MOLECULAR CLONING, RECOMBINANT EXPRESSION AND CHARACTERISATION OF SERINE AND CYSTEINE PROTEASE INHIBITORS FROM *TRICHINELLA ZIMBABWENSIS*

by

Thando Glory Maseko

B. Sc (Hons) Biochemistry

Submitted in the fulfilment of the academic requirements for the

MSc degree

in the

Discipline of Biochemistry

School of Life Sciences

University of KwaZulu-Natal

Pietermaritzburg

2019

PREFACE

The experimental work described in this dissertation was carried out in the School of Life Science, University of KwaZulu-Natal, Pietermaritzburg, from January 2018 to December 2019, under the supervision of Professor THT Coetzer.

The studies represent original work by the author and have not otherwise been submitted in any other form to another University. Where use has been made of the work of others, it has been duly acknowledged in the text.

_____

Thando Maseko (candidate)

December 2019

As the candidate's Supervisor, I agree to the submission of this dissertation.

_____

Prof. Theresa H.T. Coetzer

DECLARATION – PLAGIARISM

I, Thando Glory Maseko, declare that

1. The research reported in this dissertation, except where otherwise indicated, is my original research

2. This dissertation has not been submitted for any degree or examination at any other university.

3. This dissertation does not contain other persons' data, pictures, graphs or other information unless specifically acknowledged as being sourced from other persons.

4. This dissertation does not contain other persons' writing unless specifically acknowledged as being sourced from other researchers. Where other written sources have been quoted, then:

    a) Their words have been re-written, but the general information attributed to them has been referenced
    b) Where their exact words have been used, then their writing has been placed in italics and inside quotation marks, and referenced

5. This dissertation does not contain text, graphics or tables copied and pasted from the Internet, unless specifically acknowledged, and the source being detailed in the dissertation and in the Reference section

Thando Maseko

December 2019

ACKNOWLEDGEMENTS

I thank God who makes all things possible (Luke 19:26).

I would like to express my heartfelt and sincerest gratitude to my amazing supervisor Prof. Coetzer for her support, guidance, wisdom, encouragement, patience and immense knowledge. I cannot thank you enough for your role in my development as a scientist. I appreciate the discipline and work ethic you have instilled in me as a developing researcher.

I would like to extend special thanks to the Biochemistry department: Prof. Goldring, Dr. Khoza, Dr. Hewer, Prof Nielser for your input, involvement and role in my development.

I thank the National Research Foundation for funding my studies.

I would like to appreciate Dr Lauren Eyssen 'Taylor'; I cannot put in words how much I appreciate your advice, support, life lessons shared and always showing me light during my tunnel seasons. You are such a role model and inspiration.

Nxalati Mkhombo, you are gold. One will put one thousand to flight and two will put ten thousand to flight. Thank you for walking this journey with me from the start till the end. I appreciate your support, encouragement, your heart, friendship and co-parenting our baby rats with me.

To the lab 45 *Trichinella* squad; Nomusa Zondo, Faiaz Shaik Abdool and Nxalati Mkhombo, thank you for sharing the load and making a journey that would've been difficult alone, a manageable one. I would like to extend special thanks to Lucky Marufu and Ephraim Chauke for your much-appreciated suggestions, encouragement and constant assistance. I would thank lab 45: Bhavana Ramjeawon, Chanelle Grantham, Ziphezinhle Mbhele, Pretty Gumede, Bongumusa Mthethwa and ex-member Murtala Bindawa. I appreciate your support, input and friendship.

I thank my loving, and supportive mom, Patience Maseko, who has held my hand in support throughout my educational career. Kept me grounded through the emotional rollercoaster initiated by experimental results. Thank you for all the sacrifices that you have made to enable my development as a researcher and scientist. You are a God-given blessing. I would also like to thank aunty Penelope Hammond and uncle Frederick Hammond who gave me a warm home away from home. Special thanks to One life church for keeping me encouraged, enabling a balanced lifestyle and developing my drumming and bass playing abilities, which made me happy when experimental results weren't.

To my friends; Sphindile Gambushe, Mbali Mfeka, Sne Mgungwana, Kgaogelo Lentswana, words can never be enough to appreciate your support in this season.

ABSTRACT

Trichinellosis is a disease caused by parasitic helminths of the genus *Trichinella*. Infection occurs by ingestion of meat contaminated with infective *Trichinella* larvae. Cases of *Trichinella zimbabwensis*, a non-encapsulating species of *Trichinella* infecting mammals and reptiles, have been reported in Ethiopia, Mozambique and South Africa. The parasite life cycle alternates between the enteric and skeletal muscle phases of infection. *Trichinella* species release various excretory-secretory products that enable successful parasitism. These include cysteine protease inhibitors, cystatins and serine protease inhibitors. To illustrate, cystatins have roles in cellular invasion and immune evasion while serpins inhibit blood coagulation, resist host protease damage and interfere with host immunoregulatory signals. The potential roles of endogenous parasite cysteine and serine protease inhibitors in *T. zimbabwensis* make these inhibitors attractive targets for the development of novel antiparasitic interventions.

The genes encoding a cysteine protease inhibitor, cystatin B, and a Kazal-type serine protease inhibitor, SPINK4, were identified in the *T. zimbabwensis* genome. Following the synthesis of cDNA from nematode extracted mRNA, the respective genes were amplified and cloned into *E. coli* expression vectors. The recombinantly expressed proteins, r*Tz*cystatin B and r*Tz*SPINK4, were purified using immobilised metal affinity chromatography, their inhibitory activity evaluated and antibodies were produced in chickens. The antibodies were used for the detection of the recombinant proteins on western blots and ELISA. Recombinant *Tz*cystatin B inhibited the activity of the catalytic domain of the cathepsin L-like peptidase from *Trypanosoma congolense* (*Tco*CATL), the homologues from *T. vivax* (*Tvi*CATL) and *Theileria parva* (*Thp*CATL) as well as cathepsin B from *T. zimbabwensis* (*Tz*CATB). Conversely, r*Tz*SPINK4 was unable to inhibit either host serine proteases, chymotrypsin or trypsin. Future studies will be aimed at exploring the effect of the *T. zimbabwensis* protease inhibitors on host proteases involved in antigen processing. This may indicate a possible role for the nematode protease inhibitors in host immunoregulation.

TABLE OF CONTENTS

LIST OF FIGURES

LIST OF TABLES

LIST OF ABBREVIATIONS

2 x YT	2 x yeast extract, tryptone
ABTS	2,2-azino-di-[3-ethylbenzthiazoline sulfonate]
AMC	7-amino-4-methylcoumarin
Bis-Tris	2-bis(2-hydroxyethyl)amino-2-(hydroxymethyl)-1,3-propanediol
BMGY	Buffered media glycerol yeast
BMM	Buffered minimal media
BRU	Biomedical research unit
BSA	Bovine serum albumin
CATB	Cathepsin B
CATL	Cathepsin L
C-terminal	Carboxy terminal
DNA	Deoxyribonucleic acid
DTT	Dithiothreitol
ELISA	Enzyme-linked immunosorbent assay
ES	Excretory-secretory
h	Hour
HRPO	Horseradish peroxidise
IMAC	Immobilised metal ion affinity chromatography
IgG	Immunoglobulin G
IgY	Immunoglobulin Y
IPTG	Isopropyl-β-D-thiogalactopyranoside
kDa	kilodalton
LAMP	Loop-mediated isothermal amplification
LEKTI	Lymphoepithelial Kazal-type-related inhibitor
MEC	Molecular exclusion chromatography
min	Minute (s)
M	Molecular weight
N-terminal	Amino terminal
OD600	Optical density at 600 nm
PAGE	Polyacrylamide gel electrophoresis
PAR	Protein-activated receptors
PBS	Phosphate buffered saline

PCR	Polymerase chain reaction
PDB	Protein Database
PEG	Polyethylene glycol
RT	Room temperature
SBTI	Soya bean trypsin inhibitor
SDS	Sodium dodecyl sulphate
TAE	Tris-acetate-EDTA
TBS	Tris buffered saline
TB	Terrific broth
TPP	Three phase partitioning
Tris	2-amino-2-(hydroxymethyl)-1,3-propandiol
X-gal	Isopropyl-β-D-thiogalactopyranoside
YNB	Yeast nitrogen base
YPD	Yeast extract peptone dextrose

Chapter 1: Literature review

1.1 Introduction

Trichinellosis is a food-borne disease and is continuously emerging and re-emerging in various parts of the world. *Trichinella*, a genus of parasitic helminths, is the causative agent for Trichinellosis (Bruschi *et al.*, 2010). This disease was reported in the early 18th century in London by Sir Richard Owen and Sir James Paget who observed the worms in a cadaver (Neghina *et al.*, 2012). Since then, human cases of the diseases have been reported in 55 countries (Rostami *et al.*, 2017).

Different species within the *Trichinella* genus have been found to not only infect different hosts but behave differently within the respective hosts (Gottstein *et al.*, 2009). The members of this genus are characterised by the presence or absence of a collagen capsule in the skeletal muscle stage (Mitreva and Jasmer, 2006). Infection occurs by ingestion of meat contaminated with infective *Trichinella* larvae (Nagano *et al.*, 2001). The *Trichinella* life cycle alternates between enteric and striated skeletal muscle stages in the host (Gottstein *et al.*, 2009).

Successful parasitism is dependent on the ability of the parasite to evade host immune responses (Tormo *et al.*, 2011). Helminths such as *T. zimbabwensis* have been termed masterful immunoregulators because of their ability to release various excretory-secretory (ES) products such as proteases and protease inhibitors able to aid in host immunosuppression (Hewitson *et al.*, 2009). Proteases are hydrolytic enzymes responsible for various intra and extracellular physiological processes such as digestion, apoptosis, signal transduction, blood coagulation and complement activation (Turk *et al.*, 2002; Yang *et al.*, 2015b). This proteolytic activity needs to be carefully controlled by endogenous protease inhibitors (Habib and Fazili, 2007). Endogenous protease inhibitors are selective for specific classes of proteases, such as cystatins for cysteine proteases and serpins (serine protease inhibitors) for serine proteases (Xu *et al.*, 2017b). In addition, classes of protease inhibitors also include metallo, aspartic, glutamic and threonine protease inhibitors (Yang *et al.*, 2015b). Endogenous serpins inhibit host blood coagulation, resist host protease damage, assist in host epithelial cell invasion and larval migration as well as interfere with host immunoregulatory signals (Xu *et al.*, 2017b; Yang *et al.*, 2015b).

Endogenous cysteine protease inhibitors have also been associated with immunoevasion and cellular invasion (Sajid and McKerrow, 2002; Dubin, 2005). The roles of serine and cysteine protease inhibitors in parasites such as *T. zimbabwensis* make these inhibitors attractive agents for the development of novel antiparasitic interventions.

1.2 Classification and host range of *Trichinella*

Helminths are worm-like parasites, which share similar morphologies, and have been categorised as Trematodes (flukes), Cestodes (tapeworms) and Nematodes (roundworms) (Castro, 1996). Members of the Phylum Nematoda may occur as free-living organisms in a wide range of habitats ranging from deep sea sediments to arid deserts, or as obligate parasites within multiple hosts (Wang *et al.*, 2017a). The Phylum Nematoda consists of three classes which include the Enoplia, Chromadoria and Dorylamia; the latter include vertebrate parasites such as the gastrointestinal *Trichinella*; intestinal whip worms such as *Trichuris* and giant kidney worm, *Dictophyme* (De Ley, 2006; Smythe *et al.*, 2019). The *Trichinella* genus belongs to the Trichinellida order which belongs to one of the sister clades within the class Dorylamia and family Trichinellidae (Smythe *et al.*, 2019). There are currently nine recognised species of *Trichinella* and three genotypes (Fig. 1.1). These species are categorised by the presence or absence of a collagen capsule surrounding the worm's nurse cell in the host tissue (Gottstein *et al.*, 2009). The collagen capsule around the parasite in encapsulated species aids in the provision of nutrients from the host (Pozio *et al.*, 2001). The non-encapsulated species affect the full length of the infected cell (Fig 1.2), the nurse cell is not sealed off by a collagen capsule as observed in the encapsulating species (Xu *et al.*, 1997; Wu *et al.*, 2001; Ko *et al.*, 2009). Encapsulated species of *Trichinella* include *T. nativa*, *T. murrelli*, *T. brivoti*, *T. patagoniensis*, *T. nelson*i and *T.spiralis* and the T6, T8 and T9 genotypes while the non-encapsulated species include *T. pupae, T. pseudospiralis* and *T. zimbabwensis* (Gottstein *et al.*, 2009; Korhonen *et al.*, 2016).

Cases of *Trichinella* infection have been reported in Africa, Australia, Asia and Europe (Table 1.1) (Korhonen *et al.*, 2016). The most prevalent species being *T spiralis* and the least prevalent, *T. zimbabwensis* which has been reported in Mozambique, South Africa, Zimbabwe and Ethiopia (Gottstein *et al.*, 2009; La Grange *et al.*, 2009). *Trichinella zimbabwensis* larvae were discovered in farmed Zimbabwean crocodiles (Mukaratirwa *et al.*, 2013). The diet of these crocodiles included a wide variety of animal carcasses thus the source is unknown (Pozio *et al.*, 2002b). In addition, the lifespan of non-encapsulating *Trichinella* larvae in the host muscle is unknown (Ortega and Sterling, 2018). No human infections by *T. zimbabwensis* have been reported (Ortega and Sterling, 2018).

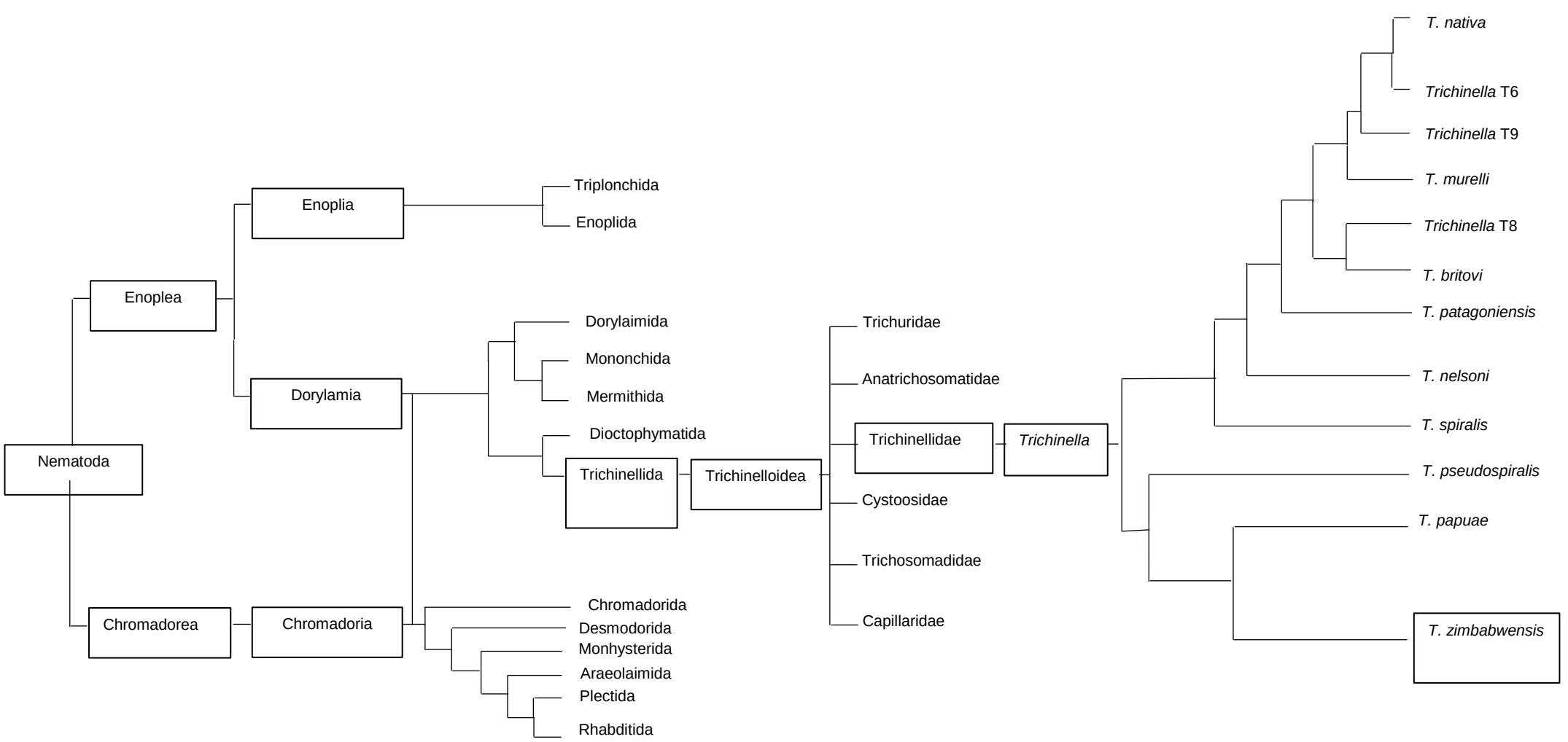

Figure 1.1: Classification and phylogenetic relationship of *Trichinella* species. (Blaxter *et al.*, 1998; Parkinson *et al.*, 2004; De Ley, 2006; Smythe *et al.*, 2019).

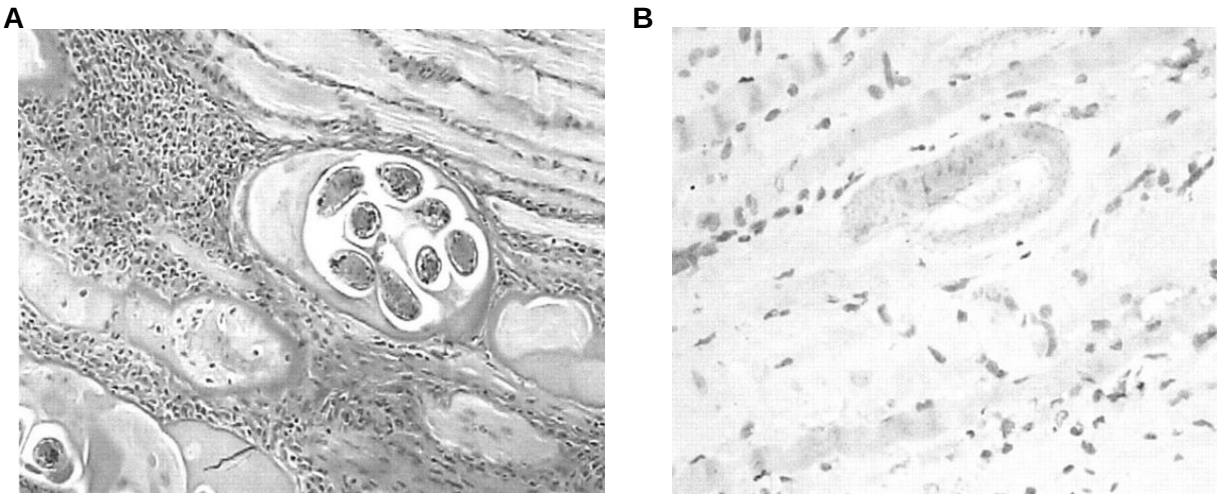

Figure 1.2: Histological image of encapsulated *T. brivoti* and non-encapsulated *T. pseudospiralis*. Histological image of the diaphragms of mice that had been infected with (A) *T. brivoti* (B) *T. pseudospiralis.* (Bruschi and Murrell, 2002).

Table 1.1: Host range and distribution of *Trichinella* species

Genotype	Species	Host	Geographic distribution
T1	*T. spiralis*	*Meriones persicus*	USA, Asia, Egypt, New Zealand
T2	*T. nativa*	*Ursus maritimus* *Vulpes lagopus* *Canis domesticus*	Asia, Europe, Greenland, Alaska[1]
T3	*T. brivoti*	*Nyctereutes procyonoides*	Europe, Western Asia[2,3]
T4	*T. pseudospiralis*	*Sus scrofa domesticus*	Europe[2]
T5	*T. murelli*	*Ursus americanus*	USA, Australia[3]
T6	-	*Alopex logopus* *Canis lupus* *Lynx rufus*	North America[5]
T7	*T. nelson*	*Acinonyx jubatus* *Panthera pardus* *Panthera leo*	South Africa, Tanzania[2]
T8	-	*Panthera leo*	South Africa, Namibia[6]
T9	-	*Vulpes vulpes* *Nyctereutes procyonoides*	Japan[7,8]
T10	*T. pupae*	*Crocodylus porosus* *Sus scrofa*	South America[2]
T11	*T. zimbabwensis*	*Crocodylus niloticus* *Varanus indicus* *Panthera leo*	Zimbabwe, Ethiopia, Mozambique, South Africa[2,6]
T12	*T. patagoniensis*	*Puma concolor*	Argentina[9]

[1]:Walden (2013); [2]: Feidas *et al.* (2014); [3]: Ortega and Sterling (2018); [4]: Goździk *et al.* (2017); [5]: Pozio (2016); [6]: Mukaratirwa *et al.* (2013); [7]: Lihua *et al.* (2015); [8]: (Kanai *et al.*, 2007); [9]: Farina *et al.* (2017).

1.3 Life cycle

The general life cycle of *Trichinella* (Fig. 1.3) is initiated by the ingestion of meat contaminated with infective *Trichinella* larvae which marks the onset of the enteric phase of the infection (Zhang *et al.*, 2016). The larvae are released from the muscle following pepsin digestion and

travel to the columnar epithelium in the small intestine where they develop, reach sexual maturity within 4-5 days post infection and mate (Mitreva and Jasmer, 2006; Walden, 2013). The females can produce up to 1500 larvae which are deposited into the intestinal mucosa; enter the lymphatic system, join the peripheral blood circulation and ultimately reach the striated muscle (Mitreva and Jasmer, 2006; Walden, 2013). Within the striated muscle, the *Trichinella* remodel the cells to promote survival (Wu *et al.*, 2001).

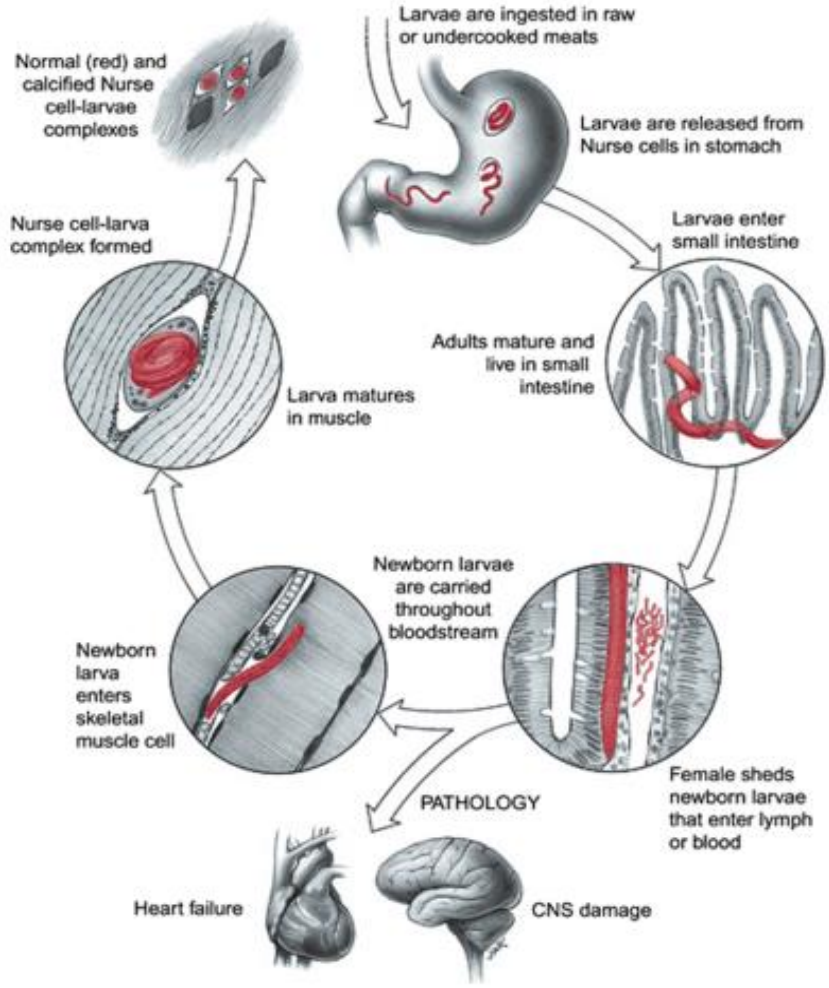

.

Figure 1.3: Life cycle of *Trichinella* species. See text for details of the individual stages (Mitreva and Jasmer, 2006).

1.4 *Trichinella* excretory – secretory (ES) products

The *Trichinella* parasites release ES products during the enteric phase of the infection which assist in the establishment of the infection (Todorova, 2000; Han *et al.*, 2019). In the host, antigen recognition by the immune system leads to an immune response such as the production of T cells, and release of cytokines to aid in inflammation (Janeway Jr *et al.*, 2001). The enteric phase of the *Trichinella* infection is characterised by the induction of a mixed type

1 helper T cell (Th1)/type 2 helper T cell (Th2) immune response, predominantly the latter, which would lead to worm expulsion (Ilic *et al.*, 2012). The Th2 immune response is characterised by the production of cytokines such as IL-4, IL-5, IL-9, IL-3; immunoglobulin IgE responses; and the presence of eosinophils as well as alternatively activated macrophages (M2-type) (MacDonald *et al.*, 2002; Nutman, 2015). However, due to the presence of ES products, the Th1/Th2 immune responses are altered, which may lead to inhibition of macrophage function, suppression of dendritic function and anti-inflammatory or tissue repair effects observed instead (Xu *et al.*, 2017b; Han *et al.*, 2019). To illustrate, a serpin from *T. spiralis* was able to induce the polarisation of M2 macrophages (Xu *et al.*, 2017b).

Excretory-secretory products identified from *Trichinella* include cystatins, serpins, glycans, mucins, lectins or homologues of cytokines which aid in host penetration, larval migration as well as evasion of immune responses (Todorova, 2000; Ilic *et al.*, 2012). Helminth cystatins inhibit T-cell activation by inhibiting the activity of cathepsins in antigen presenting cells and eliciting the production of cytokine IL-10 while the serpins inhibit neutrophil proteases (Nutman, 2015). The released products also enable parasite survival within the host; for example, *T. spiralis* glycoproteins released by the stichosome of muscle larvae are thought to promote nurse cell formation (Sofronic-Milosavljevic *et al.*, 2015). The components of ES products are still being studied to determine the role of these products in immune evasion (Xu *et al.*, 2019).

1.5 Proteases

The hallmarks of successful parasitism include parasite survival and propagation within the respective hosts; these processes are facilitated by proteases (Atkinson *et al.*, 2009). Proteases are hydrolytic enzymes that regulate intra and extracellular physiological processes in both parasites and hosts (Turk *et al.*, 2005). These processes include host protection from harmful proteases released by other microorganisms as well the degradation of host proteins by parasites for nutrient acquisition (Atkinson *et al.*, 2009; Wang *et al.*, 2013b). Hydrolytic enzymes from the serine, cysteine, glutamic, metallo, threonine and aspartic proteases and asparagine lyases degrade both intra and extracellular proteins (Turk *et al.*, 2000; Turk *et al.*, 2012). The activity of these proteases is regulated by protease inhibitors (Rawlings *et al.*, 2015).

1.5.1 Cysteine proteases

Parasite cysteine proteases have roles in tissue penetration, nutrition and immune evasion (Qu *et al.*, 2015). In contrast, host cysteine proteases localised in both intra and extra lysosomal compartments have roles in antigen presentation and protein processing among others (Turk *et al.*, 2012).

The cysteine proteases have been grouped into the following ten clans; clan CA, CD, CE, CF, CH, CL, CM, CN, CO and CP; however, some clans remain unassigned (Barrett and Rawlings, 1996; Rawlings *et al.*, 2012). Clan CA is the best studied clan and has 12 families distinguished by having a papain-like fold (Fig 1.4). Clan CA includes proteases from parasitic helminths; one such family is the C1 family of cysteine proteases which are among the best studied cysteine proteases (Atkinson *et al.*, 2009). Cathepsins, papain-like proteases within the C1 family of proteases, are present in various locations such as the nucleus, cytoplasm, plasma membrane and tissue which function in protein degradation (Turk *et al.*, 2012; Caffrey *et al.*, 2018). Cathepsins B and L are major protozoan and helminth parasite proteases (Chung *et al.*, 2005; Caffrey *et al.*, 2018). Helminth cathepsin B-like proteases have roles in nutrient acquisition (Duffy *et al.*, 2006). These include degradation of host haemoglobin by the gastrointestinal nematode *Haemonchus contortus* and host tissue degradation by *Ancylostoma cranium* and *Trichuris muris* (Caffrey *et al.*, 2018). In the *Fasciola* species, which are trematodes, cathepsins B and L have roles in excystation and host intestinal wall penetration (Grote *et al.*, 2018).

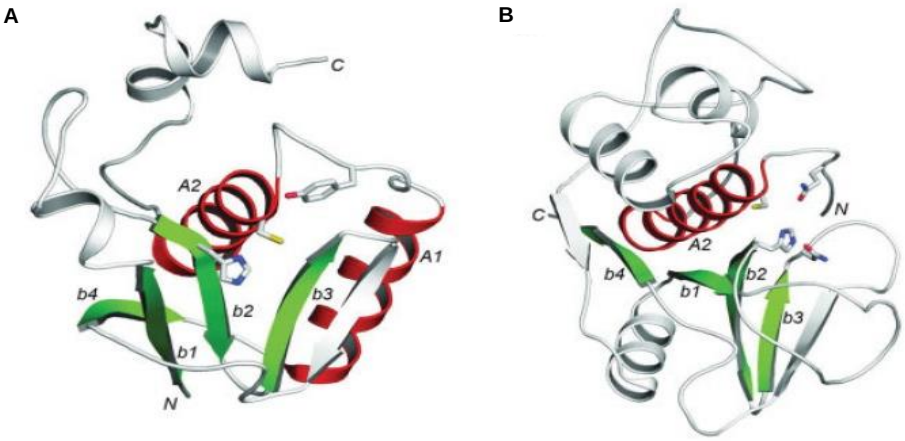

Figure 1.4: Structure of papain-like fold. (A) circularly mutated papain-like fold (pdb: 3ebq) **(B)** papain-like fold (pdb: 1khq). Figure modified from Pei and Grishin (2009).

Trichinella species secrete cysteine proteases such as cathepsin B, which helps regulate migration and parasite survival (Sajid and McKerrow, 2002). A cathepsin B from *T. spiralis* was most expressed during the early adult stage while a cathepsin F was expressed in all life stages, localised in the parasite cuticle and schistosome (Zhan *et al.*, 2013; Qu *et al.*, 2015). In addition, a cysteine protease from *T. spiralis*, expressed in all the stages of the parasite's life cycle, and located in the cuticle, stichosome and reproductive organs, was thought to be involved in the invasion, moulting and survival of the parasite (Song *et al.*, 2018a).

Structural studies show that cysteine proteins are comprised of two domains that join to form an active site cleft, which contains the conserved active site cysteine, histidine and asparagine

residues (Turk *et al.*, 2012). The catalytic mechanism of cysteine proteases (Fig. 1.5) is initiated by the nucleophilic cysteine attack on the carbonyl carbon of the scissile bond, which produces a tetrahedral intermediate. The latter becomes an acyl enzyme following the release of the first product with an amine terminus. The carbonyl carbon of the acyl enzyme is attacked by a nucleophilic water molecule, which leads to the release of the second product containing a carboxylic acid moiety (Bromme, 2001; Verma *et al.*, 2016) (Elsässer *et al.*, 2017).

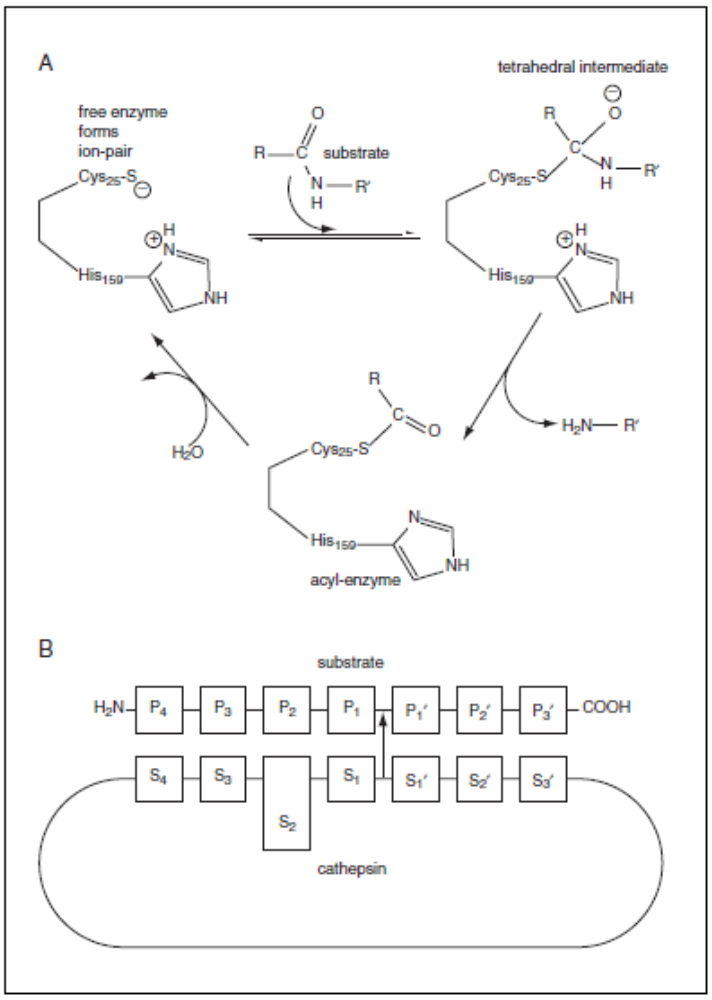

Figure 1.5: Catalytic mechanism for substrate hydrolysis by papain-like cysteine proteases and Schechter and Berger nomenclature for protease interaction with peptide substrates. (A) Catalytic mechanism illustrating the attack of a substrate by the catalytic cysteine, formation and disintegration of tetrahedral formation resulting in the release of a first product, acyl enzyme hydrolysis and release of second product **(B)** Schechter and Berger cathepsin substrate binding regions. Protease active sites are comprised of subsites labelled S1, S2, S1' and S2'. Peptide substrates are labelled P1, P2 and P1', P2' on either side of the scissile bond where hydrolysis occurs (Bromme, 2001).

1.5.2 Serine proteases

Serine proteases have various physiological functions such as digestion, apoptosis, signal transduction, blood coagulation, complement cascade activation and wound healing (Yang et al., 2015). There are 40 families of serine proteases which belong to 13 families; Clan PA

trypsin-like proteases are the best studied family of serine proteases (Di Cera, 2009). Serine proteases from parasitic nematodes *Trichuris muris* were shown to degrade mucin, a component of the intestinal mucus barrier, that has roles in worm expulsion (Hasnain *et al.*, 2012). A serine protease from the muscle stage of *T. spiralis* and one expressed in all stages of the life cycle has roles in invasion and nurse cell formation while another serine protease, located in the oesophagus of the same parasite has roles in moulting and nutrition (Yang *et al.*, 2015b). Serine protease also have roles in the nutrition, host invasion, immune evasion and migration of other nematodes such as *Onchorcerca volvulus* (Yang *et al.*, 2015b).

The serine protease catalytic triad comprises a nucleophilic serine, electrophilic aspartate and basic histidine (Antalis *et al.*, 2011). The catalytic histidine accepts a proton from the catalytic serine forming a methanolate anion that attacks the scissile bond to form a tetrahedral intermediate (Fig. 1.6), characterised by the presence of the oxyanion hole which stabilises the intermediate (Hunkapiller *et al.*, 1976). Cis/trans conformational acyl enzymes are formed from the collapse of the tetrahedral intermediate by proton transfer to the amide of the scissile bond by the histidine leading to the dissociation of the N-terminal half of the polypeptide; the water molecule enables the release of the C-terminal half of the polypeptide (Di Cera, 2009).

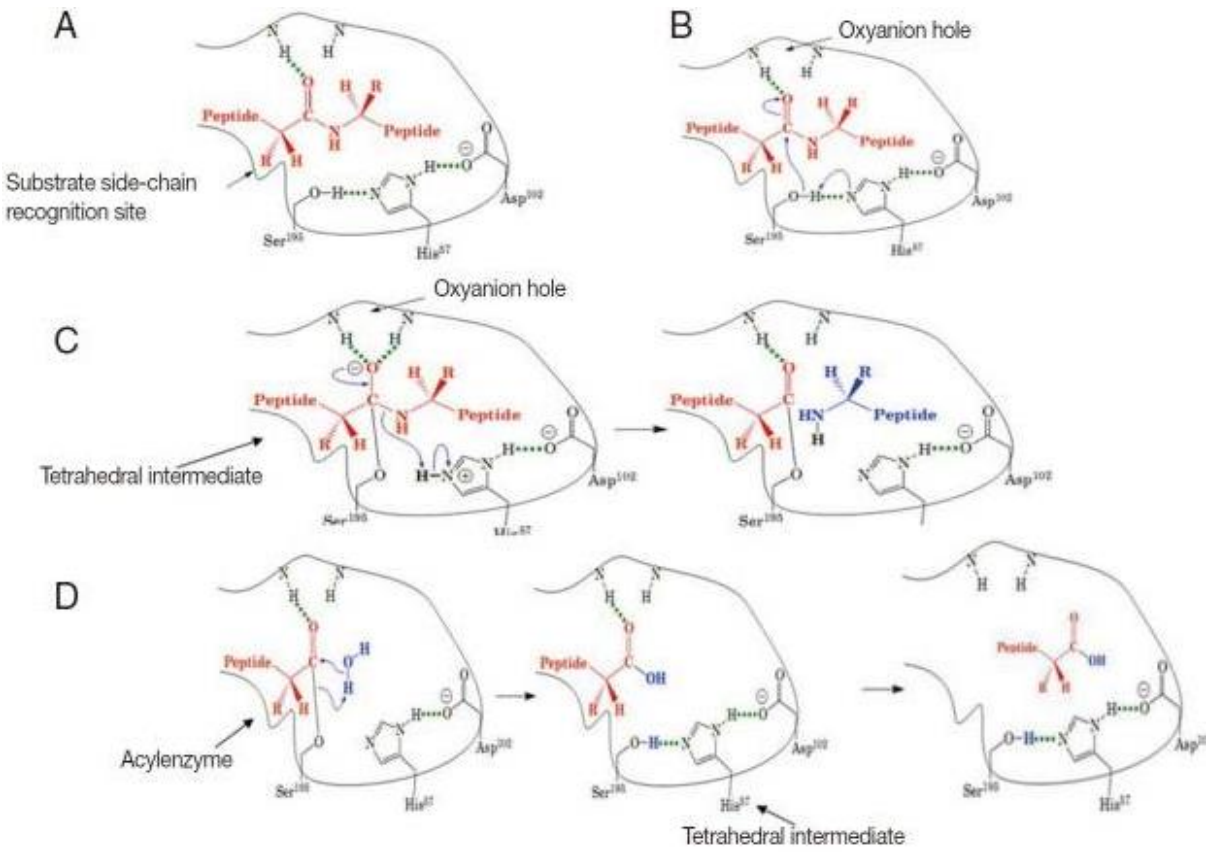

Figure 1.6: Catalytic mechanism of serine proteases. (A) binding of substrate to proteases; **(B)** nucleophilic attack; **(C)** protonation; **(D)** diacylation (Yang *et al.*, 2015b).

1.6. Protease inhibitors

1.6.1 Cysteine protease inhibitors

The activity of cysteine proteases is regulated by various inhibitors which include endogenous peptide and protein inhibitors (Turk *et al.*, 2012). There are 51 Clans of cysteine protease inhibitors with 93 families; the cystatins belong to clan IH and the family I25 (Chakraborti and Dhalla, 2017). This family is comprised of four subfamilies namely: I25A, the stefins; I25B, the cystatins and kininogens; I25C, the metalloprotease inhibitors and unclassified cystatins (Turk *et al.*, 2005). Cystatins in nematodes, trematodes and ticks have been identified as cystatins from the I25 superfamily (Lee *et al.*, 2013). The stefins inhibit proteases from the C1 family of papain-like cysteine proteases; while the cystatins inhibit, in addition to papain-like proteases from the C1 family, also legumain-like proteases from the C13 family, while the kininogens inhibit proteases from the S8 subtilase family and M13 metalloprotease family (Turk *et al.*, 2005; van Wyk *et al.*, 2014).

The cystatins are competitive inhibitors that bind tightly, but non-covalently to target cysteine proteases (Hartmann and Lucius, 2003). Cystatins target proteases with lysosomal functions as well as endosomal functions such as protein degradation, endosomal antigen presentation and signalling pathways (Turk *et al.*, 2005). The stefins A and B, now termed cystatin A and B, are intracellular and involved in endogenous protein regulation and act primarily against members of the papain-like C1 peptidase family (Turk *et al.*, 2002; Guo, 2015; Zerovnik, 2006). The term cystatin was initially used for a partially characterised inhibitor of papain from chicken egg white; subsequently identified cysteine protease inhibitors were found to be related to the chicken cystatin hence termed members of this superfamily (Turk and Bode, 1991).

Cystatin B interacts with cysteine proteases in a reversible, tight-binding fashion using the two hydrophobic wedge-shaped β hairpin loops and the N-terminus (Fig 1.7) (Hartmann and Lucius, 2003). However, the active site of the cysteine protease is not directly involved since the cystatin binds the cysteine protease around the catalytic cleft preventing further interaction with any substrate (Chakraborti and Dhalla, 2017). The first hairpin loop includes the conserved QVVAG sequence and the second hairpin loop a conserved Pro and Trp residue that participate in the interaction with the cysteine protease. The N-terminal domain around Gly-11 interacts with the S1, S2 and S3 pockets of the cysteine protease (Hartmann and Lucius, 2003). Mutagenesis studies have shown that this glycine residue plays a significant role in inhibition and binding affinity (Turk *et al.*, 2005). In addition, cysteine-3 (papain numbering) from human and bovine cystatin B was shown to be a key residue for cathepsin B inhibition (Pol and Björk, 2001).

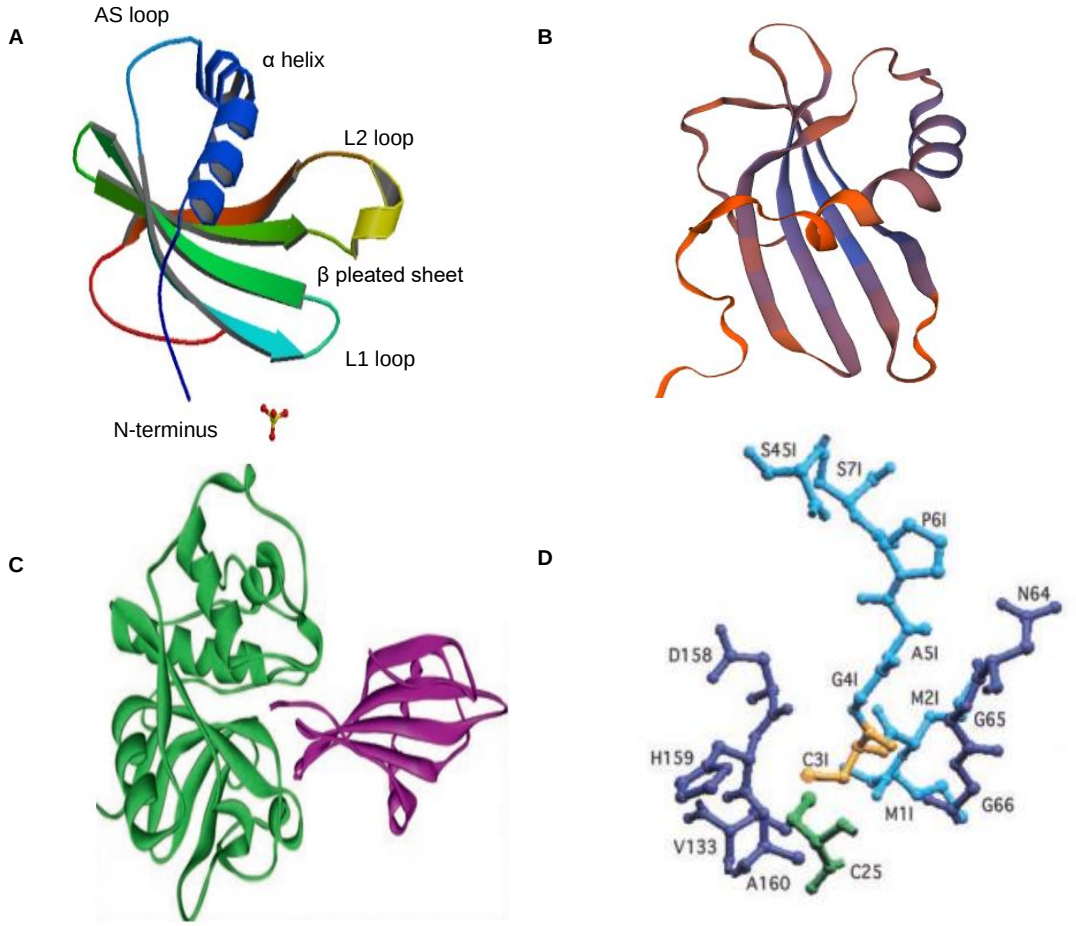

Figure 1.7: Structure of human stefin B, modelled *Trichinella zimbabwensis* cystatin B and a human stefin B-papain complex. (A) Structure of human stefin B (PBB 4N6V); **(B)** *T. zimbabwensis* cystatin B as predicted by Swiss model; **(C)** Interaction of papain (green) and human stefin B (purple); **(D)** Interaction of human wild-type cystatin B and papain; papain (violet), catalytic cysteine of papain (green), cystatin B (blue), cysteine-3 (yellow). Figure modified from (Pol and Björk, 2001; Chakraborti and Dhalla, 2017).

Endogenous nematode cystatins have the ability to regulate both parasite and host protease activity (Guo, 2015). A multi-cystatin-like domain protein (MCD) protein was identified from the ES proteins of *T. spiralis* muscle larvae. Analysis of the MCD-1 structure showed an absence of the conserved QxVxG motif; however, also showed that the MCD protein shared sequence similarities with type 2 cystatins (Robinson *et al.*, 2007). In addition, a strongly antigenic cystatin-like protein was identified in *T. spiralis* containing three domains that also do not contain the conserved QVG motif but two GXA/TXYXD motifs instead (Tang *et al.*, 2015). The cystatin B protein from *T. zimbabwensis* was modelled using Swiss model and shown to resemble the structure of the human stefin B (Fig. 1.7). The modelled structure of *T. zimbabwensis* cystatin B appears to be similar to the structure of the human stefin B. The *T. zimbabwensis* cystatin B is shown to consist of five antiparallel β pleated sheets, which are wrapped around the α helix to form the characteristic cystatin fold (Fig. 1.7).

1.6.2 Serine protease inhibitors

Serine protease inhibitors are classified into three groups, namely: non-canonical and canonical serine protease inhibitors as well as serpins based on the mechanism of inhibition (Krowarsch *et al.*, 2003). The 6-8 kDa non-canonical inhibitors utilise the N-terminus for inhibition. The reversible, tight-binding interaction of 3-21 kDa canonical inhibitors with their target proteases resembles the Michaelis substrate-enzyme complex, while the irreversible 45-55 kDa serpin forms the standard acyl-enzyme complex (Krowarsch *et al.*, 2003). There are four main families of canonical serine protease inhibitors which include the Kunitz, Kazal, Trypsin-like inhibitor and Bowman-Birk families (Fig. 1.8) (Ranasinghe and McManus, 2013).

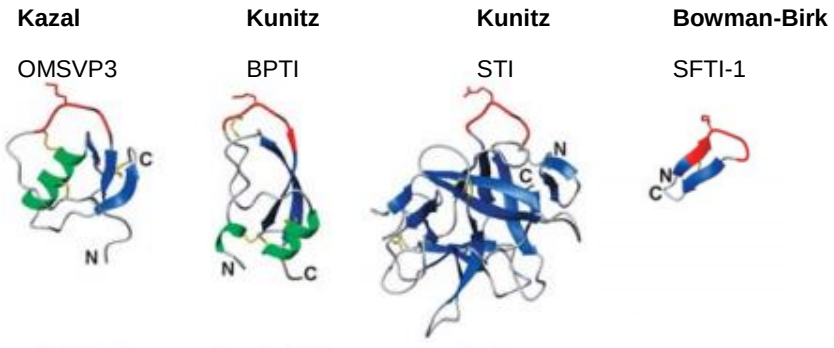

Figure 1.8: Structures of canonical serine protease inhibitors. (A) Kazal-type OMSVP3, PDB: 2ovo **(B)** Kunitz-type pancreatic trypsin inhibitor (BPTI), PDB: Ipi2 **(C)** Kunitz-type soybean trypsin inhibitor, PDB: lavu **(D)** Bowman-Birk Inhibitor-type Sunflower Trypsin Inhibitor (SFTI-1). Figure modified from (Krowarsch *et al.*, 2003).

The Kazal-type serine protease inhibitors (SPINKs), a branch of serine protease inhibitors, belong to the I12 family of inhibitors (Fig. 1.8) (Krowarsch *et al.*, 2003). The I12 family of inhibitors is known to inhibit proteases within the serine protease S1 and S8 families, which include trypsin-like and subtilisin-like proteases (Di Cera, 2009). The Kazal-type serine protease inhibitors act as anticoagulants in leeches, mosquitoes and ticks and protect parasitic protozoa from host digestive enzymes (Ranasinghe and McManus, 2013). Blood sucking parasites such as leeches mosquitoes, ticks and bugs use protease inhibitors to eliminate proteases from the host biological systems (Rimphanitchayakit and Tassanakajon, 2010; Blisnick *et al.*, 2017). Bdellin B-3, a non-canonical Kazal-type inhibitor,isolated from the leech *Hirudo medicinalis*, inhibits trypsin and plasmin (Fink *et al.*, 1986). *Rhodnius prolixus* (kissing bug that is the main vector for *Trypanosoma cruzi* that causes Chagas disease) uses the Kazal-type inhibitor rhodnin (Fig. 1.10, panel A), a thrombin inhibitor, to prevent blood coagulation (Friedrich *et al.*, 1993a). A Kazal-type inhibitor, *Toxoplasma gondii* protease inhibitor (TgPI-1) inhibits trypsin, chymotrypsin, pancreatic elastase and neutrophil elastase and is thought to protect the protozoan parasite from the host digestive enzymes to enable the parasite to propagate (Rimphanitchayakit and Tassanakajon, 2010).

The Kazal-type serine protease inhibitors may comprise of a single or multiple domains (Blisnick *et al.*, 2017). A 6-21 kDa canonical Kazal domain is made up of a short α-helix enfolded by a three stranded β-pleated sheet and three peptide loops where the second loop, termed the reactive site loop, house the P_1 site necessary for inhibitor specificity (Fig. 1.9) (Ranasinghe and McManus, 2013). The Kazal domain has a C-X-C-X-PVCG-X-Y-X-C-X-C-X-C motif where the position of the cysteines determine whether the inhibitor is a classical or non-classical Kazal inhibitor (Negulescu *et al.*, 2015).

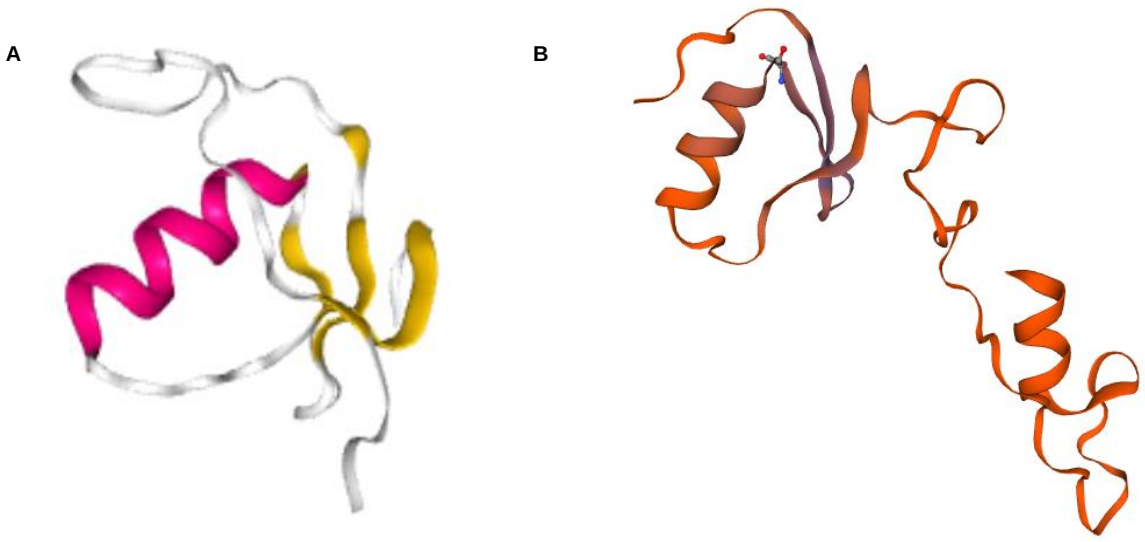

Figure 1.9: Structure of pancreatic secretory trypsin inhibitor (SPINK1) and modelled *T. zimbabwensis* SPINK4. (A) SPINK1, PDB ID 1HPT.1. **(B)** *T. zimbabwensis* SPINK4 as predicted by Swiss model.

The canonical Kazal inhibitors follow a standard (Laskowski) mechanism (Fig. 1.10) (Farady and Craik, 2010). The SPINKs competitively inhibit target serine proteases as each Kazal domain mimics the substrate and binds with the aid of the exposed reactive site loop thus trapping the protease to form a non-covalent Michaelis complex (Ranasinghe and McManus, 2013). The Kazal domains interact with target proteases primarily by the P_1 site amino acid residue, which determines the specificity of the inhibitor (Fig. 1.10). In addition, there are twelve other points of interaction which include the P_1, P_2, P_3, P_4, P_5, P_6 as well as the P_1', P_2', P_3', P_{14}' and P_{18}' sites (Rimphanitchayakit and Tassanakajon, 2010). SPINKs with lysine or arginine at the P_1 site inhibit trypsin-like proteases, those with phenylalanine, tyrosine and leucine inhibit chymotrypsin-like proteases, while SPINKs with alanine, arginine or methionine inhibit elastase-like proteases (Negulescu *et al.*, 2015). The modelled structure of *Trichinella zimbabwensis* SPINK4 illustrates the presence of a characteristic Kazal-domain which consists of an α-helix, a three stranded β -pleated sheet and peptide loop. In addition, a second domain is observed.

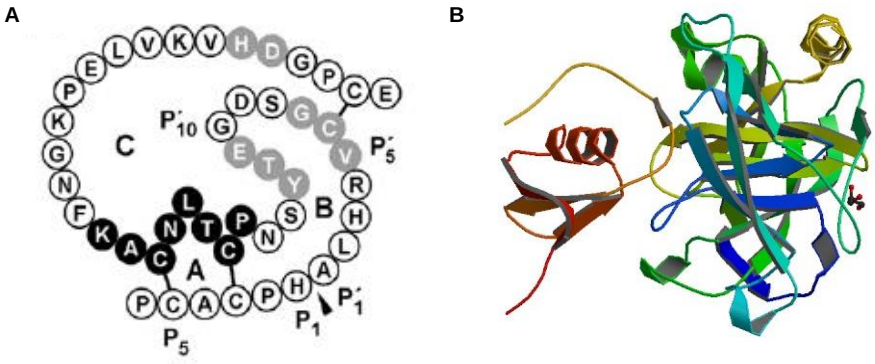

Figure 1.10: Interaction of human kallikrein 4 and SPINK2 (Nishimiya *et al.*, 2019). **(A)** Primary structure of invertebrate Kazal-type inhibitor, rhodonin; **(B)** Interaction of kallikrein with SPINK2. Figure modified from (Rimphanitchayakit and Tassanakajon, 2010).

1.7 Diagnosis of *Trichinella* infection

Trichinellosis is diagnosed using direct and indirect methods (Gómez-Morales *et al.*, 2014). A direct method entails the *post mortem* inspection of meat using tissue digestion of at least 1 g of tissue sample and parasite detection by microscopy (Gottstein *et al.*, 2009). Indirect methods of diagnosis include serological tests such as the enzyme-linked immunosorbent assay (ELISA), which is a preferred diagnostic test, along with indirect fluorescent antibody tests and western blots (Bai *et al.*, 2017). These serological tests detect characterised *Trichinella* antigens, to illustrate, *T. spiralis* muscle larval antigens have been classified into 8 groups according to their recognition by monoclonal and polyclonal antibodies (Yang *et al.*, 2016). The TSL-1 antigens are a family of glycoproteins which share a carbohydrate (3.6-dideoxyhexose sugar) tyvelose epitope; and are recognised by monoclonal antibodies specific for the *T. spiralis* muscle stage (Goyal *et al.*, 2002; Yepez-Mulia *et al.*, 2007). Antibodies have been produced against these 40-70 kDa TSL-1 antigens from the stichosome of muscle larvae, which share a tyvelose; and are now used in serological tests (Magrone *et al.*, 2014). Immunochromatographic lateral flow strip tests have also been developed for the serological detection of Trichinellosis from blood serum of humans or animals by detecting anti-*Trichinella* antibodies using gold labelled ES antigens (Bai *et al.*, 2017). The antigens used are obtained from the muscle larval stage (Zhang *et al.*, 2009; Bai *et al.*, 2017). Multiplex PCR, which uses the DNA sequences of each of the *Trichinella* genotypes produces a unique and distinct banding pattern for each genotype which aids in the differentiation of species and genotypes (Zarlenga *et al.*, 2001).

1.8 Prevention and control

1.8.1 Vaccination

There is a need to prevent Trichinellosis in animals and humans (Xu *et al.*, 2017a). Vaccine immunogens, tested on porcine and mouse models, have included crude ES antigens, recombinant proteases, surface antigens and antigens involved in the intracellular processes of the *T. spiralis* parasites while candidate antigens include whole worms, recombinant ES products, proteases, surface proteins and proteins used in intracellular processes (Zhang *et al.*, 2018). The ES antigens include crude proteins with sizes ranging from 20 kDa – 55 kDa. To illustrate, 37.97 kDa *T. spiralis* 87 (*Ts*87) protein which was abundantly present on the cuticular surface of *T. spiralis* which produces a predominantly Th2 response (Gu *et al.*, 2008). Larval stage antigens include 43 kDa glycoprotein (gp43) found in secretions and on the parasite *T. spiralis* surface and thought to have roles in the invasion of intestinal epithelial cells (Andrade-Becerra *et al.*, 2017; Zhang *et al.*, 2018). Recombinant proteins include 35.5 kDa *T. spiralis* serine protease (TsSP-1.2) which was localised in the cuticle and internal organs of *T. spiralis;* and present in all the stages of the parasite while surface proteins include aquaporins (Wang *et al.*, 2013a; Zhang *et al.*, 2018). Whole worms may include heat sterilised *T. spiralis* larvae and inactivated muscle larvae (Andrade-Becerra *et al.*, 2017). A DNA vaccine comprised of a larval serine protease and Nudix hydrolase from *T. spiralis,* have been tested on mice and was shown to promote both helper T cell 1 (Th1) and Th2 responses since the Th2 response is commonly suppressed by the parasite (Xu *et al.*, 2017a; Bai *et al.*, 2017). A Nudix hydrolase which aids in the hydrolysis of pyrophosphates, and thought to be involved in the invasion of intestinal epithelial cells by *T. spiralis*, was expressed in all the stages of the *T. spiralis* life cycle and thought to be a house keeping gene (Long *et al.*, 2015). Trichinellosis vaccine development studies are ongoing and prove to be promising for the control of the *T. spiralis* infection (Zhang *et al.*, 2018).

1.8.2 Treatment of Trichinellosis

The benzimidazole antihelminthic agents including mebendazole and albendazole, improved versions of thiabendazole which produced unwanted side effects such as headaches, vertigo and vomiting, have been effective against Trichinellosis (Kocięcka, 2000; Abongwa *et al.*, 2017). The benzimidazole drugs kill the parasites by destroying their cell structures due to the inhibition of microtubule polymerisation (Abongwa *et al.*, 2017). Albendazole is the choice drug for the treatment of *Trichinella* infection and acts on the alimentary canal of nematodes during all their developmental stages (Kocięcka, 2000). Glucocorticosteriods are administered during chronic stages of infection in combination with albendazole (Wang and Cui, 2008; Abongwa *et al.*, 2017).

1.9 Rationale of study

Trichinellosis is a food-borne zoonosis which infects mammals and reptiles (Zolfaghari Emameh *et al.*, 2018). This continuously re-emerging disease has health impacts which include the clinical infection of humans and negative economic impacts on the international meat trade and porcine production (Gottstein *et al.*, 2009). There is a need for further development of vaccines and vaccine candidates based on antigens from different stages of the parasite's life cycle and treatment (Andrade-Becerra *et al.*, 2017).

1.10 Objectives of the present study

The overall objective of this study was to identify a cysteine and a serine protease inhibitor in the genome of *Trichinella zimbabwensis* muscle larvae. The specific experimental aims within this objective included:

- The cultivation of *Trichinella zimbabwensis* muscle larvae *in vivo* in rats.
- The isolation of the parasites from infected rat tissue for the extraction of total RNA and synthesis of cDNA from the isolated RNA.
- The identification of cysteine and serine protease inhibitor genes from the *T. zimbabwensis* genome using bioinformatics, and design of gene-specific primers to be used for amplification of the genes by PCR.
- The amplification of *Tzcystatin B* and *TzSPINK4* genes by PCR using synthesised cDNA as a template and the designed gene-specific primers.
- The cloning of the *Tzcystatin B* and *TzSPINK4* genes into cloning vectors and recombinant expression of *Tz*cystatin B and *Tz*SPINK4 proteins using the *E. coli* expression system.
- The purification of recombinant *Tz*cystatin B (r*Tz*cystatin B) and *Tz*SPINK4 (r*Tz*SPINK4) proteins.
- The proteolytic cleavage of fusion tags from the purified r*Tz*cystatin B and r*Tz*SPINK4 fusion proteins.
- The immunisation of chickens with purified *Tz*cystatin B and *Tz*SPINK4 proteins to produce chicken anti-*Tz*cystatin B and chicken anti-*Tz*SPINK4 IgY antibodies and analysis of the progress of antibody production by ELISA.
- The detection of recombinant and native *Tz*cystatin B and *Tz*SPINK4 in western blots using the antibodies produced in chickens.
- The determination of the inhibitory activity of *Tz*cystatin B protein on endogenous and exogenous cathepsins and commercial cysteine proteases using synthetic substrates.
- The determination of the inhibitory activity of *Tz*SPINK4 protein on serine proteases; trypsin, chymotrypsin and thrombin using synthetic substrates.

Chapter 2: Recombinant expression, purification and characterisation of serine protease inhibitor Kazal type-4 (SPINK4) from *Trichinella zimbabwensis* muscle larvae

2.1 Introduction

The Kazal-type serine protease inhibitors have been found in mammals, birds, fish and blood sucking insects (Qian *et al.*, 2015). These inhibitors control the activity of serine proteases from the S1 peptidase family, which include the kallikreins, chymotrypsin, trypsin, elastase, matriptase and thrombin (Sigle and Ramalho-Ortigão, 2013; Kalinska *et al.*, 2016). Some of these proteases, such as thrombin and the kallikreins, are thought to be involved in inflammation and immune responses (Steinhoff *et al.*, 2004). To illustrate, the tissue kallikreins have been implicated in the mediation of pro-inflammatory pathways and activation of protein-activated receptors (PARs) which may lead to cytokine production (Yiu *et al.*, 2014).

The recombinant expression and characterisation of serine protease inhibitor Kazal-type 4 (SPINK4) from *Trichinella* species and other parasitic nematodes has not been documented to date. However, immunoproteomic studies on *T. spiralis* adult worm proteins recognised by early infection sera showed that the *Ts*SPINK4 protein was recognised by pig and mouse infection sera at seven days post infection (Yang *et al.*, 2015a). Recombinant expression of these Kazal-type serine protease inhibitors from human and arthropod species such as *Nasonisa vitripennis*, a parasitoid wasp (Qian *et al.*, 2015); *Phlebotomus papatasi*, vector for Leishmania parasites (Sigle and Ramalho-Ortigão, 2013); *Rhodnius prolixus,* a blood sucking insect and main vector for Chagas parasites (Friedrich *et al.*, 1993b) were recombinantly expressed and in the case of blood feeding insects had roles in the prevention of blood coagulation during feeding (Meyer-Hoffert *et al.*, 2010).

The transcription levels of two *Nasonia vitripennis* Kazal-type serine protease inhibitors, *Nv*KSPI-1 and *Nv*KSPI-2, implicated in host immune evasion, were found to be higher in venom apparatus than in other tissues (Qian *et al.*, 2015). The *Nv*KSPI-1 and *Nv*KSPI-2 genes were ligated to a pGEX-4T-2 vector and expressed using *E. coli* BL21 (DE3) bacterial cells by IPTG induction and purified by immobilized metal affinity chromatography. The recombinant proteins had molecular weights of 33 kDa (*Nv*KSPI-1) and 36 kDa (*Nv*KSPI-2). Whereas *Nv*KSPI-1 inhibited only pancreatic trypsin, NvKSPI-2 did not inhibit pancreatic trypsin, chymotrypsin or proteinase K (Qian *et al.*, 2015).

Transcriptomic studies on the midgut of *Phlebotomus papatasi* showed that there were two Kazal-type inhibitors expressed in the midgut of the larva and pupa (Sigle and Ramalho-Ortigão, 2013). The mature form of the Kazal-type serine protease inhibitor from *P. papatasi,*

*Pp*Kzl2, without the signal peptide was amplified using cDNA reverse transcribed from total RNA obtained from dissected midguts of the sand flies (Sigle and Ramalho-Ortigão, 2013). The *PpKzl2* gene was cloned into a VR1020-TOPO vector and expressed using a mammalian freestyle Chinese hamster ovary-S expression system. The *Pp*Kzl2 inhibited human α-thrombin, trypsin and bovine α-chymotrypsin (Sigle and Ramalho-Ortigão, 2013).

Transcriptomic studies on lactating rodents, challenged with *Nippostrongylus brasiliensis*, a parasitic nematode, showed that the extracellularly expressed *SPINK4* gene was regulated, shown by a 2.5 fold change in expression, following a second challenge with the parasite (Athanasiadou *et al.*, 2011). In addition, transcriptomic studies on the response of zebra finch, *Taeniopgyia guttata,* following a challenge with bacterial lipopolysaccharide showed that the *SPINK4* gene was largely upregulated (Scalf *et al.*, 2019). A recent study on Hepatitis B Virus (HBV) illustrated that an HBV protein enhanced the expression of SPINK1 levels during disease progression of HBV-related disease and is considered to be a potential biomarker for the diagnosis of HBV-related diseases (Zhu *et al.*, 2019).

The SPINKS, grouped in family I1 of protease inhibitors, have a conserved C-C-PVCG-Y-C-C-C motif-containing domain (Rimphanitchayakit and Tassanakajon, 2010). The conserved cysteine 1 and 5, cysteine 2 and 5, cysteine 2 and 6 form intra-domain disulphide bridges (Rimphanitchayakit and Tassanakajon, 2010; Negulescu *et al.*, 2015). The structure is comprised of a central alpha helix, three stranded beta pleated sheet and loops of peptide segments, one of which houses the reactive site P1 which determines the specificity of the Kazal-type inhibitor; however, 11 other positions of contact exist between the Kazal inhibitor and target protease (Negulescu *et al.*, 2015; Rimphanitchayakit and Tassanakajon, 2010). Trypsin-like enzymes are inhibited by Kazal inhibitors with lysine or arginine in the P1 site, chymotrypsin-like enzymes by inhibitors with tyrosine, phenylalanine in the P1 site and elastase-like enzymes by inhibitors with serine, methionine, leucine or alanine in the P1 site (Negulescu *et al.*, 2015).

The SPINK4 was aligned with human SPINKS that inhibit various S1 peptidase family proteases. SPINK4 was found to share a sequence similarity of 35.62% with SPINK1, 32.89% with SPINK 7, 25.68% with SPINK6 and 25% with SPINK9 (Fig. 2.1).

Figure 2.1: A comparison of SPINK sequences from different species. Multiple sequence alignment was generated using Clustal omega (https://www.ebi.ac.uk/Tools/msa/clustalo/). SPINK4 sequence from *Trichinella zimbabwensis* (KRZ12928.1), Homo sapiens SPINK1 (KR710681.1), SPINK6 (NM_205841.4), SPINK7 (NM_032566), and SPINK9 (NM_001040433.2) sequences obtained from NCBI Genbank (https://www.ncbi.nlm.nih.gov/genbank/). The symbols shown represent: conserved residues, (*); residues with similar properties, (:); residues with weakly similar properies, (.).

In this study, the gene encoding SPINK4 from *T. zimbabwensis* was obtained from NCBI Genbank (https://www.ncbi.nlm.nih.gov/genbank/).The gene was amplified by PCR using cDNA reverse transcribed from total RNA extracted from the *T. zimbabwensis* larval parasites. The recombinant protein was purified, the activity tested against various serine proteases and used for antibody production. The antibodies were used for the detection of the recombinantly expressed *Tz*SPINK4 on western blots and ELISA.

2.2 Materials and methods

2.2.1 Materials:

Molecular biology, protein purification and characterisation: The Direct-zol RNA miniprep plus R2070 kit was purchased from Zymo Research (Orange, CA, USA) and the PCR reaction mixture components, Firepol Taq polymerase, PCR reaction buffer and 25 mM $MgCl_2$ from Solis Biodyne (Tartu, Estonia). EcoRI, BamHI, XhoI restriction enzymes (nomenclature as per Roberts *et al.* (2003)) and T4 DNA ligase were obtained from Thermo Scientific (Waltham, MA, USA). The pMD-19T simple cloning vector, TaKaRa Ex Taq Hot start Version Taq polymerase and the TaKaRa 1 kb DNA ladder were purchased sourced from Clonetech (Californina, USA). The O'GeneRuler 1 kb DNA ladder, 5-bromo-4-chloro-3-indolyl-β-D-galactopyranoside (IPTG), isopropyl-β-D-thiogalactopyranoside (X-gal) and dithiothreitol (DTT) were obtained from (Fermentas, Vilnius, Lithuania). The pGEM-T and pGEM-T easy cloning vectors were purchased from (Promega, Madison, WI, USA) and the pET-28a,

pET-32a, pET-100 expression vectors from Novagen (Darmstadt, Germany). Nunc-Immuno 96-well plates were purchased from Nunc (Intermed, Denmark) and nickel-nitriloacetic acid (Ni-NTA) agarose resin for immobilised metal affinity chromatography (IMAC) was obtained from Qiagen (Hilden, Germany). The peptide substrate Benzyloxycarbonyl (Z)-Phe-Arg-7-amino-4-methylcoumarin (AMC), cysteine protease inhibitor *trans*-Epoxysuccinyl-L-leucylamido(4-guanidino)butane (E-64), bovine serum albumin (BSA), and Freund's complete and incomplete adjuvants were purchased from (Sigma, St. Louis, MO. USA) and *2,2'-Azino-bis*(*3-ethylbenzothiazoline-6-sulfonic acid*) (ABTS) sourced from Roche (Mannheim, Germany). All other reagents were of the highest purity available were obtained from Merck, RSA.

Sprague Dawley (SD) rats: The male SD rats were obtained from the Biomedical Resources Unit (BRU) at the University of KwaZulu-Natal (Westville campus).

***Escherichia coli* cells**: *E. coli* JM 109 cells with a T7 expression system were purchased from Novagen (Darmstadt, Germany) and protease deficient *E. coli* BL21 (DE3) cells from NEB labs (MA, USA).

2.2.2 Protein quantification

The Bradford protein determination method (Bradford, 1976) was used to determine the protein concentration of all samples. A calibration curve was constructed using BSA in a range of 0–100 µg (Fig. 2.2). Briefly, triplicate samples of 0 – 100 µl of the 100 µg/ml BSA standard solution were diluted to 100 µl with distilled water. Subsequently, 900 µl of Bradford reagent (0.06% (w/v) Coomassie brilliant blue G-250, 2% (v/v) perchloric acid) was added and the samples vortexed. The absorbance of the samples was read at 595 nm after three minutes incubation time. A calibration curve was constructed and used to determine the protein concentration in samples of unknown concentration (Fig. 2.2).

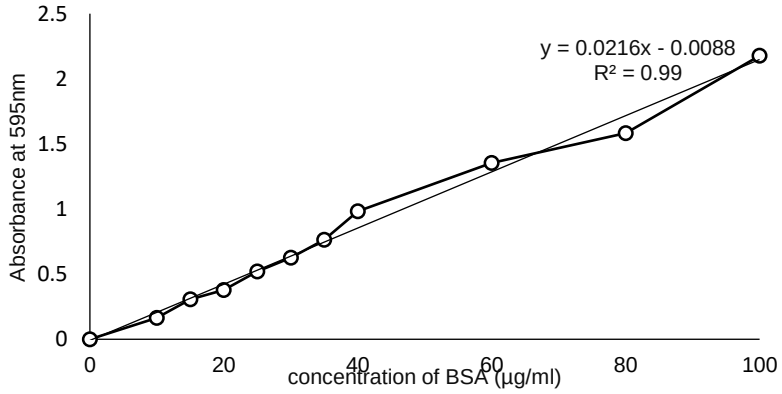

Figure 2.2: Standard curve relating BSA concentration to absorbance using Bradford assay. Bovine serum albumin dilutions (5 to 100 µg/ml) were combined with Bradford reagent. Following a 5 min incubation of the samples at RT, absorbance values were read at 595 nm. The equation of the trend was y= 0.0291x-0.0291 with a correlation coefficient of 0.9925.

2.2.3 *In vitro* cultivation of *Trichinella zimbabwensis* parasites and isolation from rat tissue

All protocols involving animals were approved by the UKZN Research Ethics committee with approval number (AREC/077/016D).

Male Sprague-Dawley (SD) rats were obtained and kept in the animal house in an environment with 12 h light/12 h dark cycles containing bedding and environmental enrichment to promote physical activity and mental stimulation (Hutchinson *et al.*, 2005). The rats had *ad libitum* access to food and water. The rats were 90 – 150 g at the time of infection unless otherwise stated. The rats were orally infected with 300 – 500 *T. zimbabwensis* larvae in 1% (w/v) saline solution.

For parasite isolation, an infected rat was sacrificed using carbon dioxide three months post infection (pi). The infected muscle tissue was digested using the modified pepsin-HCl method (Pozio *et al.*, 2002a). Briefly, the muscle tissue was weighed and mixed with pre-heated distilled water in a 5 L beaker (2 L per 100 g rat muscle). Digestion was facilitated by the addition of pepsin (20 g per 100 g rat muscle) and 37% (v/v) HCl (8 ml per 2 L distilled water) and the mixture stirred for 30 min at 42°C. This mixture is now referred to as digestion fluid.

The digestion fluid was sieved through 800 µm followed by 250 µm sieves to remove undigested particles. To enable sedimentation of parasites, the sieved digestion fluid was poured into 2 L separating funnels and left to stand for 40 min at RT. Post sedimentation, 50 ml digestion fluid was collected per separating funnel into a 250 ml beaker. The 50 ml digestion fluid was diluted with an equal volume of distilled water. The diluted collected digestion fluid was further sedimented within the beaker in 15 min intervals at RT after which 30 ml was aspirated and checked for the presence of parasites using a light microscope. The aspiration process was continued until 5 ml of the digestion fluid remained which should contain parasites. The presence of larval parasites was ascertained microscopically, and the digestion fluid further aspirated to 1 ml. The parasites were stored at –70°C until used for RNA extraction.

2.2.4 Extraction of total RNA from *Trichinella zimbabwensis* muscle larvae and cDNA synthesis

Parasites (100 µl) were thawed and suspended in Tri-reagent (300 µl) from the Direct-zol RNA miniprep plus R2070 kit. The resultant mixture was ground using a chilled pestle and mortar containing liquid nitrogen. This process was repeated until the parasite mixture was ground into a fine powder which was transferred to a microfuge tube. The ground powder was dissolved in Tri-reagent (100 µl) and 500 µl of 100% (v/v) ethanol. Subsequently, RNA was isolated using the kit according to the manufacturer's instructions.

The cDNA was synthesised from the isolated *T. zimbabwensis* RNA using the LunaScript R supermix kit. Briefly, isolated RNA (8 µl) was mixed with oligo primer (2 µl) or random primer (2 µl) to assess which primer yield the highest concentration of synthesised cDNA. The RNA-oligo primer and RNA-random primer mixtures were incubated at 70°C for 5 min for RNA denaturation. Subsequently, cDNA was synthesised as per the manufacturer's instruction.

2.2.5 Primer design for *TzSPINK4* gene amplification

The *T. zimbabwensis Tz*SPINK4 DNA coding sequence (GenBank accession number: KRZ12928.1) was selected for primer design. The *Tz*SPINK4 coding nucleotide sequence was obtained by the extraction and joining of coding sequence (CDS) regions within the *T. zimbabwensis* whole genome shotgun sequence using the BioEdit program (http://www.mbio.ncsu.edu/BioEdit/bioedit.html). The coding sequence was used to design primers using the Snapgene molecular biology software (https://www.snapgene.com). The ThermoFisher scientific Tm calculator was used to determine the annealing temperature of the primers, while the Oligonucleotide Properties Calculator (http://biotools.nubic.northwestern.edu/OligoCalc.html) was used to determine regions of self-complementarity within the primers. A BamHI restriction site was introduced in the forward primer, while a XhoHI restriction site was introduced in the reverse primer. The primer sequences are shown in Table 2.1 and were synthesised by Inqaba Biotechnical Industries (Pretoria, RSA).

Table 2.1 *TzSPINK4* gene oligonucleotide sequences used for PCR

Primer name	Nucleotide sequence 5' – 3'	Annealing temp.
TzSPINK4 Fwd	AAAAGGATCC ATG ATT TCA CTC GCT TGC TTG TAC TTG	53.9 °C
TzSPINK4 Rev	AAAACTCGAG TTA CGG GAT ATC AGC AGC ACG	

The underlined sequences represent the BamHI (forward primer) and XhoI (reverse primer) restriction sites.

2.2.6 Polymerase chain reaction (PCR) amplification of the *TzSPINK4* gene

The amplification of the *SPINK4* gene by PCR was performed using a PCR mastermix comprising of 0.025 U TaKaRa Ex Taq HS, 1 x Ex Taq buffer (containing Mg^{2+}), 2.5 mM dNTPs, 1 µM of the forward and reverse *SPINK4* gene primer, 400 ng cDNA in a final reaction volume of 50 µl. PCR conditions were as follows: denaturation of DNA was carried out at 95°C for 3 min followed by 34 cycles of denaturation at 95°C for 30 s; subsequently, annealing at 53.9°C for 30 s and DNA extension at 72°C for 1 min. The final extension was performed at 72°C for 5 min, upon completion of amplification, incubated at 4°C in the BioRad T100

thermocycler. A sample of the PCR amplification products were analysed by agarose gel electrophoresis as outlined in Section 2.2.7.

2.2.7 Analysis of DNA by agarose gel electrophoresis

The amplification of the *TzSPINK4* gene by PCR using the cDNA as a template, was analysed by agarose gel electrophoresis. A 1% (w/v) agarose gel was prepared by dissolving 0.5 g agarose powder in 50 ml 1 x TAE buffer (40 mM Tris, 20 mM acetic acid, 1 mM EDTA, pH 8.3) and heating the solution until the agarose had fully dissolved. The solution was cooled and gel red (2.5 µl per 50 ml TAE) was added prior to pouring into the casting tray. The DNA samples containing 1 x loading dye were electrophoresed on a 1% (w/v) agarose gel at 80 V for 50 minutes. After electrophoresis, the bands were visualised by UV light using the G-box system (Syngene). A standard curve was constructed to determine the size of DNA electrophoresed on the 1% (w/v) agarose gel (Fig. 2.3). The relative distance travelled by each DNA marker on the gel was plotted against the respective log DNA size.

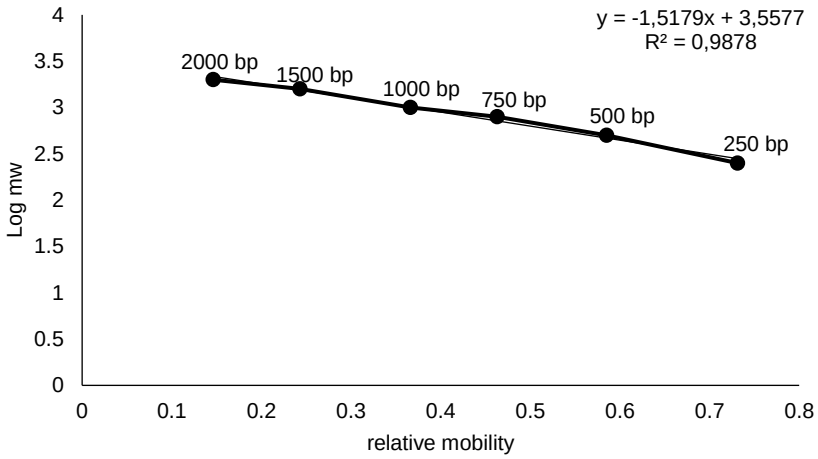

Figure 2.3: Standard curve showing relative mobility of DNA in relation to the log of the respective molecular weight. A: The 1 kb O'Gene Ruler DNA ladder was electrophoresed on a 1% (w/v) agarose gel. The equation of the trendline was y= -1.5179x + 3.5577 with a correlation coefficient of 0.9878.

2.2.8 Cloning of the *TzSPINK4* gene into pGEM-T and pGEM-T easy vectors

2.2.8.1 Ligation of the *TzSPINK4* gene insert into pGEM-T and pGEM-T easy vectors

The purified *TzSPINK4* gene amplicon was ligated to pGEM-T and pGEM-T easy cloning vectors (50 ng) using a 3:1 molar ratio of *SPINK4* gene insert to cloning vector as determined using the NEB ligation calculator (https://nebiocalculator.neb.com/#!/ligation) in the presence of 1 x rapid ligation buffer and 1 U T4 DNA ligase (Fig. 2.4). The ligation mixture was incubated at 16°C for 16 h.

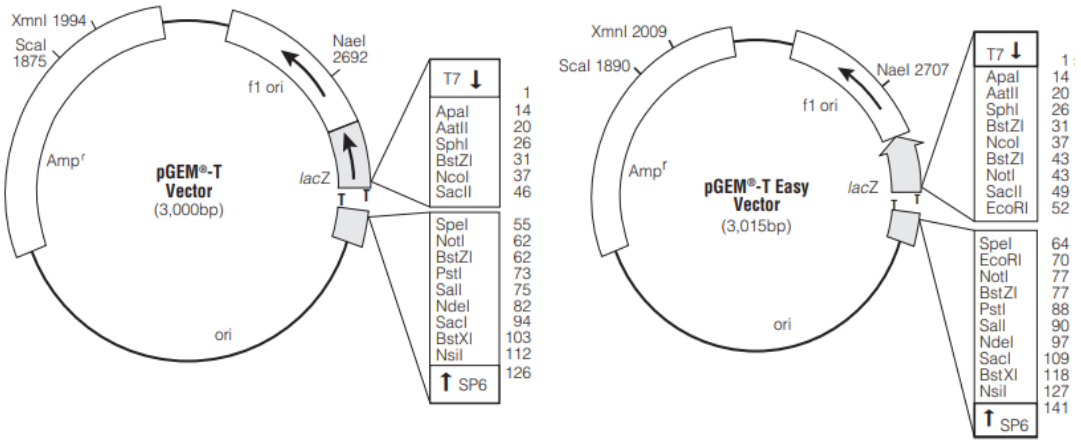

Figure 2.4: pGEM-T and pGEM-T easy cloning vector maps. The T vectors contain thymine which hybridises to adenine that flanks the gene insert in the presence of ligases

2.2.8.2 Preparation of competent *E. coli* JM 109 and BL21 (DE3) cells

E. coli JM109 and BL21 (DE3) cells were cultured overnight at 37°C in 5 ml 2 x YT medium containing no antibiotic. The overnight culture was diluted 1 in 100 ml and cultured at 37°C, 200 rpm until an optical density (OD) of 0.4 at 600 nm was reached. The culture (50 ml) was centrifuged (2700 *g,* 10 min, 4°C) and the supernatant discarded. The pellet was resuspended in sterile 0.1 M $MgCl_2$ (8 ml) and 0.1 M $CaCl_2$ (2 ml). The mixture was centrifuged (2700 *g*, 10 min, 4°C) and the supernatant discarded. The pellet was resuspended in 4 ml 0.1 M $CaCl_2$ and 2.7 ml 60% glycerol. The cells were frozen rapidly in liquid nitrogen and stored at - 80°C. The cells were tested for competence by transformation with control DNA.

2.2.8.3 Transformation of *TzSPINK4*-pGEM-T, *TzSPINK4*-pGEM-T easy into *E. coli* JM109 cells and selection of recombinant colonies

The *TzSPINK4* amplicon-cloning vector ligation mixture was transformed into competent *E. coli* JM109 cells. Transformation was performed by incubating the ligation mixture (5 µl) with competent *E. coli* JM 109 (50 µl) cells for 30 min on ice. The *E. coli* JM109 cells were heat shocked by incubation at 42°C for 60 s and cooled on ice for 5 min. Subsequently, 80 µl SOC medium [2% (w/v) tryptone, 0.5 % (w/v) yeast extract, 10 mM NaCl, 2.5 mM KCl, 10 mM $MgSO_4$, 20 mM glucose] was added to the transformation mixture and incubated at 37°C for 1 h at 200 rpm. The transformation mixture (100 µl) was plated onto a 2 x YT bacteriological agar plate [1.6 % (w/v) tryptone, 1% (w/v) yeast extract, 0.5 % (w/v) NaCl, 1% (w/v) bacteriological agar containing 50 µg/ml ampicillin, 20 µg/ml X- gal, 10 µg/ml IPTG]. The plates were incubated at 37°C for 16 h.

2.2.8.4 Identification of recombinant *TzSPINK4*-pGEM-T, *TzSPINK4*-pGEM-T easy vector clones

Recombinant colonies were selected by Blue-white colony screening. In alpha complementation, the *E. coli* bacteria contain an alpha peptide while the vector contains a lacZα sequence in the multiple cloning site which encodes the omega peptide. The alpha peptide and lacZα sequence together code for a functional β-galactosidase enzyme which hydrolyses X-gal. Colonies formed by non-recombinant cells appear bright blue because the lactose analogue will be hydrolysed to 5,5'-dibromo-4,4'-dichloro-indigo by the β-galactosidase enzyme. The presence of the *TzSPINK4* gene insert in the plasmid disrupts the lacZ gene thus a functional β-galactosidase gene is not coded for. Therefore, colonies formed by recombinant cells appear white because the X-gal is not hydrolysed (Dale *et al.*, 2011). The recombinant white colonies were each selected from agar plate and dispersed in water (10 µl) and were as template DNA for colony PCR (Section 2.2.8.5).

2.2.8.5 Colony PCR to confirm presence of the *TzSPINK4* insert

Colony PCR was performed on the recombinant *TzSPINK4*-pGEM-T and *TzSPINK4*-pGEM-T easy agar colonies to ascertain the presence and size of the *TzSPINK 4* insert. Final concentrations of the PCR mastermix components are given in Table 2.2.

Table 2.2: PCR mastermix components

Components	Concentration	Volume (µl)
10x buffer B (Solis Biodyne)	1 x	5.0
25 mM MgCl	2 mM	4.0
10 mM dNTP	200 µM	1.0
Forward primer (10 µM)	0.3 µM	1.5
Reverse primer (10 µM)	0.3 µM	1.5
Template	-	2.0
dH_2O	-	34.5
Firepol Taq polymerase (5U/ µl)	0.05 U	0.5
Total volume		50.0

The PCR reaction was conducted, in separate reactions, using either the gene primers or the vector primers. The vector primers utilised for the pGEM-T and pGEM-T easy vector were the M13 forward and reverse primers shown in Table 2.3.

Table 2.3: Vector primer nucleotide sequences used for PCR

Primer name	Nucleotide sequence (5' – 3')	Annealing temp.
M13 Fwd	GTT TTC CCA GTC ACG AC	42.8°C
M13 Rev	CAG GAA ACA GCT ATG AC	

2.2.8.6. Isolation of plasmid DNA by miniprep

Recombinant *TzSPINK4*-pGEM-T and *TzSPINK4*-pGEM-T easy vector colonies were diluted in distilled water (10 µl). This mixture (2 µl) was used to inoculate 2 x YT (5 ml) broth containing ampicillin (50 µg/ml) and incubated at 37°C for 16h with agitation. Three ml of culture was centrifuged (12 000 *g*, 10 min, 4°C) and the supernatant discarded. Plasmid DNA was isolated from the pelleted recombinant cells using the GeneJet Plasmid Miniprep kit as per the manufacturer's instructions.

2.2.8.7 Restriction digestion of plasmid DNA isolated by plasmid miniprep

The presence of the *TzSPINK4* insert DNA in the pGEM-T and pGEM-T easy vectors was further confirmed by restriction digestion. Small scale restriction digests were performed on the plasmid DNA isolated by miniprep. Plasmid DNA (1000 ng) was digested with BamHI (1 µl) and *Xanthomonas campestris* I (formerly *Xanthomonas holcicola*) XhoI (1 µl) in 1 x fast digestion buffer. The final volume was made up to 20 µl using distilled water. The digestion was carried out at 37°C for 20 min. The restriction digestion products were analysed by 1% (w/v) agarose gel electrophoresis (Section 2.2.7) to confirm excision of insert, the size of the excised insert and the orientation of the insert. Subsequently, the 450 bp *TzSPINK4* insert was excised from the agarose gel using Zymogen DNA gel extraction kit as per the manufacturer's instructions.

2.2.9 Subcloning of *Tz*SPINK4 into pET-28a, pET-32a and pET-100 expression vectors

The restriction digested bacterial expression vectors pET-28a and pET-32a (50 ng) and the pET100 TOPO vector (Fig. 2.5), synthesised with the BamHI and XhoI restriction sites by GeneArt were ligated to the digested *TzSPINK4* insert in a 3:1 molar ratio of insert to vector as calculated using the NEB ligation calculator. To the expression vector and insert mixture was added 1 x rapid ligation buffer and 1 U T4 DNA ligase. This ligation mixture was incubated at 37°C for 20 min. The ligation mixture was transformed into *E. coli* JM109 cells as described in Section 2.2.8.3.

The *TzSPINK4*-pET-28a transformation (100 µl) mixture was plated on a 2 x YT bacteriological agar plate [1.6 % (w/v) tryptone, 1% (w/v) yeast extract, 0.5 % (w/v) NaCl, 1% (w/v)

bacteriological agar containing 50 µg/ml ampicillin, 20 µg/ml X- gal, 10 µg/ml IPTG] containing kanamycin (34 µg/ml) while the pET-32a and pET-100 transformation mixtures were plated on a 2 x YT bacteriological agar plate containing ampicillin (50 µg/ml).

2.2.10 Recombinant expression of *Tz*SPINK4 in *E. coli* (BL21) cells by auto and IPTG induction

2.2.10.1 Recombinant expression by IPTG induction

The 450 bp *SPINK4* gene from *T. zimbabwensis* codes for a protein of 150 amino acids with an expected molecular weight of approximately ~16.6 kDa. Single recombinant *TzSPINK4*-pET-32a and *TzSPINK4*-pET-100 colonies were used to inoculate 2 x YT liquid medium (5 ml) containing ampicillin (50 µg/ml). In addition, a single recombinant *TzSPINK4*-pET28a colony was used to inoculate 2 x YT liquid medium (5 ml) containing kanamycin (34 µg/ml). The flasks were incubated at 37°C for 16h with agitation. Subsequently, a 1:100 dilution of the 2 x YT cultures with fresh 2 x YT medium (250 ml) containing the respective antibiotics was performed, and the new culture grown at 37°C with agitation until an $OD_{600\ nm}$ of 0.6 - 0.8 was reached.

Expression was induced with IPTG (1 mM) at 37°C for 4 h with agitation. The IPTG concentration for induction of expression and temperature at which expression was carried out and induced was optimised using 0.1, 0.3 and 1 mM IPTG concentrations, and expression conducted for 4 h at 37°C, 24 h and 48 h at 16°C. The empty pET expression vectors were subjected to the same conditions as controls. Induction at 37°C for 4 h was found to be optimal for IPTG induction. The bacterial cells were harvested by centrifugation (6000 *g*, 20 min, 4°C). The pelleted cells were resuspended in 1% (v/v) Triton X-100-PBS (10 ml) containing lysozyme (1 mg/ml) and incubated at 37°C for 30 min. The cells were frozen at -20°C for 16 h, thawed at RT and sonicated 4 times for 30 s on ice. The soluble and insoluble fractions were obtained by centrifugation (6000 *g*, 10 min, 4°C).

2.2.10.2 Recombinant expression by auto induction

Recombinant expression of *Tz*SPINK4 from pET-28a, pET-32a expression vectors (Fig. 2.5) was performed in the *E. coli* BL21 (DE3) host by inoculating terrific broth medium [1.2% (w/v) tryptone, 2.4 (w/v) yeast extract, 0.4% v/v glycerol, 0.17 M KH_2HPO_4, 0.72 M K_2HPO_4] containing kanamycin (34 µg/ml) and ampicillin (50 µg/ml), respectively, with a recombinant colony. The inoculated medium was incubated at 37°C for 16 h with agitation. The temperature at which expression was performed was optimised by incubation at 37°C for 16 h and 24 h and at 16 °C for 16 h, 24 h and 48 h.

Expression at 16°C for 24 h was found to be optimal for auto-induction. The cells were harvested, and soluble and insoluble fractions obtained as described in Section 2.2.10.1.

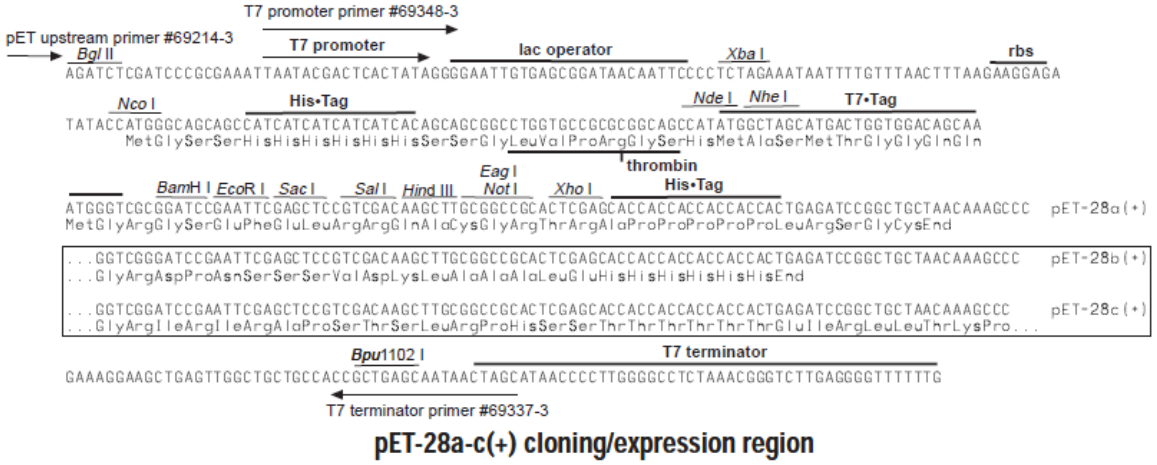

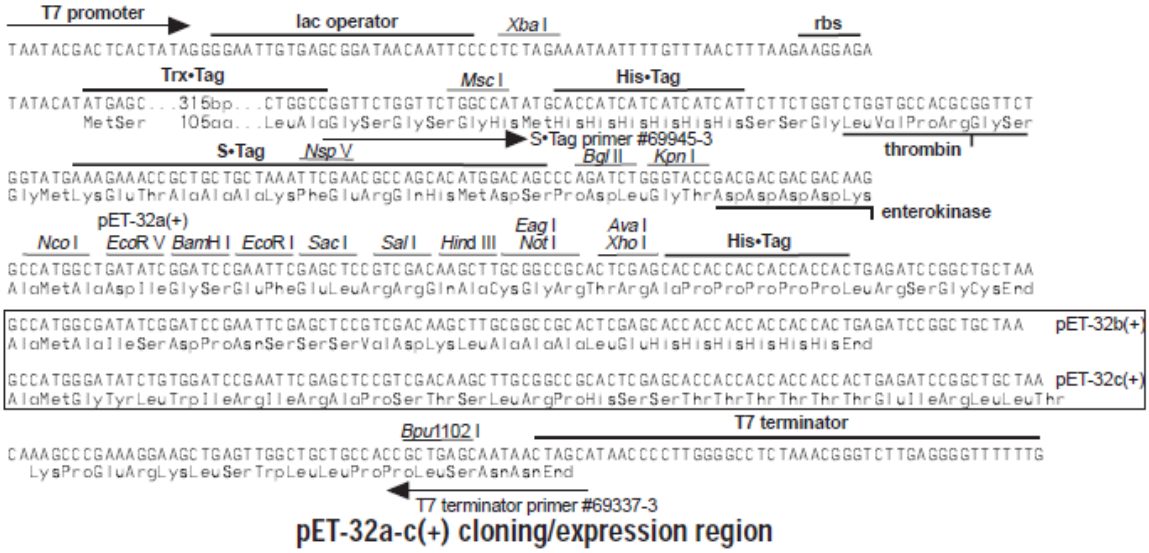

.

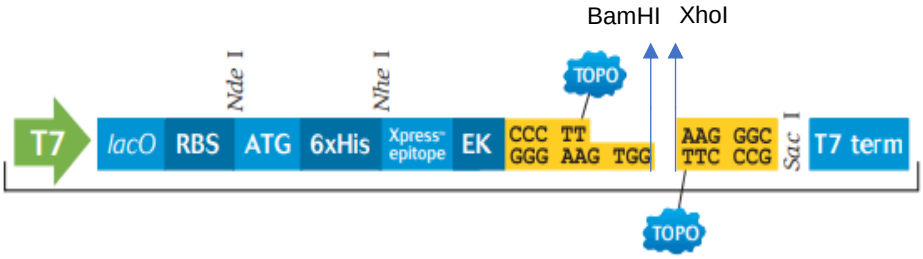

Figure 2.5: Vector map of the pET-28a, pET-32a and pET100/D TOPO expression vectors

2.2.11 Analysis of recombinant expression

2.2.11.1 SDS-PAGE analysis of recombinant expression of proteins

Recombinant protein expression was analysed on two 10% reducing Tris-tricine SDS-PAGE gels (Schägger, 2006; Haider *et al.*, 2012). The gels were electrophoresed using a Bio-Rad gel electrophoresis system at 80 V for 85 min. Tris-tricine SDS-PAGE is commonly used to resolve proteins smaller than 30 kDa. However, it can separate proteins 1 – 100 kDa in size. One set of gels was stained with Coomassie Brilliant Blue R-250 and the other used for western blotting. The gels were viewed on the G-box system (Syngene). A calibration curve was constructed to determine the molecular weight of proteins separated on 10% Tris-tricine reducing SDS-PAGE gels (Fig. 2.6). The relative distance travelled by protein markers on the gel was plotted against the respective log molecular weights.

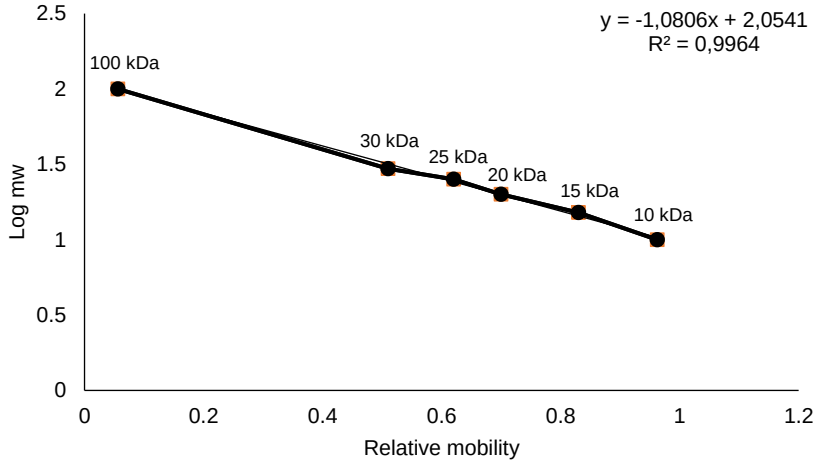

Figure 2.6: Standard curve showing relative mobility of proteins in relation to the log of the respective molecular weight. The commercial protein molecular weight marker used for the 10% Tris-tricine reducing SDS-PAGE gel had a trendline with the equation y= -1.0806x + 2.0541 with a correlation coefficient of 0.9964.

2.2.11.2 Detection of proteins using western blotting

Protein expression may be confirmed using an immuno- (western) blotting technique. The proteins separated by reducing SDS-PAGE were transferred onto a nitrocellulose membrane using the Bio-Rad blotting system at 40 mA for 6 h. Following protein transfer, the nitrocellulose membrane was incubated in Ponceau S stain [0.1% (w/v) Ponceau S, 1% (v/v) acetic acid] for 20 min to ascertain protein transfer. The Ponceau S stain was removed by rinsing the nitrocellulose membrane with distilled water. Residual Ponceau stain was removed by the addition of a few drops of 500 mM NaOH followed by rinsing with distilled water. The unoccupied sites on the membrane were blocked with 5% (w/v) low fat milk in Tris buffered saline (TBS) [20 mM Tris, 20 mM NaCl, pH 7.4] for 1 h. The nitrocellulose membrane was then washed three times with TBS and incubated with primary antibody (mouse anti-His

monoclonal antibody (1:5000) or chicken anti-*Tco*CATL N-terminal peptide IgY (2.4 μg/ml) in TBS containing 0.5% (w/v) BSA for 2 h. The membrane was washed three times with TBS and incubated in HRPO-linked goat anti-mouse IgG (1:5000) in TBS containing 0.5% (w/v) BSA for 1 h. The nitrocellulose membrane was washed three times in TBS and incubated with substrate solution [0.06% (w/v) 4-chloro-1-naphthol, 0.1% (v/v) methanol, 0.0015% (v/v) H_2O_2 in PBS] for 10 min in the dark until bands became visible. The image was captured using the G-box (Syngene).

2.2.12 Purification of His-tagged *Tz*SPINK4 expressed from pET-32a and pET-28a vectors by nickel immobilised metal-ion affinity chromatography (IMAC)

Recombinant *Tz*SPINK4 expressed from the pET-28a and pET-32a vectors contains a polyhistidine (6xHis) sequence commonly referred to as a His-tag which enabled purification using a nickel-nitrilotriacetic acid (Ni-NTA) agarose column. Proteins bound to the column were eluted with high concentrations of imidazole. Qiagen Ni-NTA agarose resin (1 ml) was added to a 10 ml chromatography column. The column was equilibrated with 10 column volumes of equilibration buffer [20 mM NaH_2PO_4, 300 mM NaCl, 10 mM imidazole, pH 7.4]. The soluble *Tz*SPINK4 lysate (2 ml) from recombinant expression was incubated with the resin for 3 h using an end-over-end rotator at 4°C. The unbound fraction was collected in 1 ml volumes. The nickel column was then washed with 30 ml of wash buffer [20 mM NaH_2PO_4, 300 mM NaCl, 20 mM imidazole, pH 7.4] until an absorbance at 280 nm of 0.03 was reached. The bound *Tz*SPINK4 protein was eluted in 1 ml fractions with 10 ml of elution buffer [20 mM NaH_2PO_4, 300 mM NaCl, 250 mM imidazole (optimised as indicated below), pH 7.4]. To determine the lowest concentration of imidazole necessary for elution of the *Tz*SPINK4-pET-28a the protein was eluted using elution buffer containing increasing concentrations for imidazole. The Ni-NTA affinity column was equilibrated, loaded and washed as previously described. The bound *Tz*SPINK4-pET-28a protein was eluted in 2 ml fractions by running with 4 ml of elution buffer containing 50 mM, 100 mM, 150 mM, 200 mM and 250 mM imidazole concentrations. The column was regenerated with 10 ml of 6 M guanidine hydrochloride, washed with 10 ml distilled water and stored in 20% ethanol. The unbound, wash and elution fractions were electrophoresed on a 10% Tris-tricine SDS-PAGE gel, (Section 2.2.11.1).

2.2.13 Antibody production and immunoglobulin isolation

2.2.13.1 Chicken immunisation

Two chickens were used to raise antibodies against purified recombinant *Tz*SPINK4. During the immunisation schedule, 50 μg *Tz*SPINK4 was used per chicken per immunisation. The purified *Tz*SPINK4 protein (50 μg, 1ml) was mixed with an equal volume of Freund's complete adjuvant and triturated until a stable water-in-oil emulsion was formed. The chickens were

immunised intramuscularly on each side of the breast bone with the triturated *Tz*SPINK4. Booster injections were given at weeks 2, 4 and 6 with the same amount of purified recombinant *Tz*SPINK4 mixed with an equal volume of Freund's incomplete adjuvant. Eggs from both chickens were collected prior immunisation and weekly for 16-weeks post the first immunisation. The eggs were stored at 4°C.

2.2.13.2 Immunoglobulin (IgY) isolation

Chicken IgY was isolated from eggs collected during the immunisation schedule (Goldring and Coetzer, 2003). The egg white was discarded, and the yolk volume determined using a measuring cylinder. Two yolk volumes of 100 mM sodium phosphate buffer pH 7.6, containing 0.02% NaN_3 were added. A concentration of 3.5% (w/v) polyethylene glycol (PEG) 6000 was dissolved into the yolk solution. The resulting solution was filtered through Whatman No. 1 filter paper. A further 8.5% (w/v) PEG 6000 was dissolved in the filtrate and the solution centrifuged (12 000 *g*, 10 min, RT). The supernatant was discarded, and the pellet was resuspended in a volume equivalent to that of the original yolk volume. The 12% (w/v) PEG 6000 added and dissolved using sodium phosphate buffer before the IgY pellet was collected by centrifugation (12 000 *g*, 10 min, RT). The supernatant was discarded, and the pellet dissolved with a sixth of the yolk volume using sodium phosphate buffer [100 mM NaH_2PO_4 buffer containing 0.1% NaN_3, pH 7.6]. The concentration of IgY was determined by diluting the sample 1:50 with sodium phosphate buffer and reading the absorbance at 280 nm $E_{280\,nm}^{1\,mg/ml}$ = 1.25 (Goldring *et al.*, 2005).

2.2.13.3 Enzyme-linked immunosorbent assay ELISA

The progress of antibody production against *Tz*SPINK4 during the immunisation period was analysed using the ELISA technique. The experiment was performed in duplicates. Purified recombinant *Tz*SPINK4 (1 µg/ml, 100 µl per well) was used to coat the 96 well Nunc-Immuno Maxisorp ELISA plate which was incubated at 4°C for 16 h. The ELISA plate was washed three times with 1% (v/v) Tween-20-PBS using the BIOTEK ELx50 Microplate washer. The unoccupied sites of the coated wells were blocked with 0.5% (w/v) BSA-PBS (200 µl per well) for 1 h at 37°C and washed three times as previously described. The plates were then incubated with primary antibody, 100 µg/ml chicken anti-cystatin IgY in 0.5% (w/v) BSA-PBS (100 µl per well) at 37°C for 2 h. The plate was washed three times with 1% (v/v) Tween-20-PBS and incubated with secondary antibody, rabbit anti-chicken IgY (whole molecule) in in 0.5% (w/v) BSA-PBS (120 µl per well). The plate was washed three times with 1% (v/v) Tween-20-PBS and incubated with substrate solution 0.05% (w/v) ABTS, 0.0015% (v/v) H2O2 in 0.15 M citrate-phosphate buffer, pH 5] in the dark for 15 min. The reaction was stopped by the addition of the stopping buffer [0.15 M citrate buffer, pH 5 containing 0.1% (w/v) NaN_3].

A similar protocol was used to determine the optimum dilution of IgY to use in western blots. All steps were identical, except for the primary antibody incubation step where a series of dilutions of IgY (100, 50, 25, 10, 5, 1, 0.1 µg/ml), isolated from eggs pooled during weeks of maximal IgY production, were incubated in place of the fixed 100 µg/ml IgY.

2.2.14. Assays for inhibition of protease activity with *Tz*SPINK4

2.2.14.1 AMC standard curve

The relationship between the amount of fluorescence released from a hydrolysed substrate and concentration of AMC was quantified using an AMC standard curve. The AMC standard curve was constructed using AMC concentrations in a range of 5 – 10 000 nM (Fig. 2.7). Briefly, 50 µl of the standard concentrations were mixed with 50 µl of assay buffer [50 mM Tris-HCl buffer, 150 mM NaCl, 10 mM $CaCl_2$, pH 7.5] containing 5 mM dithiothreitol (DTT) and incubated at 37°C. The fluorescence (Ex360nm and Em460nm) was read using an Optima Spectrophotometer from BMG Labtech.

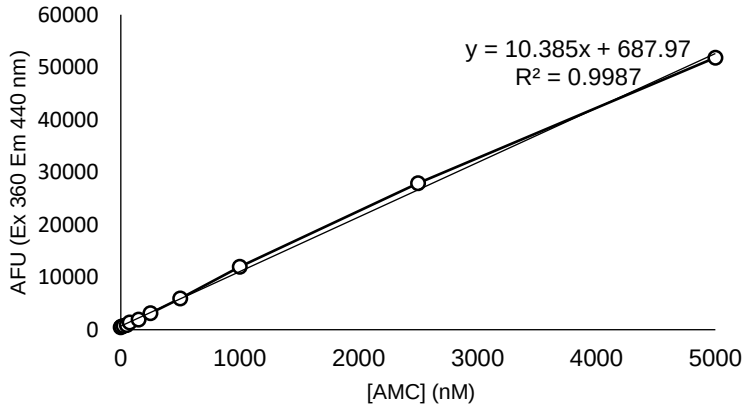

Figure 2.7: AMC standard curve showing fluorescence versus AMC concentration. AMC was diluted to various concentrations and incubated with MCA buffer at 37°C and fluorescence measured at Ex_{360nm} Em_{460nm}. The equation for the trendline is given by y = 10. 385x + 687.97.

2.2.14.2 Inhibition studies

The inhibitory activity of *Tz*SPINK4 against chymotrypsin, trypsin and thrombin was tested. Briefly, the enzymes, 1 µM trypsin, 1 µM chymotrypsin (diluted in 0.1% Brij 35) were incubated with 1, 5 and 10 µM *Tz*SPINK4 and assay buffer [50 mM Tris-HCl buffer, 150 mM CaCl, 10 mM $CaCl_2$, pH 8] and 1 U, 0.5 U, 0.025 U thrombin (diluted in 0.1% Brij 35) with 5 µM *Tz*SPINK4 and thrombin buffer [200 mM Tris-HCl buffer, 1.5 M NaCl, 25 mM $CaCl_2$, pH 8] containing 5 mM dithiothreitol (DTT) for 30 min at 37 °C for 30 min. Subsequently, 20 µM Z-Phe-Arg-AMC synthetic substrate was added. The fluorescence (Ex360nm and Em460nm) measured using the Optima Spectrophotometer from BMG Labtech.

2.3 Results

2.3.1 Total RNA extraction and amplification of *TzSPINK4* gene from *T. zimbabwensis* muscle larvae

Total RNA was extracted from *T. zimbabwensis* muscle larvae and utilised for the synthesis of cDNA. The synthesised cDNA along with gene specific primers were used for PCR for the amplification of the *TzSPINK4* gene. The total RNA was represented by two prominent bands which were approximately 1800 bp and 2000 bp in size (Fig. 2.8, panel A). The gene which encodes *T. zimbabwensis* SPINK4 was amplified at approximately 450 bp (Fig. 2.8, panel B).

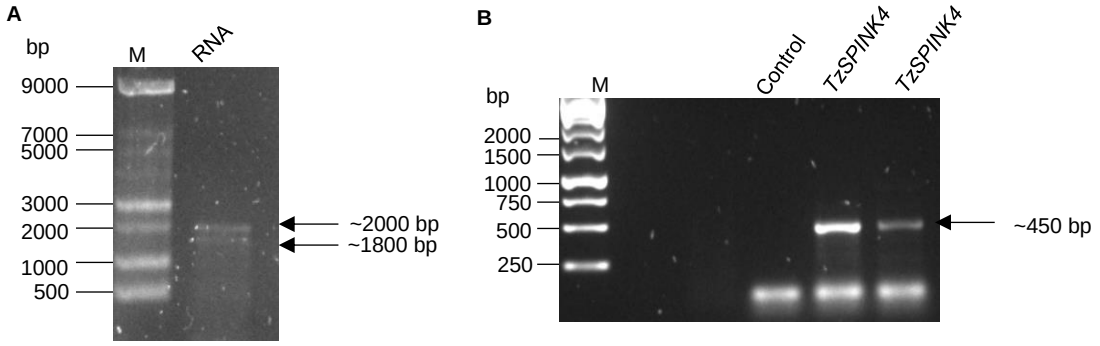

Figure 2.8: Agarose gel analysis of *Tz*SPINK4 gene amplification using cDNA synthesised from total RNA extracted from *T. zimbabwensis*. (A) Total RNA was extracted from the *T. zimbabwensis* muscle larvae and analysed on a 1% (w/v) agarose gel, M: ssRNA. **(B)** The *TzSPINK4* gene amplicon and non-template control were analysed on a 1% (w/v) agarose gel, M: O'Gene Ruler

2.3.2 Cloning of *TzSPINK4* gene amplicon into pGEM-T, pGEM-T easy cloning vectors.

The *TzSPINK4* gene amplicon was purified and ligated to the ~3000 bp pGEM-T, ~3015 bp pGEM-T easy cloning vectors. Blue-white colony screening was employed for the selection of the recombinant colonies. The plasmid DNA of the recombinant *TzSPINK4*-pGEM-T colonies (Fig. 2.9, panel A) and recombinant *Tz*SPINK-4-pGEM-T easy colonies (Fig. 2.9, panel B) was isolated and represented by three bands which correspond to the coiled, supercoiled and nicked conformations. The presence of the *TzSPINK4* gene insert was confirmed by colony PCR using M13 vector primers as well as the *TzSPINK4* gene primers. The amplification of the *TzSPINK4* gene insert in pGEM-T vector using the M13 vector primers produced amplicons with an approximate size of 650 bp in comparison to the pGEM-T easy amplicons with an approximate size of 550 bp (Fig. 2.9, panels C and D). The additional base pairs may be attributed to the amplification of vector DNA that flanks the gene. However, the pGEM-T easy vector that is 15 bp bigger than the pGEM-T vector was found to have amplicons with a size less than the pGEM-T vector.

Colony PCR performed using gene specific primers yielded an amplicon with a size of approximately 450 bp in pGEM-T and pGEM-T easy (Fig. 2.9, panels E and F). However, faint contaminating bands of higher molecular size are observed in both the vectors.

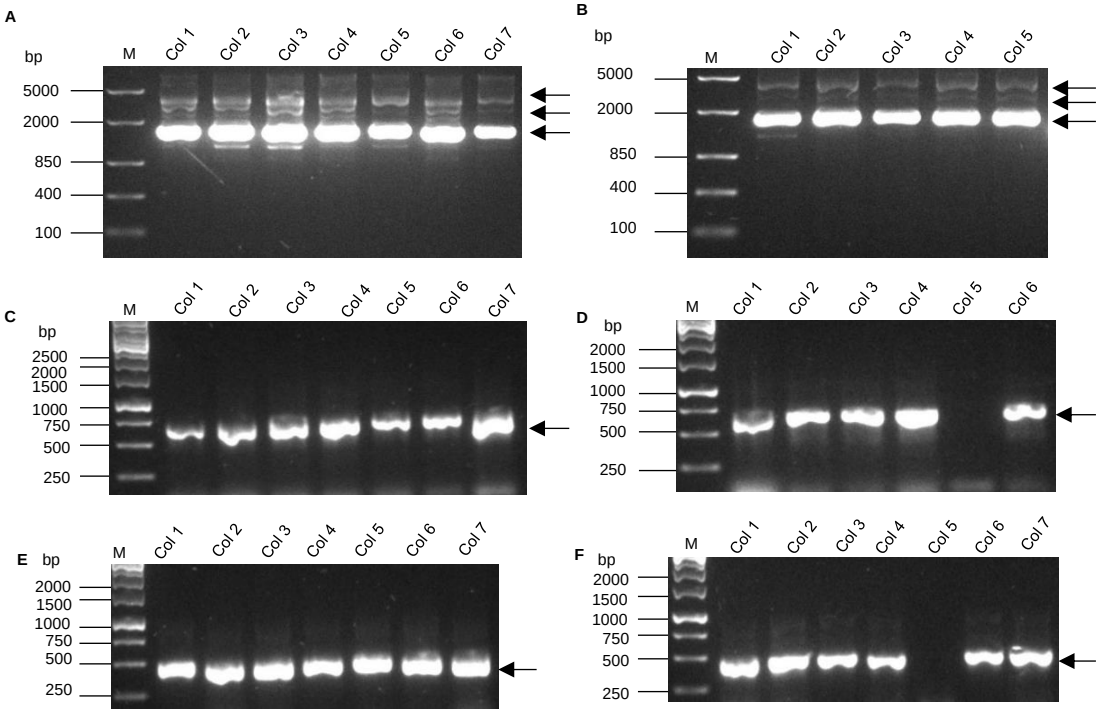

Figure 2.9: Screening of recombinant *Tz*SPINK4-pGEM-T and *Tz*SPINK4-pGEM-T easy colonies. The *TzSPINK4* gene amplicon was ligated to the respective cloning vectors and transformed into the *E. coli* JM109 cells. The plasmid DNA from the recombinant colonies was isolated from recombinant clones and electrophoresed on a 1% (w/v) agarose gel: **(A)** ***TzSPINK4*-pGEM-T colonies **(B)** *recombinant *TzSPINK4*-pGEM-T easy colonies, M: Fast Ruler midrange. Colony PCR was performed to confirm presence of gene insert in: **(C)** □*TzSPINK4*-pGEM-T colonies using M13 vector primers **(D)** □*TzSPINK4*-pGEM-T easy colonies using M13 primers. **(E)** □*TzSPINK4*-pGEM-T colonies using gene primers **(F)** □*TzSPINK4*-pGEM-T easy colonies using gene primers; M, O'Gene Ruler. The arrows in (A) and (B) represent the DNA conformations; (C) to (F): *Tz*SPINK4 colony PCR amplicons. The (*) represents amplicons and the (□) plasmid DNA.

2.3.3 Restriction digestion analysis of *TzSPINK4*-pGEM-T and *TzSPINK4*-pGEM-T easy colonies to confirm presence of *TzSPINK4* gene

The colony PCR, performed using gene specific primers, showed that the amplicons had an approximate molecular size of ~450 bp for both the vectors. To further confirm the presence and size of the gene to be used for subcloning, a small-scale restriction digestion was performed using the BamHI and XhoI restriction enzymes. The products of the double restriction digestion of *Tz*SPINK-4-pGEM-T included a digested ~3000 bp pGEM-T vector and an expected ~450 bp *TzSPINK4* gene insert (Fig. 2.10, panel A). The digestion of *Tz*SPINK-4-pGEM-T easy did not yield a ~450 bp *TzSPINK4* gene insert with the correct size (result not shown). The 450 bp *TzSPINK4* gene insert was extracted from the agarose gel, purified and used for subcloning into pET expression vectors (Fig. 2.10, panel B).

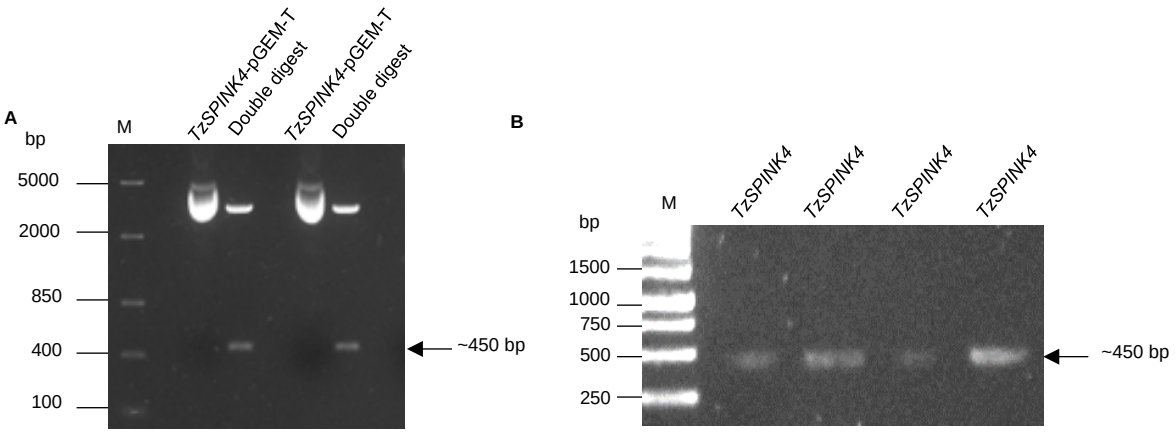

Figure 2.10: Analysis of the restriction digestion products of *Tz*SPINK4-pGEM-T by BamHI and XhoI restriction enzymes. **(A)** The *TzSPINK4*-pGEM-T plasmids were digested with BamHI (fwd) and XhoI (rev) restriction enzymes for 20 min at 37°C and a sample of digestion products electrophoresed on a 1% (w/v) agarose gel; M: Fast Ruler midrange. **(B)** A sample of the purified gel-extracted *TzSPINK4* gene insert electrophoresed on a 1% (w/v) agarose gel; M: O'Gene Ruler. The arrows represent the *Tz*SPINK4 gene insert

2.3.4 Subcloning of the *TzSPINK4* gene insert into pET-28a, pET-32a and pET-100 expression vectors

The purified *TzSPINK4* gene insert was ligated to pET28a, pET-32a and pET-100 expression vectors. The expression vectors were previously digested with BamHI and XhoI restriction enzymes prior to ligation (result not shown). The ligation mixtures were transformed into *E. coli* JM109 cells for storage and *E. coli* BL21 (DE3) cells for expression. The presence of the *TzSPINK4* gene insert in the recombinant colonies was ascertained by colony PCR. The ten recombinant *TzSPINK4*-pET-28a colonies had amplicons with an expected molecular size of ~450 bp (Fig. 2.11, panel A). The recombinant *TzSPINK4*-pET-32a amplicons from colonies 1,2,6,8 and 9 were of the size at ~450 bp. However, the amplicons from colonies 3,4,7,10,11,12 had a prominent band at 450 bp and faint bands at approximately 850 bp (Fig. 4, panel B). A single recombinant *TzSPINK4*-pET100 colony in *E. coli* BL21 (DE3) was shown to contain the gene *SPINK4* insert (Fig. 2.11, panel C).

2.3.5 Recombinant expression of *SPINK4* in the pET-28a, pET-32a and pET-100 expression vectors

The *TzSPINK4* gene from *T. zimbabwensis* encodes a protein that is 150 amino acids long with an expected molecular weight of ~16.6 kDa and a pI of 4.46 as predicted by Expasy server, a Bioinformatics Resource Portal. *Tz*SPINK was expressed by IPTG induction from three recombinant pET28a-*Tz*SPINK4 clones (Fig. 2.12, panel A). A protein band was detected at 21 kDa from clone 2 and 3 by the mouse anti-His monoclonal antibody (Fig. 2.12, panel B). This size corresponds to the expected size of His-tagged *Tz*SPINK4 protein.

The recombinant *Tz*SPINK4 clones from pET-28a and pET-32a construct were also expressed using autoinducing terrific broth medium. Following recombinant expression using the pET-32a expression vector, a protein band of 33 kDa, as well as other prominent high and low molecular weight protein bands, were observed. High and low molecular weight bands were also observed following expression using the pET-28a vector (Fig. 2.12, panel C). Recombinant expression of *Tz*SPINK4 from the pET-32a construct by IPTG induction showed that two prominent bands were obtained with molecular weights of approximately 35 kDa and 42 kDa (Fig. 2.12, panel D). There was no recombinant expression of *Tz*SPINK4 from the pET-100 construct.

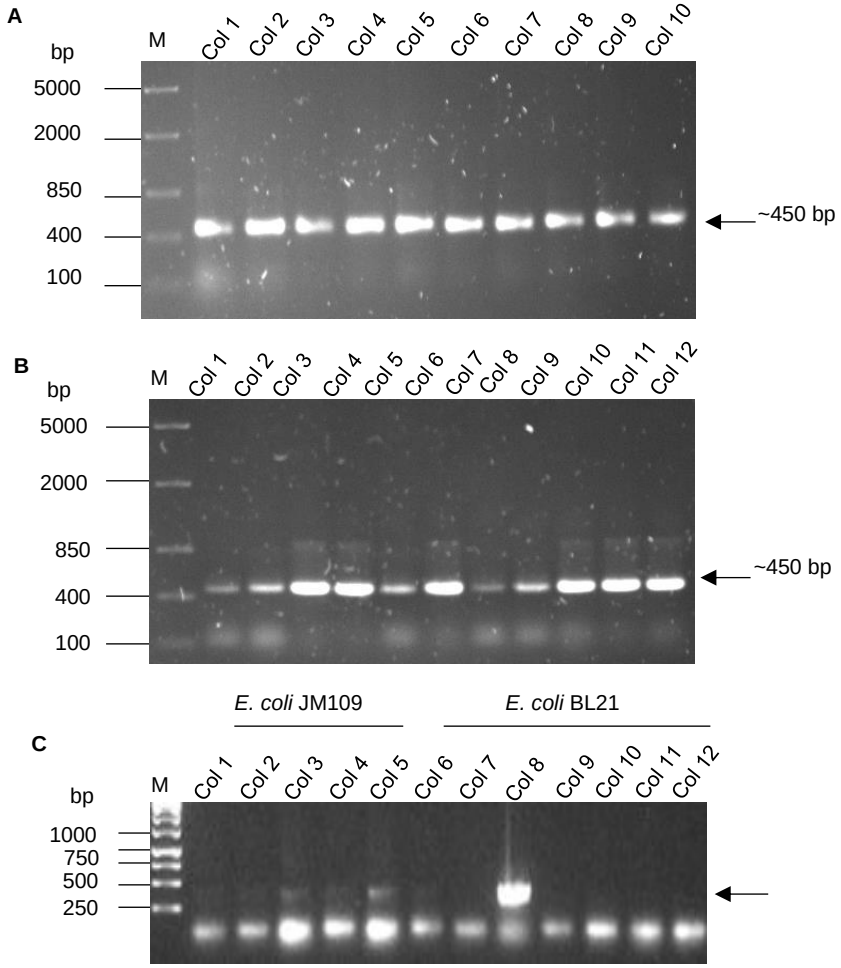

Figure 2.11: Screening of recombinant *Tz*SPINK4-pET-28a, *Tz*SPINK4-pET-32a and *Tz*SPINK4-pET-100 colonies by PCR amplification. The TzSPINK4 gene was ligated to the pET-28a, pET-32a and pET100 expression vectors transformed into *E. coli* cells. Colony PCR was performed on the: **(A)** TzSPINK4-pET-28a colonies. **(B)** TzSPINK4-pET-32a; M: Fast Ruler midrange. **(C)** TzSPINK4-pET-100; M: O'Gene Ruler. The amplicons were electrophoresed on a 1% (w/v) agarose gel**.**

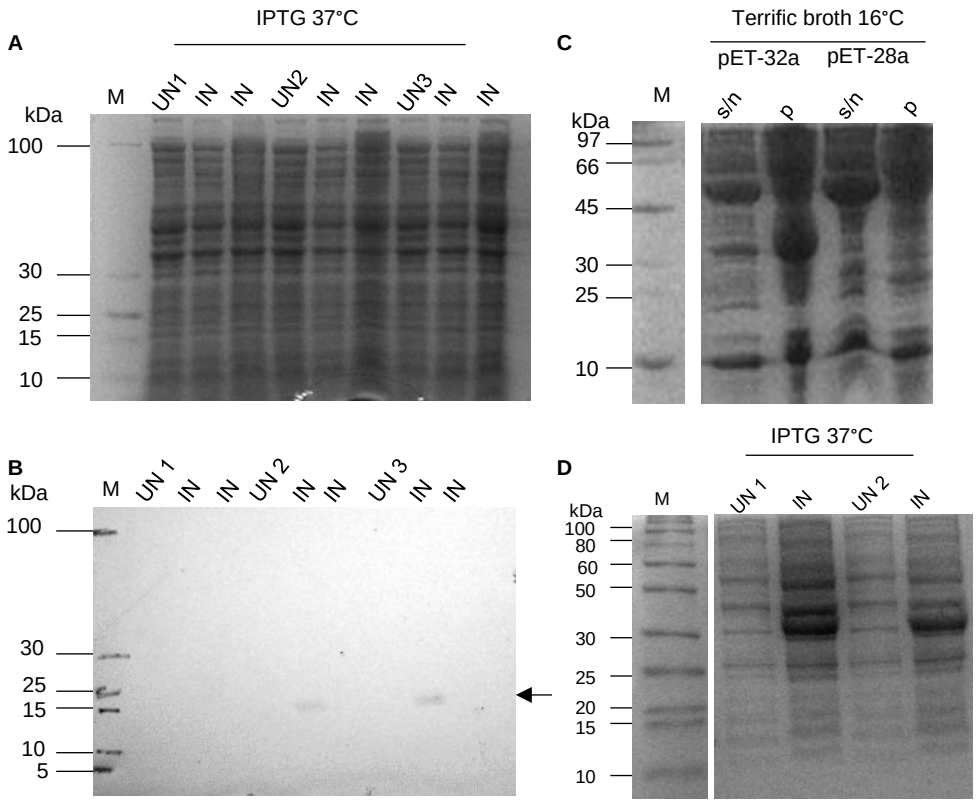

Figure 2.12: Analysis of *T. zimbabwensis* SPINK4 expression from the pET-28a and pET-32a constructs by IPTG induction and auto induction. **(A)** The induced and uninduced samples from recombinant expression of colonies 1-3 from the pET-28a construct in E. coli BL21 (DE3) cells were electrophoresed on a 10% Tris-Tricine SDS-PAGE gel. **(B)** The electrophoresed proteins were transferred onto nitrocellulose and probed with a primary mouse anti-His monoclonal antibody and goat anti-mouse IgG HRPO as a secondary antibody. **(C)** The auto induced expression supernatant and pellet following expression using the pET-28a and pET-32a were electrophoresed on a 10% Tris-Tricine gel. **(D)** Following expression of TzSPINK4 from the pET-32a construct by IPTG induction, the uninduced and induced samples from colony 1 and 2 were electrophoresed on a 10% Tris-tricine SDS-PAGE gel.

2.3.6 Purification of *Tz*SPINK4 by nickel affinity chromatography

The recombinantly expressed *Tz*SPINK4 was purified from the pool of proteins due to the high binding affinity of the histidine fusion protein to the immobilised nickel. A prominent band of ~20 kDa along with two contaminating bands of high molecular weight were eluted from the column in the experiment with the expression lysates containing the pET-28a vector (Fig. 2.13, panel A). The 20 kDa protein band represented the expected size because of the protein size is ~16.6 kDa and an added 4 kDa results from the presence of the His-tag. This purified protein was used for subsequent experiments. A protein with a molecular weight of approximately 38 kDa was eluted from the experiment with the expression lysates containing the pET-32a vector, which is slightly higher than the expected 36 kDa size. (Fig. 2.13, panel B). A higher protein yield was obtained from purification using expression lysates containing the pET-28a vector in comparison to the those containing the pET-32a vector (Fig. 2.13).

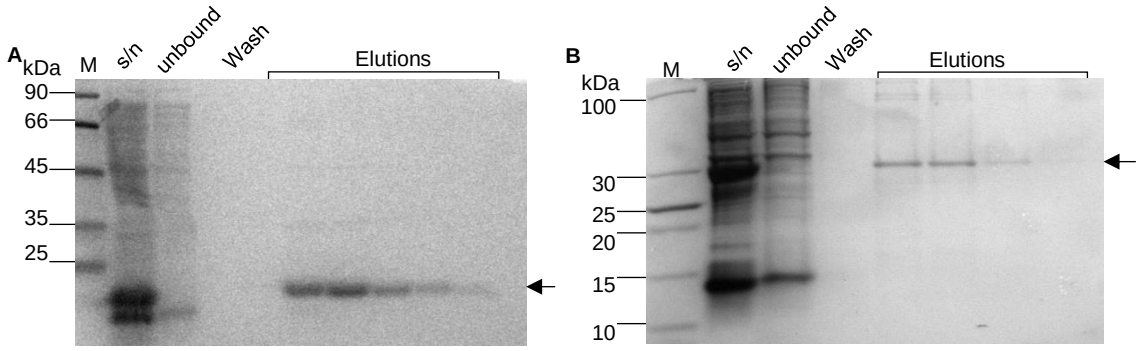

Figure 2.13: Purification of recombinant *Tz*SPINK4 by nickel affinity chromatography. Samples from the **(A)** elution profile of *Tz*SPINK4 expressed in pET-28a and from the **(B)** elution profile- of *Tz*SPINK4 expressed in pET-32a analysed on a 10% reducing Tris-tricine SDS-PAGE gel. The arrows represent the *Tz*SPINK4 protein.

2.3.7 Production of chicken anti-*Tz*SPINK4 antibodies

The purified His-tagged *Tz*SPINK4 was used to immunise two chickens for the purpose of antibody production against the protein. An ELISA was performed to analyse antibody production over the immunisation period. The production of antibodies by chicken 1 was found to peak at week 4 and similar levels of antibody was maintained over the remainder of the 16-week period while the antibody production by chicken 2 peaked at week 4 and similar levels of antibody observed till week 11 where a decrease in levels of antibody was shown. (Fig. 2.14, panel A). A checkerboard ELISA was performed and showed increasing concentrations of antibody produced higher signals and that a concentration of 1 µg/ml was enough for the detection of the recombinant protein in a western blot (Fig. 2.14, panels B and C).

The chicken anti-*Tz*SPINK4 IgY antibodies were used to confirm recombinant expression. Recombinant expression of *Tz*SPINK4 from the pET-32a construct by IPTG induction showed that two prominent bands were obtained with molecular weights of approximately 35 kDa and 42 kDa (Fig. 2.15, panel A). These protein bands were detected by both the mouse anti-His antibody and the chicken anti *Tz*SPINK4 (Fig. 2.15, panels B and C). The expected size of with the pET-32a fusion tags was ~36.5 kDa.

2.3.8 Inhibition of serine protease activity with *Tz*SPINK4

The inhibitory activity of *Tz*SPINK4 with serine proteases such as trypsin, chymotrypsin and thrombin was assessed. The *Tz*SPINK4 protein showed no inhibitory activity against 1 µM trypsin, 1 µM chymotrypsin and 0.025 U, 0.5 and 1 U of thrombin (result not shown).

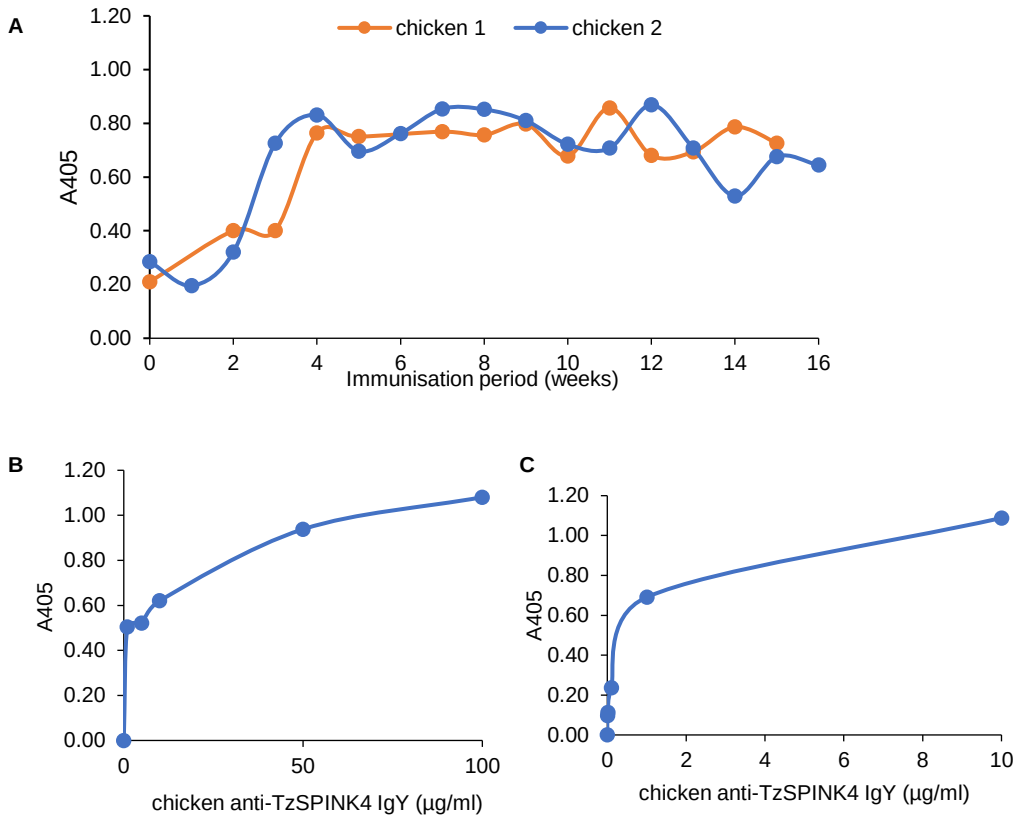

Figure 2.14: ELISA of chicken anti-*Tz*SPINK IgY antibodies. The ELISA plates were coated with 1 µg/ml of purified recombinant *Tz*SPINK4 and detected by chicken anti- TzSPINK4 IgY as a primary antibody and rabbit anti-chicken IgY- HRPO conjugate as a secondary antibody using the ABTS·H_2O_2 detection system. **(A)** Analysis of the production of antibodies against TzSPINK4 over a16 week ELISA. **(B)** and **(C)** checkerboard ELISA to determine the lowest antibody concentration that is able to produce an adequate signal. The absorbance readings at 405 nm are averages of duplicate experiments.

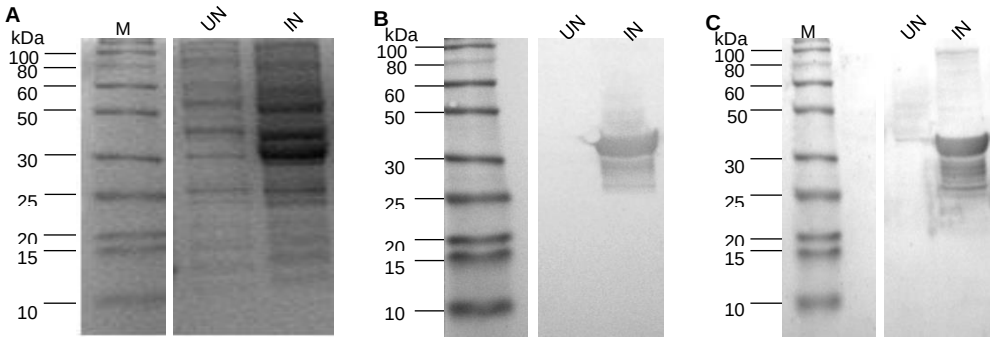

Figure 2.15: Detection recombinant TzSPINK4 using chicken anti-*Tz*SPINK4 antibodies. (A). The induced and uninduced samples from recombinant expression of *Tz*SPINK4 from the pET-32a construct in *E. coli* BL21 (DE3) cells were electrophoresed on a 10% Tris-Tricine SDS-PAGE gel. The electrophoresed proteins transferred onto nitrocellulose and probed with **(B)** a primary mouse anti-His monoclonal antibody and goat anti-mouse IgG HRPO as a secondary antibody as well as **(C)** chicken anti-*Tz*SPINK4 and rabbit anti-chicken IgY HRPO as a secondary antibody. UN, uninduced; IN, induced.

.

2.4 Discussion

In this study, the gene encoding the serine protease inhibitor, SPINK4 was amplified from *T. zimbabwensis* muscle larvae. The amplified *TzSPINK4* gene was cloned and the *Tz*SPINK4 protein recombinantly expressed in *E. coli* BL21 cells. The recombinant *Tz*SPINK4 protein was affinity purified and used to produce antibodies in chickens, which were used to confirm recombinant expression. The interaction of purified *Tz*SPINK4 with serine proteases was assessed. The 450 bp *TzSPINK4* gene was amplified by PCR using the synthesised cDNA as a template.The amplified *TzSPINK4* gene was cloned. The *Tz*SPINK4 was recombinantly expressed as a 20 kDa His-tagged protein and as a 38 kDa fusion protein which were purified by nickel affinity chromatography. Antibodies against the 20 kDa *Tz*SPINK4 were raised and the protein shown to have no inhibitory activity against trypsin, chymotrypsin and thrombin.

Trichinella infected rat muscle provided a source of parasites from which total RNA was isolated that was reverse transcribed into cDNA. This cDNA was used for the amplification of the 450 bp *TzSPINK4* gene, which was cloned into pGEM-T and pGEM-T easy cloning vectors. Similarly, the genes of two Kazal-type inhibitors from the gastrointestinal nematode, *N. vitripennis,* 65 amino acid *N. vitripennis* Kazal-type serine protease inhibitors-1 (*NvKSPI-1)* and 87 amino acid *NvKSPI -2* were amplified using cDNA reverse transcribed from total RNA isolated from *N. vitripennis* tissue*.* These genes were cloned into the pGEM-T easy vectors (Qian *et al.*, 2015). In a further study the *SPINK9* gene, which encodes the LEKTI-2 protein, was obtained by rapid amplification of cDNA ends (RACE) performed on total RNA isolated from human skin samples using gene specific sense and antisense primers. Subsequently, the *SPINK9* cDNA was cloned into the pGEM-T vector (Meyer-Hoffert *et al.*, 2009)

The *TzSPINK4* gene was subcloned into the pET-100, an expression vector which adds an N-terminal His-tag; pET-28a, a bacterial expression vector which adds a N and C-terminal His-tag, thrombin cleavage site and T7 epitope as well as the pET-32a vector which adds a 109 amino acid thioredoxin tag, N-terminal and C-terminal His-tags, S-tag, thrombin and enterokinase cleavage tags (Fig. 2.5). No expression was obtained from the pET-100 construct. The Expasy server predicted that the *Tz*SPINK4 sequence would translate into a ~16.6 kDa protein. Analysis of expression and purification by nickel affinity chromatography showed *Tz*SPINK4 to have an apparent molecular weight of ~21 kDa and ~38 kDa using the pET-28 and PET-32a vectors respectively. The size differences between the expected size of 16.6 kDa and the sizes obtained following expression from the pET-28a and pET-32a constructs was attributed to the presence of fusion tags. The ~21 kDa *Tz*SPINK4 was used for antibody production in chickens. Chicken anti-*Tz*SPINK4 antibody production was highest

at week 4 and between weeks 6 to 8. The antibodies were able to detect recombinant *Tz*SPINK4 on a western blot.

The purified *Nv*KSPI-1 and *Nv*KSPI-2 proteins containing the GST fusion protein from recombinant expression in the pGEX construct were found to have molecular sizes of 33 kDa and 36 kDa respectively (Qian *et al.*, 2015). The 7 kDa Lymphoepithelial Kazal-type-related inhibitor (LEKTI) 2 protein , encoded by SPINK5, was used to produce polyclonal antibodies in goats that were affinity purified and used for immunohistochemical studies and protein detection on western blots (Meyer-Hoffert *et al.*, 2009). The immunohistochemical studies showed the LEKTI-2 protein to be localised in the stratum granulosum and stratum corneum of human skin (Meyer-Hoffert *et al.*, 2009).

The purified *Tz*SPINK4 had no inhibitory activity against serine proteases such as trypsin, chymotrypsin and thrombin. Similarly, although the LEKTI-2 protein encoded by the *SPINK9* gene inhibited kallikrein 5, it showed no inhibitory activity against bovine trypsin, cathepsin G, chymotrypsin, human elastase, thrombin, matriptase and plasmin (Meyer-Hoffert *et al.*, 2009). LEKTI domains, encoded by the *SPINK5* gene showed inhibition against trypsin, subtilisin A, cathepsin G, human elastase and kallikreins 5, 7 and 14 (Mitsudo *et al.*, 2003). The *Nv*KSPI-1, was shown to inhibit trypsin and the *Nv*KSPI-2 shown to inhibit the activation of insect prophenoloxidase which is an innate immune protein (Qian *et al.*, 2015). Purified recombinant SPINK6 inhibited kallikreins 5, 7, 8 and14 but showed no inhibitory activity against bovine trypsin, cathepsin G, chymase, human chymotrypsin, human leukocyte elastase, human plasmin, human thrombin and matriptase (Meyer-Hoffert *et al.*, 2010).

The *N. vitripennis* eggs are laid in the host along with venom, which contains *Nv*KSPIs, to ensure the development of their offspring by inhibiting the host immune responses (Qian *et al.*, 2015). The human kallikreins, among other functions, have roles in the activation of protein-activated receptors (PARs), that mediate inflammation (Sotiropoulou *et al.*, 2009). The PARs have been shown to be expressed by cells that have roles in the immune response and inflammation and regulate the secretion of inflammatory mediators such as TNF-α (Steinhoff *et al.*, 2004). Future studies include assessing the inhibitory activity of *Tz*SPINK4 on cathepsin G, human leukocyte elastase and the kallikreins.

A further objective of this study was to identify a cysteine protease inhibitor in *T. zimbabwensis.* In the next chapter results are presented on the identification, recombinant expression and characterisation of *Tz*cystatin B, a cysteine protease inhibitor from the larval stage of *T. zimbabwensis*.

Chapter 3: Cloning and expression of recombinant *Tz*cystatin B from *Trichinella zimbabwensis* muscle larvae

3.1 Introduction

The most abundant protease inhibitors within parasites are the cysteine protease inhibitors or cystatins and serine protease inhibitors, or serpins (Hewitson *et al.*, 2009). Cystatins, have been found in the phyla Nematoda, Platyhelminthes and Arthropoda amongst others (Klotz *et al.*, 2011). The isolation and recombinant expression of these cystatins in non-encapsulating species of *Trichinella* such as *T. zimbabwensis* has not yet been reported. However, the recombinant expression of an antigenic 45.9 kDa cystatin-like protein in *T. spiralis* (r*Ts*CLP), an encapsulating species of *Trichinella*, has been reported (Tang *et al.*, 2015). The *TsCLP* gene was amplified from cDNA that had been reverse transcribed from mRNA isolated from infective larvae; subcloned in the pET-28a expression vector and expressed in *E. coli*. Following expression, the r*Ts*CLP was used to raise antibodies in rabbits which were shown to induce protective immunity in mice (Tang *et al.*, 2015). The expression and characterisation of cystatins and cystatin-like protease inhibitors from homologous gastrointestinal nematodes such as *Heligmosoides polygrus, Nippostrongylus brasiliensis, Haemonchus contortus*, *Acanthocheilonema viteae* and parasitic filarial nematode *Onchocerca volvulus* has been reported (Hewitson *et al.*, 2009).

The role of the *H. polygrus* cystatin as immunomodulator in mice was studied. The *HpCystatin* gene was amplified from cDNA reverse transcribed from RNA isolated from adult worms. The amplified gene was subcloned into pET-32a containing a His-tag and Tobacco Etch virus (TEV) recognition site. The 16 kDa r*Hp*Cystatin was affinity purified, used to raise monoclonal antibodies in mice, and characterised following cleavage of the His tag using the TEV protease. However, the monoclonal antibodies produced against r*Hp*Cystatin recognised a slightly smaller 14 kDa protein from the excretory-secretory products. The r*Hp*Cystatin was found to inhibit cathepsins B, C, L and S (Sun *et al.*, 2013). Similarly, Nippostatin, a 14 kDa type 2 cystatin from *N. brasilienses,* which primarily infects rats, was amplified from cDNA reverse transcribed from RNA isolated from adult worms. The amplicon was cloned into pGEM-T Easy and subcloned into pET (the author did not specify which pET vector was used) containing a His-tag and leader sequence of the influenza virus hemagglutinin epitope and expressed in *E. coli*, affinity purified and used for antibody production in mice (Dainichi *et al.*, 2001).

The purified rNippostatin was found to inhibit mammalian cathepsins L and B (Dainichi *et al.*, 2001; Hartmann and Lucius, 2003). The *H. corticus* cystatin gene was amplified, cloned into pMD19-T vector and expressed using pET-32a in the *E. coli* host. The affinity purified 35 kDa

r*Hc*Cystatin that would contain a 12 kDa thioredoxin fusion tag was tested for inhibitory activity and an expressed empty pET-32a was used as a control (Wang *et al.*, 2017b; Terpe, 2003). The r*Hc*Cystatin effectively inhibited papain and human cathepsin L, reduced the activity of human cathepsin B and failed to inhibit human caspase 1 (Wang *et al.*, 2017b). Polyclonal antibodies against r*Hc*Cystatin were produced in mice which were used for immunohistochemical localisation studies of native *Hc*Cystatin (Wang *et al.*, 2017b).

The *A. viteae* cystatin and the homologous *O. volvulus* cystatin have been found to be more similar to the type 3 cystatins. The 17 kDa cystatin C from the filarial parasite *A. viteae* was cloned and recombinantly expressed with glutathionES-transferase (GST) and maltose binding protein (MBP) fusion tags. When the inhibitory activity was tested, the r*Av*cystatin without a fusion tag was found to be more active against papain in comparison to the r*Av*Cystatin containing the MBP and GST fusion tags. In addition, r*Av*Cystatin was found to inhibit the proliferation of thymocytes in mice (Hartmann *et al.*, 1997).

Cystatins from parasitic nematodes have been expressed in pET expression systems such a pET-32a and pET-28a. The inhibitory studies of r*Av*Cystatin against papain showed that the presence of large fusion proteins such as the 26 kDa GST tag and 42 kDa MBP tag reduced inhibitory activity. As a result, pET expression systems containing smaller sized fusion tags are recommended because of the minimal effect they have on protein structure and activity (Jia and Jeon, 2016). To illustrate, specialised pET expression systems containing a single protease cleavage recognition site and His-tag have been utilised for expression for r*Hp*Cystatin. Alternatively, the more economical pET-28a expression system which contains smaller fusion tags including the N- and C-terminal His-tags, a N-terminal T7 tag and thrombin recognition site may be used as an expression system.

In order to study *Tz*cystatin B from *T. zimbabwensis*, the sequence of the *Tzcystatin B* gene was obtained from NCBI Genbank (https://www.ncbi.nlm.nih.gov/genbank/) and aligned with the sequences of *Tzcystatin B* from species within the same genus and homologous species. The alignment showed that the sequences of the 11 kDa Tzcystatin B from *T. zimbabwensis* was 87.63% identical to the 33 kDa cystatin from *T. spiralis* (Fig. 3.1). The two cystatin sequences along with the sequences from other helminths contained the conserved QxVxG motif found in the L1 loop of cystatins. The sequence similarity of the 11 kDa *T. zimbabwensis* cystatin to 17 kDa *A. viteae* was 25.27%, 16 kDa *O. volvulus* 23.08%, 16 kDa *H. polygrus* 22.68%, 14 kDa *H. contortus* 22.22% and 14 kDa *N. brasiliensis* 21.65% (Fig. 3.1).

Figure 3.1: A comparison of the cystatin sequences from nematode species. Multiple sequence alignment generated through Clustal omega. Cystatin sequences from *Trichinella zimbabwensis* (KRZ08317.1), *Trichinella spiralis* (XP_003379766.1), *Acanthocheilonema viteae* (AAA87228.1), *Haemonchus contortus* (AAB95324.1) and *Nippostrongylus brasiliensis* (BAB59011.1) were obtained from NCBI Genbank (https://www.ncbi.nlm.nih.gov/genbank/). The symbols shown represent: conserved residues, (*); residues with similar properties, (:); residues with weakly similar properies, (.). The *Heligmosoides polygrus* and *Onchocerca volvulus* cystatin sequences were obtained from Sun *et al.* (2013).

In the present study, the gene encoding cystatin B was amplified from cDNA synthesised from total RNA isolated from *T. zimbabwensis* muscle larvae. The amplified gene was cloned and recombinantly expressed in *E. coli*. The recombinant protein was purified, the interaction with cysteine proteases evaluated and antibodies produced in chickens for the detection of recombinant protein, localisation of the inhibitors in parasite extracts and ELISA.

3.2 Materials and methods

3.2.1. Primer design for *Tzcystatin B* amplification

The 450 bp *T. zimbabwensis Tzcystatin B* DNA coding sequence (Genbank accession number: KRZ08317.1) was used to design primers (Table 3.1) for the amplification of the gene by PCR. The *Tzcystatin B* coding nucleotide sequence was obtained, and primers designed using a method described in Section 2.2.5. An EcoRI restriction site was introduced in the forward primer, while a XhoHI restriction site was introduced in the reverse primer. The primers were synthesised by Inqaba Biotechnical Industries (Pretoria, RSA).

Table 3.1: *Tzcystatin B* gene primer nucleotide sequences used for PCR

Primer name	Nucleotide sequence 5' – 3'	Annealing temp.
*Tz*CysB Fwd	AAGAATTC ATG AGT AAC ATA TGC GGA GGT GT	51.7°C
*Tz*CysB Rev	AACTCGAG CTA AAA ATA TTC GAG CTT ATC AGA ATG TTT TTT ACC A	

Sequences underlined represent the restriction sites for EcoRI in the forward and for XhoI in the reverse primer.

3.2.2 Polymerase chain reaction (PCR) for amplification of Tzcystatin B

For amplification of the *Tzcystatin B* gene the following master mix was prepared: 0.25 U TaKaRa Ex Taq HS, 1 x Ex Taq buffer (containing Mg^{2+}), 2.5 mM dNTP, 0.5 µM of each gene primer, 0.5 - 1 µM DNA in a final reaction volume of 50 µl. PCR conditions were as follows: initial denaturation of DNA was performed 95°C for 3 min; then 34 cycles of denaturation at 95°C for 30 s, annealing at 51.7°C for 30 s, DNA extension at 72°C for 1 min, final extension at 72°C for 5 min and incubated at 4°C in the Bio-Rad T100 thermocycler. A sample of the PCR product was analysed by agarose gel electrophoresis (Section 2.2.7) and the remainder purified and concentrated using the DNA Clean and Concentrator™-5 kit (Zymo Research) according to the manufacturer's instructions.

3.2.3 Cloning of *Tzcystatin B* into pGEM-T and pMD19-T vectors

3.2.3.1 Ligation of the *Tzcystatin B* insert into pGEM-T and pMD19-T (simple) vector

The purified PCR product was ligated to a cloning vector (50 ng) using a 3:1 molar ratio of insert to vector as calculated using the NEB ligation calculator (https://nebiocalculator.neb.com/#!/ligation). The purified 290 bp *Tzcystatin B* PCR product was ligated to pGEM-T and pMD19-T cloning vectors incubated with 1 x rapid ligation buffer and 1 U of T4 DNA ligase (Fig. 3.2). Incubation conditions were optimised by incubating

ligation mixtures at different temperatures: 1 h at RT then 4°C for 16 h; 1 h at 16°C then RT for 16 h; 16 h at 16°C; 16 h at 4°C and 16 h at RT.

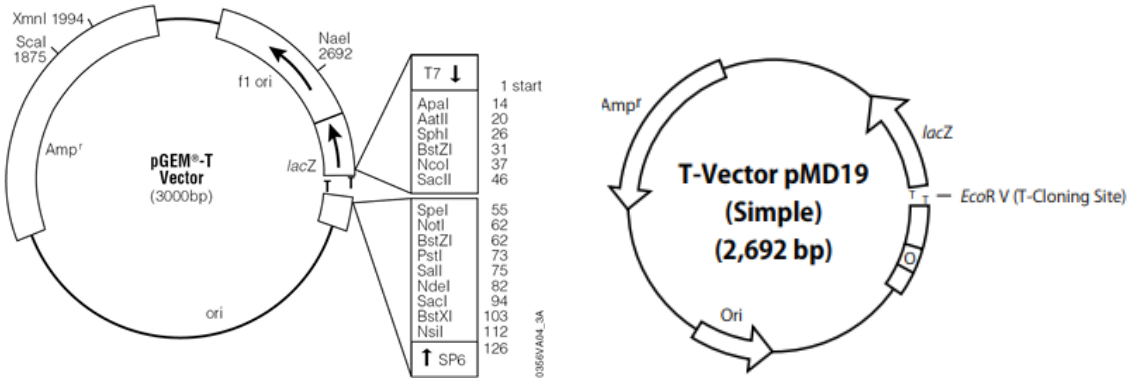

Figure 3.2: pGEM-T and pMD19-T (simple) cloning vector maps illustrating their multiple cloning sites and antibiotic resistance. T vectors utilise thymine adenine (TA) cloning where DNA strands hybridise and ligate due to the presence of 3' thymine overhangs.

3.2.3.2 Transformation of *Tzcystatin B*-pGEM-T and *Tzcystatin B*-pMD-19 (simple) T vector into *E. coli* JM109 cells

The *Tzcystatin B* gene amplicon-cloning vector ligation mixture was transformed into competent *E. coli* JM109 cells as described in Section 2.2.8.3. The transformation mixtures were plated on 2 x YT bacteriological agar plates [1.6 % (w/v) tryptone, 1% (w/v) yeast extract, 0.5 % (w/v) NaCl, 1% (w/v) bacteriological agar containing 50 µg/ml ampicillin, 20 µg/ml X-gal, 10 µg/ml IPTG] and incubated at 37°C for 16 h. The recombinant *Tzcystatin B*-pGEM-T and *Tzcystatin B*-pMD-19T colonies were selected by Blue-white colony screening.

3.2.3.3 Plasmid miniprep and restriction digestion of plasmid DNA from recombinant *Tzcystatin B*-pGEM-T and *Tzcystatin B*-pMD-19 colonies

The presence of the *Tzcystatin B* gene insert in the recombinant colonies selected by Blue-white colony screening was confirmed by colony PCR as outlined in Section 2.2.8.5. The vector primers utilised for the pGEM-T vector were the M13 forward and reverse primers as well as the SP6 forward and T7 reverse primers while for the pMD-19T vector were the M13 forward and reverse primers shown in Table 3.2. The plasmid DNA of the recombinant clones was sequenced at the Central Analytical facility (CAF), Stellenbosch University. The plasmid DNA was isolated from the recombinant *Tzcystatin B*-pGEM-T and *Tzcystatin B*-pMD-19 colonies by miniprep as outlined in Section 2.2.8.6 and restriction digested using the EcoRI and XhoI restriction enzymes. Briefly, 1000 ng of isolated plasmid DNA from the recombinant colonies was digested with EcoRI (1 µl) and XhoI (1 µl) restriction enzymes in the presence of 1 x fast digestion buffer in a final reaction volume of 20 µl. The digestion mixture was incubated at 37°C for 20 min. The restriction digestion products were analysed by agarose gel electrophoreses as outlined in Section 2.2.7. The 291 bp *Tzcystatin B* gene insert was excised

from the 1% agarose gel using the Zymogen DNA gel extraction kit as per the manufacturer's instructions.

Table 3.2: Vector primer nucleotide sequences used for PCR

Primer name	Nucleotide sequence (5' – 3')	Annealing temp.
M13 Fwd	GTT TTC CCA GTC ACG AC	42.8°C
M13 Rev	CAG GAA ACA GCT ATG AC	43.2°C
T7 terminator	CTA GTT ATT GCT CAG CGG TG	
SP6 promoter	ATT TAG GTG ACA CTA TAG	

3.2.4 Subcloning of *Tz*cystatin B into pET-28a and pET-32a expression vectors

The pET-28a and pET-32a bacterial expression vectors were restriction digested as described in Section 2.2.8.7. The restriction digested pET-28a, pET-32a (50 ng) expression vectors were ligated to the restriction digested *Tzcystatin B* in a 3:1 molar ratio of insert to expression vector as determined by the NEB ligation calculator in the presence of 1 x rapid ligation buffer and 1 U T4 DNA ligase at 16°C for 16 h. This ligation mixture was transformed into *E. coli* JM109 cells and *E. coli* BL21 (DE3) cells as per Section 2.2.8.3. The *Tz*cystatin B-pET-28a and *Tz*cystatin B-pET-32a transformation mixtures (100 µl) were plated onto 2 x YT plates containing kanamycin (34 µg/ml) for pET-28a and ampicillin (50 µg/ml) for pET-32a. Recombinant colonies were selected at random and the presence of the *Tzcystatin B* insert at the expected size was ascertained. Each colony was dispersed in 10 µl distilled water. This mixture (2 µl) was used to inoculate 5 ml 2 x YT broth containing kanamycin (34 µg/ml) and ampicillin (50 µg/ml) respectively and incubated at 37°C for 16h with agitation. The presence of the insert was confirmed by colony PCR and restriction digestion of plasmid DNA by miniprep as described in Section 2.2.8.6.

3.2.5 Recombinant expression of *Tz*cystatin B in *E. coli*

3.2.5.1 Recombinant expression by IPTG induction

The 290 bp *cystatin B* gene from *T. zimbabwensis* codes for a protein of 97 amino acids with an expected molecular weight of ~11 kDa. A single recombinant *Tz*cystatin B-pET-32a colony was used to inoculate 2 x YT liquid medium (5 ml) containing ampicillin (50 µg/ml) while a single recombinant *Tzcystatin B*-pET28a colony was used to inoculate 2 x YT liquid medium (5 ml) containing kanamycin (34 µg/ml). Recombinant expression was performed as described in Section 2.2.10.1. The IPTG concentration for induction of expression and temperature at which expression was carried out and induced was optimised using 0.1, 0.3 and 1 mM IPTG

concentrations, and expression conducted for 4 h at 37°C and 24 h at 16°C. No significant difference in expression was observed thus induction was maintained at 37°C for 4h. The recombinant expression was analysed by SDS-PAGE as described in Section 2.2.11

3.2.5.2 Recombinant expression by auto induction

Recombinant expression of *Tz*cystatin B from pET-28a, pET-32a expression vectors was performed in the *E. coli* BL21 (DE3) using a method described in Section 2.2.10.2. The temperature at which expression was performed was optimised by incubation at 37°C for 16 h, 24 h and 48 h and at 16 °C for 16 h, 24 h and 48 h. Optimal expression was observed at 37 °C for 16 h. Recombinant expression was analysed by SDS-PAGE as outlined in Section 2.2.11.

3.2.6 Purification of His-tagged *Tz*cystatin B expressed from pET-32a and pET-28a vectors by nickel immobilised metal-ion affinity chromatography (IMAC)

Recombinant *Tz*cystatin B expressed from the pET-28a and pET-32a vectors carries a His-tag which enabled purification using a nickel-nitrilotriacetic acid (Ni-NTA) agarose column. Recombinant *Tz*cystatin B, expressed from pET-28a and pET-32a, was purified using nickel affinity chromatography as described in Section 2.2.12. The unbound, wash and elution fractions were electrophoresed on a 10% Tris-tricine SDS-PAGE gel, (Section 2.2.11).

3.2.7 On and off-column cleavage of fusion tags from *Tz*cystatin B expressed from the pET-32a vector using thrombin and enterokinase

3.2.7.1 On column cleavage of *Tz*cystatin B fusion tags by thrombin and enterokinase

The Ni-NTA affinity column was equilibrated and *Tz*cystatin B-containing sample loaded, the unbound fraction collected and the column washed as described in Section 2.2.12. Subsequently, the column was equilibrated with either 20 ml thrombin cleavage buffer [20 mM Tris-HCl buffer containing 150 mM NaCl, 2.5 mM $CaCl_2$, pH 8] and mixed with 800 µl thrombin cleavage buffer containing thrombin (1 U) or 20 ml enterokinase cleavage buffer [20 mM Tris-HCl buffer containing 50 mM NaCl, 2 mM $CaCl_2$, pH 8] and mixed with 800 µl enterokinase cleavage buffer containing enterokinase (2 U). The resin was mixed with thrombin or enterokinase using an end-over-end rotor at 4°C for 16 h. The cleaved *Tz*cystatin B protein was collected in 1 ml fractions using 9 ml of thrombin or enterokinase cleavage buffer. The bound His-tag and uncleaved *Tz*cystatin B were eluted with elution buffer. The column was regenerated as described in Section 2.2.12. The collected fractions were electrophoresed on a 10% Tris-tricine SDS-PAGE gel (Section 2.2.11.1) and a duplicate gel used for a western blot (Section 2.2.11.2).

3.2.7.2 Off-column cleavage of fusion tags from *Tz*cystatin B expressed in pET-32a by thrombin and enterokinase

The *Tz*cystatin B purification fractions were buffer exchanged into thrombin or enterokinase cleavage buffer using a 5 ml HiTrap desalting column according to the manufacturer's instructions. The off-column cleavage reactions by thrombin and enterokinase were carried out using microfuge tubes containing 25 µg *Tz*cystatin B in respective cleavage buffer, 10 x thrombin reaction buffer [200 mM Tris-HCl buffer, 1.5 M NaCl, 25 mM $CaCl_2$, pH 8] or 10 x enterokinase reaction buffer [200 mM Tris-HCl buffer, 0.5 M NaCl, 20 mM $CaCl_2$, pH 8] and 1 U of thrombin or enterokinase made up to a final volume of 20 µl or 50 µl using distilled water. The thrombin and enterokinase cleavage reactions were incubated at 25°C for 16 h. The products of the cleavage were analysed on a 10% Tris-tricine reducing SDS-PAGE gel and western blot (Section 2.2.11).

3.2.8 Expression and purification of *Tco*CATL and *Tvi*CATL

The gene coding for *Tco*CATL (catalytic domain of cathepsin L-like protease from *T. congolense*) was previously cloned into the pPIC 9 yeast expression vector (Fig. 3.3) and transformed into *Pichia pastoris* GS115 yeast cells for expression (Boulangé *et al.*, 2002). A glycerol stock of the *Tco*CATL construct (25% (v/v) glycerol in dH_2O, 50% (v/v) *Tco*CATL expression culture) was streaked onto yeast extract peptone dextrose agar plates (YPD) [1% (w/v) yeast extract, 2% (w/v) peptone, 2% (w/v) dextrose, 1% (w/v) bacteriological agar] containing tetracycline (10 µg/ml) and incubated at 30°C for 72 h under non shaking conditions. Subsequently, a single colony was used to inoculate 100 ml of YPD medium [1% (w/v) yeast extract, 2% (w/v) peptone, 2% (w/v) dextrose] containing tetracycline (10 µg/ml) and incubated using baffled flask at 30°C at 200 rpm for 24 h. The 100 ml culture was added to 900 ml of buffered media glycerol yeast (BMGY) [1% (w/v) yeast extract, 2% (w/v) peptone, 100 mM potassium phosphate buffer, 1.34% (w/v) yeast nitrogen base without amino acids] containing tetracycline (10 µg/ml) and ampicillin (50 µg/ml) and cultured at 30°C at 200 rpm for 72 h. The yeast cells were harvested by centrifugation (2000 *g*, 10 min, 4°C). The harvested yeast cells were resuspended in 1 L buffered minimal media (BMM) [100 mM potassium phosphate buffer, 1.34% (w/v) YNB, 0.0004% (w/v) biotin] containing 0.5% (v/v) methanol, tetracycline (10 µg/ml) and ampicillin (50 µg/ml) in a baffled flask covered with sterile cheesecloth for expression over a 7 day period at 30°C, 200 rpm. Methanol (0.5% (v/v) was added to cultures every 24 h. Subsequently, the yeast cells were harvested by centrifugation. The supernatant was collected, and the pellet discarded. The supernatant was filtered using Whatman No. 4 filter paper used for three phase partitioning (TPP) (Pike and Dennison, 1989). To the filtrate was added 30% (w/v) ammonium sulfate and 30% (v/v) tertiary butanol. This solution was centrifuged (6000 *g*, 10 min, 4°C) using a swing out rotor. The precipitated protein

was collected and resuspended in molecular exclusion (MEC) buffer [50 mM NaH_2PO_4, 300 mM NaCl, pH 8].

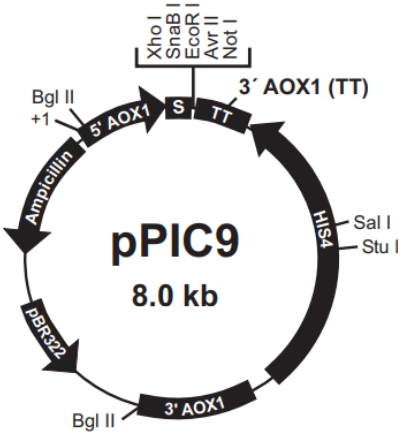

Figure 3.3: pPIC 9 vector map from Invitrogen Pichia expression kit

3.2.8.1 Purification of *Tco*CATL and *Tvi*CATL using molecular exclusion chromatography

*Tco*CATL and *Tvi*CATL expressed in *Pichia pastoris* GS115 yeast cells, were purified using HiPrep 16/16 Sephacryl S200 HR resin which has a fractionation range of 2 – 250 kDa. The S200 column was equilibrated with 180 ml MEC buffer with a flow rate of 0.05 ml/min and pressure of 0.15 kPa using the AKTA Purifier system from GE Healthcare (Uppasala, Sweden). In separate experiments, a 2 ml yeast expression sample of *Tco*CATL or *Tvi*CATL was loaded onto the MEC column. The protein was eluted in 2 ml fractions with a flow rate of 0.05 ml/min and pressure of 0.15 kPa. The S200 resin was regenerated with 60 ml of 0.2 M NaOH and stored in 20% ethanol. The eluted fractions were electrophoresed on a 12.5% reducing Tris-glycine SDS-PAGE gel (Section 2.2.11.1). The fractions containing either *Tco*CATL or *Tvi*CATL were pooled and concentrated using PEG 20 000.

3.2.9 Inhibition of cysteine protease activity with *Tz*cystatin B

The active concentrations of *Tco*CATL, *Tvi*CATL and papain were titrated using the commercial irreversible inhibitor E-64. Briefly, the enzyme, 1.7 µM *Tco*CATL or 1 µM *Tvi*CATL (diluted in 0.1 % (w/v) Brij 35) were incubated with 1-10 µM E-64 or 0 -1 µM E-64 respectively and assay buffer [50 mM Tris-HCl buffer, 150 mM NaCl, 10 mM CaCl2, pH 7.5] containing 5 mM dithiothreitol (DTT) for 30 minutes. Subsequently, 20 µM Z-Phe-Arg-AMC substrate was added. Papain (0.2 µM) was (diluted in 0.1 % (w/v) Brij 35) and incubated with 1-10 µM E-64, assay buffer [340 mM Na-acetate, 60 mM acetic acid, 4 mM Na_2EDTA, pH 5.5] containing 5 mM DTT for 30 minutes. Subsequently, 20 µM Z-Phe-Arg-AMC synthetic substrate was

added. The fluorescence (Ex360nm and Em460nm) was measured using the Optima Spectrophotometer from BMG Labtech.

The inhibitory activity of purified *T. zimbabwensis* cystatin B against *Tco*CATL, *Tvi*CATL, papain, *T. zimbabwensis* cathepsin B and *Theileria parva* cysteine protease was tested by preincubation of the proteases in triplicate experiments (diluted in 0.1 % (w/v) Brij 35) with 0, 0.5, 1, 2, 5, 10 µM *Tz*cystatin B in the respective assay buffer for 30 min. The Z-Phe-Arg-AMC substrate (20 µM) was added and the fluorescence (Ex360nm and Em460nm) measured using the Optima Spectrophotometer from BMG Labtech.

3.2.10 Gelatin zymography and reverse gelatin zymography using papain

3.2.10.1 Gelatin Zymography

The analysis of the enzymatic activity of proteases can be carried out using a gelatin zymogram (Heussen and Dowdle, 1980). The enzymatic activity of the MEC purified *Tco*CATL was analysed using a zymogram. The purified *Tco*CATL was electrophoresed on a 12.5% Laemmli non-reducing SDS-PAGE gel to which 0.1% (m/v) gelatin was incorporated. Following electrophoresis, the zymogram was incubated in two changes 2.5% (v/v) Triton X100 (15 ml) for 1h at RT to remove SDS thus renature the proteases (Heussen and Dowdle, 1980). Following protease renaturation, the gel was incubated in assay buffer for 16 h at RT. The gel was stained in 0.1% (m/v) amido black for 3 h destained in several changes of destain solution [30% methanol, 10% acetic acid and 60% dH_2O].

3.2.10.2 Reverse gelatin zymography using papain

The inhibition of papain by the *Tz*cystatin B protein also analysed using the reverse zymography method (Hanspal *et al.*, 1983). The *Tz*cystatin B protein sample was electrophoresed on a 10% Tris-tricine non-reducing SDS-PAGE gels to which 0.1% (m/v) gelatin was incorporated. Following electrophoresis, the SDS was removed as per Section 3.2.10.1. The gels were then incubated in papain (50, 100, 200,400, 600, 800 µM; diluted in PBS at 37°C for 16h. The gels were stained and destained as outlined in Section 3.2.10.1. A concentration of 400 µM papain was optimal.

3.2.11 Antibody production and immunoglobulin isolation

3.2.11.1 Chicken immunisation and IgY isolation

Two chickens were used to raise antibodies against purified recombinant *Tz*cystatin B as outlined in Section 2.2.13.1. The chicken IgY was isolated as described in Section 2.2.13.2 and the progress of antibody production analysed by ELISA as described in Section 2.2.13.3.

3.3 Results

3.3.1 Amplification of a cystatin gene from *Trichinella zimbabwensis*.

Total RNA was isolated from *T. zimbabwensis* parasites. Two prominent bands were observed representing RNA at approximately 2000 bp and 1800 bp (Fig. 3.4, panel A). The gene encoding *T. zimbabwensis cystatin B* with a size of approximately 290 bp was amplified by PCR using cDNA as a template synthesised from total RNA and gene specific primers (Fig. 3.4, panel B).

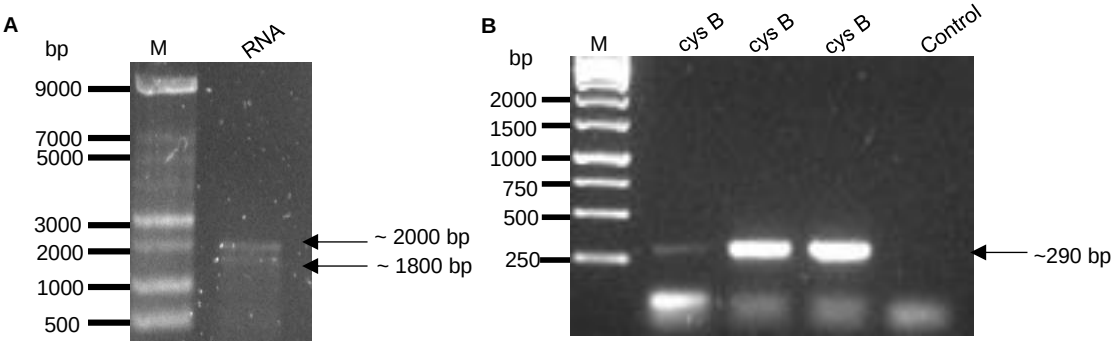

Figure 3.4: Agarose gel analysis of total RNA used for cDNA synthesis and PCR product of *T. zimbabwensis* cystatin B gene amplification. (A) Total RNA isolated from *T. zimbabwensis* muscle larvae that was used for cDNA synthesis was analysed on 1% (w/v) agarose gel, M: ssRNA. (**B)**The cystatin B gene amplicons as well as the non-template control were analysed on a 1% (w/v) agarose gel, M: 1 kb O'Gene Ruler.

3.3.2 Cloning of *Trichinella zimbabwensis cystatin B* gene amplicon into cloning vectors

The *Tzcystatin B* PCR product was purified and ligated to ~3000 bp pGEM-T and ~2692 bp pMD19-T cloning vectors. Recombinant colonies following ligation were identified by Blue-white colony screening. Plasmid DNA was isolated from the recombinant *Tz*cystatin B-pGEM-T (Fig. 3.5, panel A) and recombinant *Tz*cystatin B-pMD19-T (Fig. 3.5, panel B) colonies. Plasmid DNA assumes three conformations which are the supercoiled, coiled and nicked conformations hence three bands were observed (Fig. 3.5, panels A and B). The plasmid DNA from the recombinant colonies was used as templates for colony PCR using M13 vector primers (Fig. 3.5, panel C and D) and gene primers (Fig. 3.5, panel E). A ~500 bp colony PCR product was observed for all seven of the *Tzcystatin B*-pGEM-T colonies in contrast to the *Tzcystatin B*-pMD19-T colonies where only the first two colonies produced bands of ~500 bp with the use of the M13 vector primers. The correct size of the *Tzcystatin B* gene is ~290 bp; the additional ~210 bp may be attributed to the amplification of vector DNA on either side of the insert. Colony PCR of the same clones was conducted using gene specific primers (Fig. 3.5, panel E and F). A band representing the *Tzcystatin B* insert was obtained at the expected size of ~290 bp for all the *Tz*cystatin B-pGEM-T colonies (Fig. 3.5, panel E). On the contrary,

a ~290 bp band representing the *Tzcystatin B* insert was only obtained for colony 1, 4 and 7 of the *Tzcystatin B*-pMD19-T colonies (Fig. 3.5, panel F). The DNA from a *Tzcystatin B*-pGEM-T colony was sequenced, and the sequence was identical to the sequence obtained from NCBI Genbank (Appendix A).

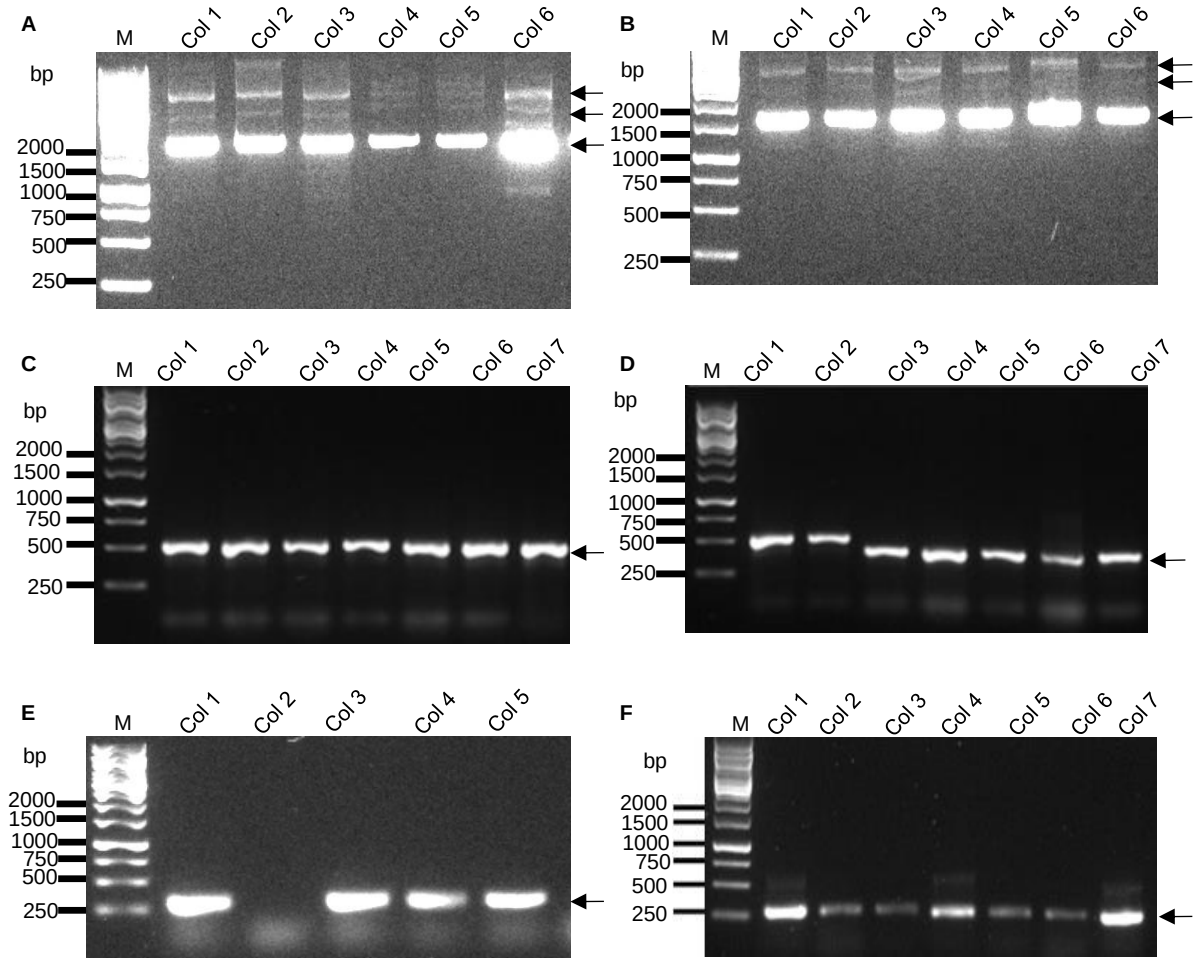

Figure 3.5: Screening of recombinant *Tz*cystatin B-pGEMT and *Tz*cystatin B-pMD19 clones. The *Tzcystatin B* PCR product was ligated to pGEM-T and pMD19-T cloning vectors and transformed into *E. coli* JM109 cells. Plasmid DNA was isolated from recombinant colonies. **(A)***Tzcystatin B*-pGEM-T clones; **(B)** *Tzcystatin B*-pMD-19T clones; colony PCR of recombinant **(C)** pGEM-T clones and **(D)** pMD-19T clones using M13 vector primers; **(E)** pGEM-T clones and **(F)** pMD-19T clones using gene primers; M: O'Gene Ruler. The arrows in (A) and (B) represent the DNA conformations; (C) to (F): *Tz*cystatin B colony PCR amplicons

The amplicons obtained from colony PCR of the *Tzcystatin B*-pGEM-T colonies using gene primers were of the expected size of ~291 bp in comparison to the Tzcystatin B-pMD19-T colonies where two bands were obtained at 500 bp and 291 bp. The presence of the *Tzcystatin B* insert in the pGEM-T clones 1, 3 and 5 was further confirmed by a small-scale restriction digestion using EcoRI and XhoI restriction enzymes. Double restriction digests of the selected colonies yielded two products, namely, the ~290 bp *Tzcystatin B* insert and the digested ~3000

bp cloning vector (Fig. 3.6). The restriction digestion was scaled up and the *Tzcystatin B* insert gel extracted and purified in preparation for subcloning into expression vectors.

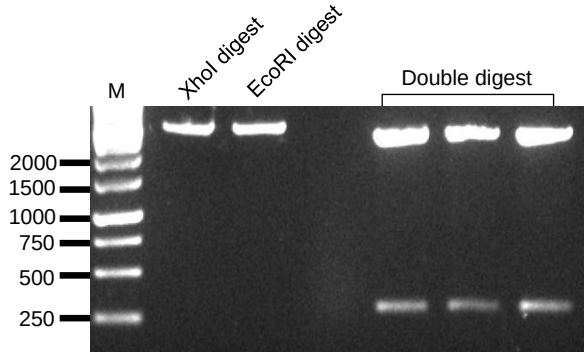

Figure 3.6: Analysis of the restriction digestion of *Tzcystatin B*-pGEM-T clones on a 1% (w/v) agarose gel. The *Tzcystatin B*-pGEM-T plasmid was restriction digested with EcoRI (fwd) for 15 min at 37°C and a further 15 min with XhoI (rev). M, O'Gene Ruler

3.3.3 Subcloning of the *Tzcystatin B* insert into pET-28a and pET-32a expression vectors

The purified ~290 bp *Tzcystatin B* insert obtained by restriction digestion of recombinant *Tzcystatin B*-pGEM-T colony 3 was ligated to expression vectors pET-28a and pET-32a. The pET-28a and pET-32a vectors used for ligation were first digested with the same restriction enzymes to create compatible sticky ends. The undigested vector is represented by three bands which are the coiled, supercoiled and linear forms of the plasmid, while the digested vectors by a single band at ~6000 bp because it has become linearised (Fig. 3.7, panel A). The ligation mixture was transformed into *E. coli* JM109 cells for storage and *E. coli* BL21 cells for expression. Colony PCR was performed on the colonies obtained from the transformation to confirm the presence of the *Tzcystatin B* insert. A prominent band with a size of approximately 290 bp for *Tzcystatin B*-pET-28a in *E. coli* JM109 (Fig. 3.7, panel B) and in *E. coli* BL21 (Fig. 3.7, panel C). A prominent band with a size of approximately 290 bp corresponding to the size of the *Tzcystatin B* insert was observed in the transformed recombinant pET-32a colonies in both *E. coli* JM109 and BL21 cells (Fig. 3.7, panels D and E).

3.3.4 Recombinant expression of *Tz*cystatin B

The ~290 bp *Tzcystatin B* gene codes for a protein with an expected molecular weight of 11 kDa and a pI of 6.97 as predicted by the ExPasy server. The expression of r*Tz*cystatin B from pET-32a (Fig. 3.8) and pET-28a (Fig. 3.9) clones in *E. coli* BL21 DE3 was carried out at 37°C using either 1 mM IPTG induction or autoinducing TB medium. Control expressions were conducted from non-recombinant pET-28a and non-recombinant pET-32a vectors. Following expression from pET-32a, a prominent band with a size of approximately 32 kDa was observed both in the soluble and insoluble fractions (Fig. 3.8, panel A). A western blot was

performed to confirm expression by detection of the polyhistidine tag introduced from the recombinant expression vectors.

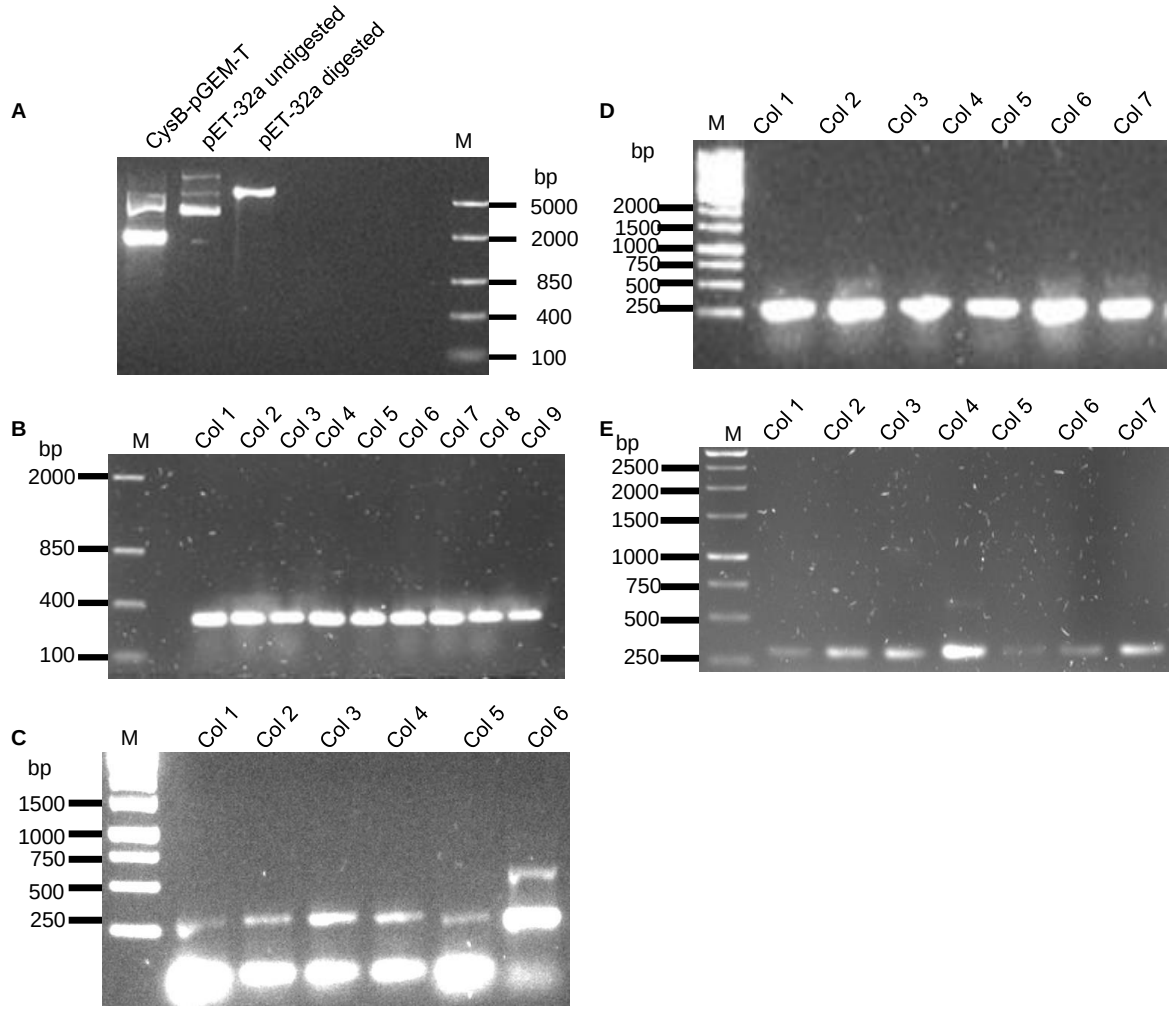

Figure 3.7: Screening for recombinant *Tz*cystatin B-pET-28a and *Tz*cystatin B-pET-32a colonies by PCR. The *Tz*cystatin B insert was ligated to pET-28a and pET-32a expression vectors that were previously digested: **(A)** restriction digested pET-32a vector; The ligation mixture was transformed into competent *E. coli* JM109 and *E. coli* BL21 cells. Colonies were selected, the plasmid DNA used for colony PCR of **(B)** *Tz*cystatin B from the pET-28a construct in *E. coli* JM109 cells and **(C)** *E. coli* BL21 (DE3) cells; **(D)** *Tz*cystatin B from the pET-32a construct in *E. coli* JM109 cells and **(E)** *E. coli* BL21 (DE3) cells using gene primers. Samples were electrophoresed on a 1% (w/v) agarose gel containing gel red. M: O'Gene Ruler.

The ~32 kDa band was detected using mouse anti-His IgG antibodies (Fig. 3.8, panel B). The pET-32a vector contains the S-tag, His-tag and thioredoxin fusion tag which adds an additional ~20 kDa to the size of the expressed protein. Therefore, the size of *Tz*cystatin B with the fusion protein is approximately 31 kDa The expression supernatant and pellet were also analysed to determine whether the protein was soluble or insoluble. Recombinant *T. zimbabwensis* cystatin B (r*Tz*cystatin B) in pET-32a was represented by a prominent band with a size of approximately 32 kDa both in the supernatant and pellet (Fig. 3.8, panel A). *Tz*cystatin B was

also expressed from the pET-32a construct in Terrific broth medium which enables expression by autoinduction, resulting in a prominent band of approximately 32 kDa (Fig. 3.8, panel C).

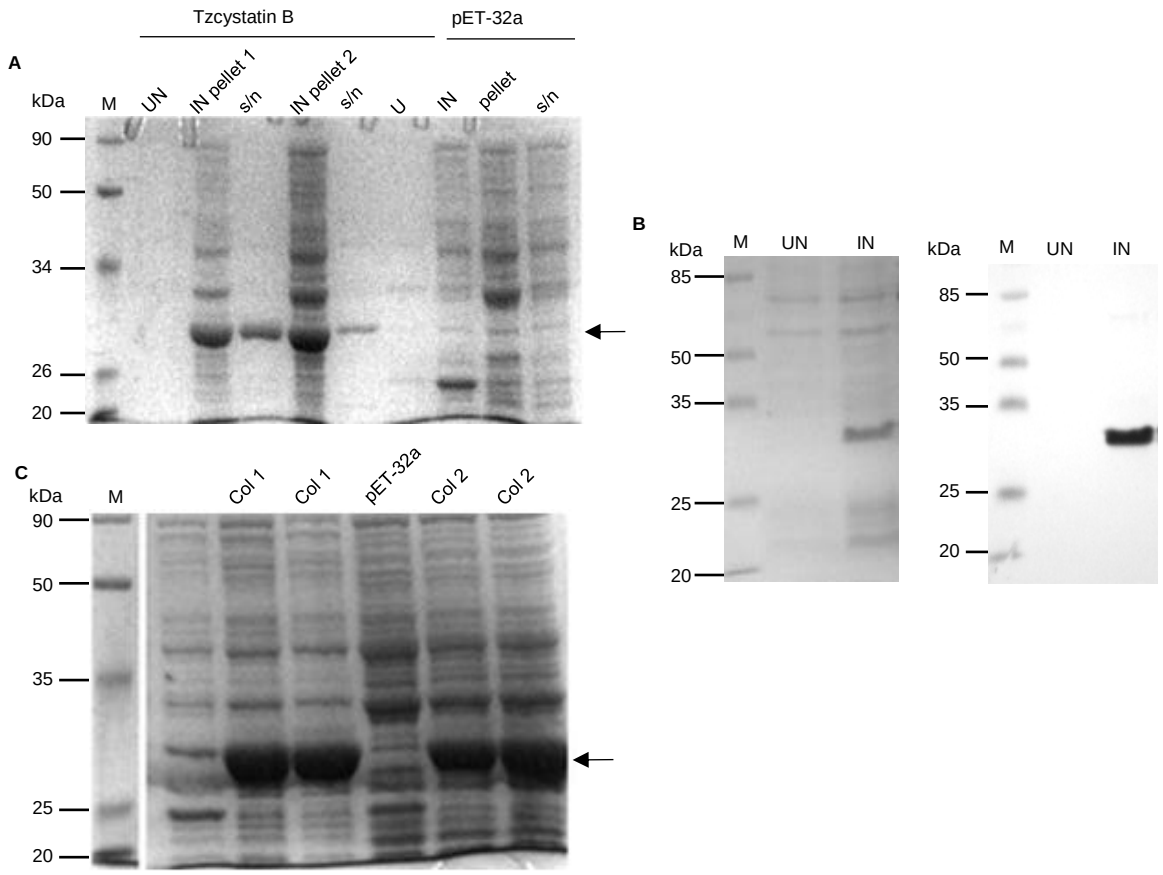

Figure 3.8: Analysis of *T. zimbabwensis* cystatin B expression from pET-32a using IPTG and autoinduction. (A) The uninduced, soluble and insoluble fractions from expression of colony 1 and 2 of *Tz*cystatin B in pET-32a and non-recombinant pET-32a were electrophoresed on a 10% reducing Tris-tricine SDS-PAGE gel and stained with Coomassie blue **(B)** The expression cell lysate was electrophoresed on a 10% Tris-tricine SDS-PAGE gel, separated proteins transferred onto nitrocellulose and probed with mouse anti-His IgG primary antibody followed by goat anti-mouse IgG HRPO and developed with the 4-chloro-1-naphtol·H_2O_2 **(C)** The auto-induced expression lysate of colonies 1 and 2 of *Tz*cystatin B in pET-32a and non-recombinant pET-32a were electrophoresed on a 10% Tris-tricine reducing SDS-PAGE gel. The arrow indicates protein band representing r*Tz*cystatin B. UN, uninduced; IN, induced; M, Molecular weight marker.

*Tz*cystatin B was also expressed from the pET-28a vector by either IPTG induction or autoinduction in Terrific broth. A prominent band was observed at approximately 16 kDa for the IPTG induced *Tz*cystatin B expression from colony 1 and auto induced expression from *Tz*cystatin B-pET-28a colonies 1 and 2. The ~16 kDa prominent band is not observed in the non-recombinant pET-28a control (Fig. 3.9). The pET-28a vector only contains N and C terminal His-tags which adds 4 kDa to the expected size of the protein. Control Soybean trypsin inhibitor (SBTI) showed a band of approximately 22 kDa and haemoglobin (Hb) monomers of 15 kDa. The SBTI and Hb were used as additional protein markers.

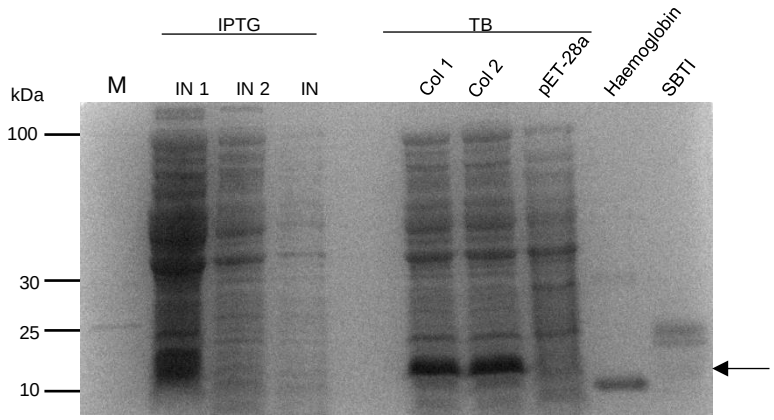

Figure 3.9: Analysis of *T. zimbabwensis* cystatin B expression from pET-28a comparing induction of expression with IPTG and autoinduction. The IPTG induced and auto-induced samples from colony 1 and 2 expression of *Tz*cystatin B from the pET-28a construct, non-recombinant pET-28a as well haemoglobin and SBTI were electrophoresed on a 10% Tris-tricine reducing SDS-PAGE gel stained with Coomassie blue. The arrow indicates protein band representing r*Tz*cystatin IN1, induced colony 1; IN2, induced colony 2, IN: induced pET-28a; M, Molecular weight marker.

3.3.5 Purification of *Tz*cystatin B using nickel affinity chromatography

The r*Tz*cystatin B expressed from both vectors was purified by immobilised metal affinity chromatography. The polyhistidine tagged r*Tz*cystatin B protein was bound to the nickel column and eluted using high concentrations of imidazole. A protein of approximately 32 kDa was eluted from the experiment with *E. coli* lysates containing the pET-32a vector along with contaminating lower and higher molecular weight proteins in the first two elutions (Fig. 3.10, panel A). This expected size corresponds to the *Tz*cystatin B expressed from the pET-32a vector. The r*Tz*cystatin B was represented by a prominent band of approximately 16 kDa, however, minor contaminating higher molecular protein bands were also present (Fig. 3.10, panel B).

The pET-32a vector, used to express *Tz*cystatin B contains a 12 amino acid S-tag, 10 amino acid His-tag tag, 109 amino acid thioredoxin tag, T7 tag as well as thrombin and enterokinase recognition sites for fusion protein cleavage. Therefore, thrombin and enterokinase were used to cleave off the fusion protein tags. On column cleavage of r*Tz*cystatin B by enterokinase proved to be ineffective (Fig. 3.11, panels A and B). A band at approximately 32 kDa was observed in the fractions after cleavage as well as in the His-tag elution fraction (Fig. 3.11, panel A). In addition, on the western blot, A 32 kDa protein band was detected by the anti-His tag antibodies in the western blot of the cleavage fractions as well as the His-tag elution fraction (Fig. 3.11, panel B). Two prominent bands were observed as products of thrombin cleavage, a ~32 kDa band and ~16 kDa band (Fig. 3.11, panel C). *Tz*cystatin B post cleavage has an expected size of 11 kDa. Therefore, the on-column cleavage of *Tz*cystatin B from its fusion protein was ineffective.

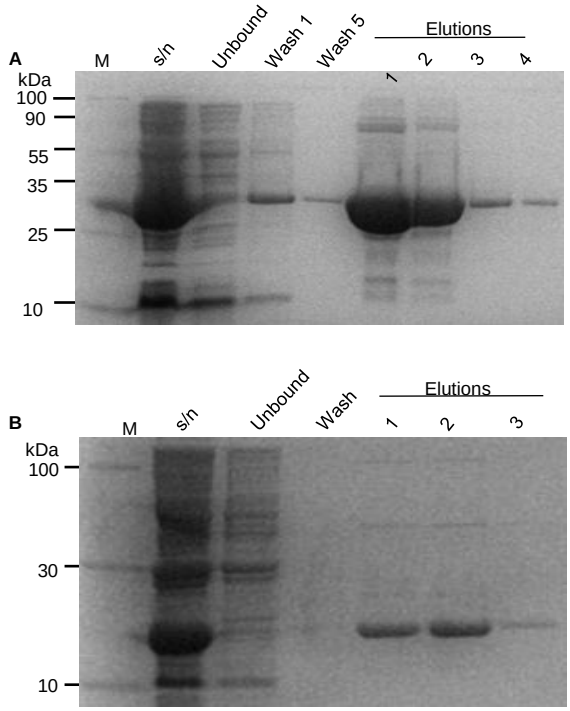

Figure 3.10: Nickel affinity purification of recombinantly expressed *Tz*cystatin B. Samples from the elution profiles of **(A)** *Tz*cystatin B expressed from pET-32a construct, **(B)** *Tz*cystatin B expressed from pET-28a construct were analysed on 10% Tris-tricine SDS-PAGE gel. M, Molecular weight marker; s/n, supernatant

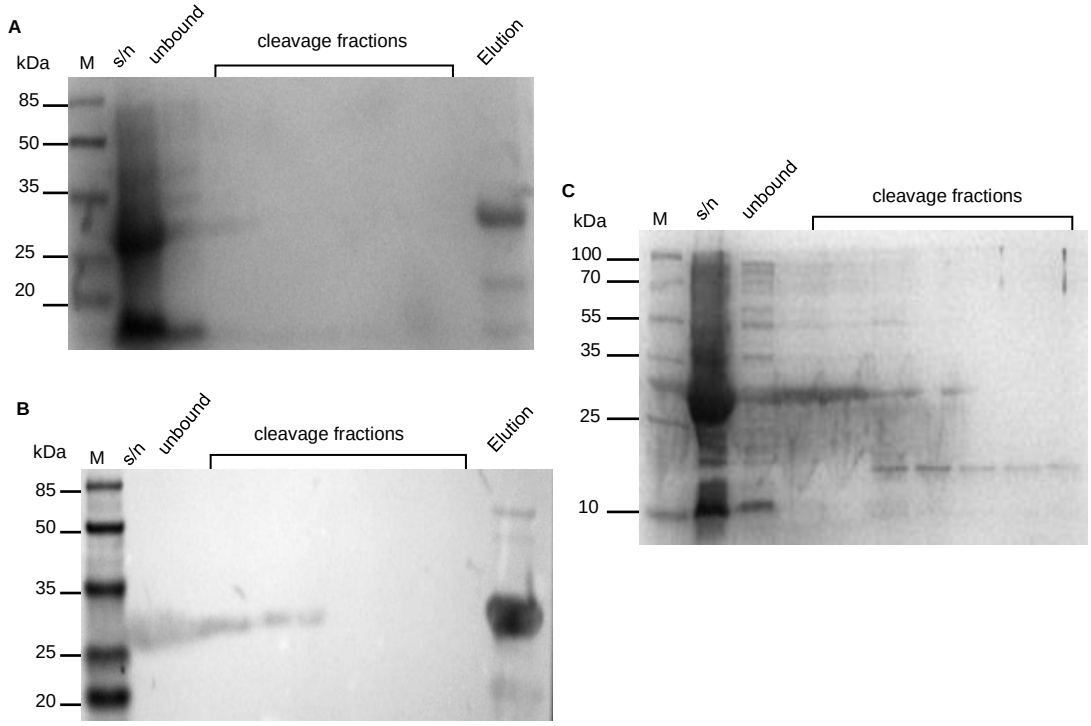

Figure 3.11: On column cleavage of *Tz*cystatin B from the His-tag, S-tag and thioredoxin fusion proteins by thrombin and enterokinase. (A) Fusion protein cleavage with enterokinase analysed by 10% Tris-tricine reducing SDS-PAGE. **(B)** Western blot of enterokinase cleavage fractions probed with mouse anti-His IgG primary antibody, followed by goat anti-mouse IgG HRPO and detected with the 4-chloro-1-naphtol·H_2O_2 **(C)** Fusion protein cleavage with thrombin analysed by 10% Tris-tricine reducing SDS-PAGE M, Molecular weight marker; s/n, supernatant.

3.3.6 On and off-column cleavage of *Tz*cystatin B-fusion protein

Purified *Tz*cystatin B-fusion protein was cleaved by thrombin and enterokinase off-column. Similar cleavage products were obtained for both the thrombin and enterokinase cleavage reactions where partial cleavage was observed. The Ni-NTA column purified 31 kDa *Tz*cystatin B-fusion protein was detected by mouse anti-His IgG was expected to produce two cleavage products with molecular sizes of 11 kDa, representing *Tz*cystatin B and 20 kDa, representing the fusion tags. Four prominent bands are observed following the enterokinase cleavage reaction while only three were observed after the thrombin cleavage reaction (Fig. 3.12, panel A). Following treatment of *Tz*cystatin B-fusion protein with enterokinase, a 31 kDa protein representing uncleaved *Tz*cystatin B was detected as well as a protein band at 20 kDa along with a lower molecular weight protein band (Fig. 3.12, panel B). Following treatment of *Tz*cystatin B by thrombin, a protein band of approximately 16 kDa was detected (Fig. 3.12, panel B).

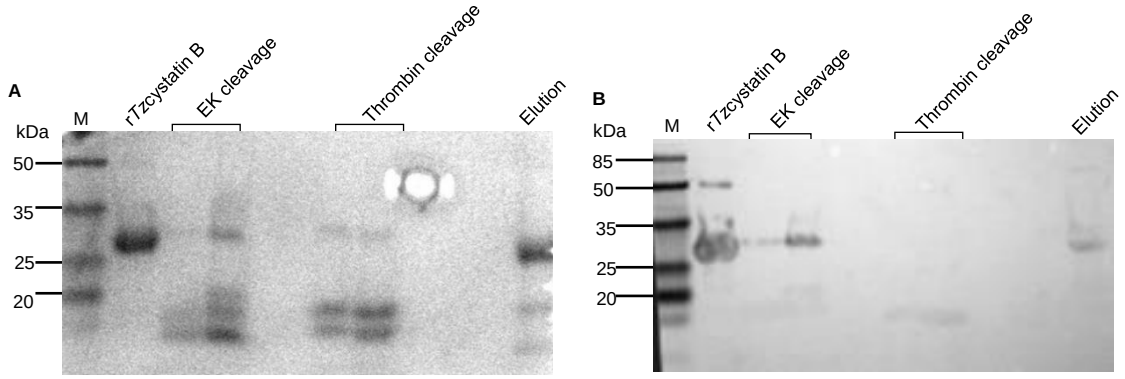

Figure 3.12: Off column cleavage of *Tz*cystatin B-pET-32a by thrombin and enterokinase. (A) 10% Tris-tricine reducing SDS-PAGE gel analysis of on column cleavage of *Tz*cystatin B – pET-32a by thrombin and enterokinase. (**B**): The thrombin and enterokinase off column cleavage fractions were electrophoresed on a 10% SDS-PAGE and transferred onto nitrocellulose and probed with mouse anti-His IgG primary antibody and goat anti-mouse IgG HRPO secondary with the 4-chloro-1-naphtol·H_2O_2. M, Molecular weight marker; EK, enterokinase

3.3.7 Expression and purification of *Tco*CATL

In order to evaluate the interaction of r*Tz*cystatin B with parasite cysteine proteases, *Trypanosoma congolense* cathepsin L-like protease (*Tco*CATL) was recombinantly expressed from the pPIC 9 yeast expression vector in GS115 yeast cells, using a construct previously prepared in our laboratory. Following *Tco*CATL expression, the soluble fraction was subjected to TPP as a first purification step. The TPP precipitated protein was further purified by molecular exclusion chromatography using an S200 column (Fig. 3.13, panel A). Two peaks were observed in the elution profile at 38.68 ml and 77.82 ml. The second peak comprising of fractions 35 – 43 contained the purified *Tco*CATL at 29 kDa (Fig. 3.13, panel B).

The purified *Tco*CATL was detected by affinity purified chicken anti-TcoCATL N-terminal peptide IgY (Fig. 3.13, panel C). The purified *Tco*CATL digested the gelatin substrate on the zymogram thus enzymatically active (Fig 3.13, panel D).

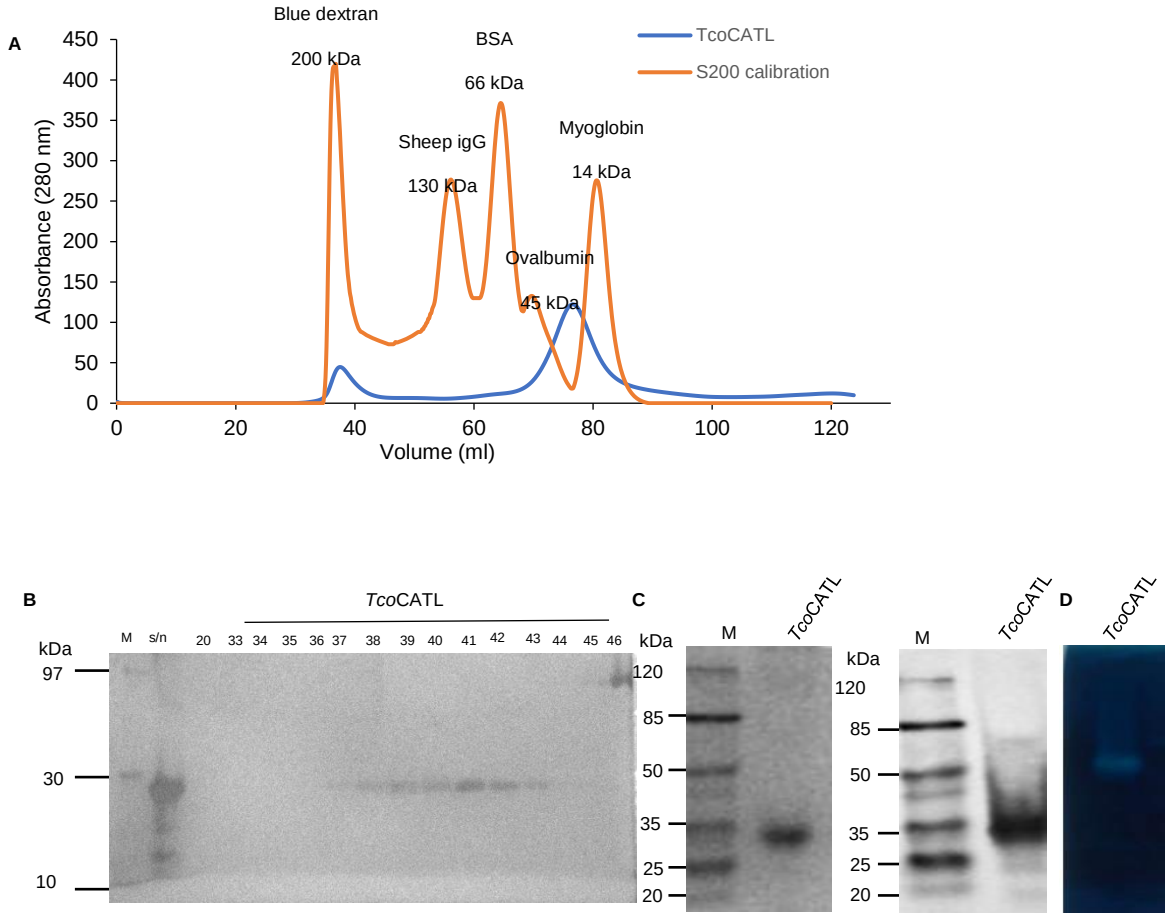

Figure 3.13: Analysis of the expression of *Tco*CATL and purification using HiPrep 16/16 Sephacryl S200 gel filtration chromatography. (A) The 30% ammonium sulfate TPP fraction following expression of *Tco*CATL was purified on a HiPrep 16/16 Sephacryl S200 column (flow rate of 0.5 ml/min). **(B)** The gel filtration fractions were analysed using a silver stained 10% Tris-tricine reducing SDS-PAGE gel. **(C)** The identity of the purified *Tco*CATL was confirmed by western blotting using chicken anti-*Tco*CATL N-terminal peptide IgY. **(D)** The enzymatic activity of purified *Tco*CATL was analysed using 12.5% SDS-PAGE zymogram. M, Molecular weight marker

3.3.8 Inhibition of cysteine protease activity with *Tz*cystatin B

The interaction of the 16 kDa *Tz*cystatin B expressed using the pET-28a expression vector construct with cysteine proteases from *T. zimbabwensis* (cathepsin B-like), *Trypanosoma congolense* (*Tco*CATL) *Trypanosoma vivax* (*Tvi*CATL) and *Theileria parva* (cathepsin L-like protease) was evaluated. These cathepsin B and cathepsin L like proteases were previously expressed and purified in our laboratory. Before the effect of r*Tz*cystatin B on *Tco*CATL activity was tested, the amount of active *Tco*CATL was determine by titrating the protease with the irreversible cysteine protease inhibitor, E-64 and the Z-Phe-Arg-AMC peptide substrate (Fig. 3.14, panel A).. Twenty percent of *Tco*CATL was active and this information was used to report

the quantity of *Tco*CATL used in the assays in terms of amount of active enzyme. The treatment of *Tco*CATL with increasing concentrations of Tzcystatin B was shown to progressively decrease the enzymatic activity of 0.2 µM *Tco*CATL.

A ~60% reduction in the activity of *Tco*CATL was observed when treated with 1 µM *Tz*cystatin B while a ~75% reduction in activity was observed when treated with 5 µM *Tz*cystatin B (Fig. 3.14, panel B). Similarly, the active site titration of *Tvi*CATL showed that only 10% of the enzyme was active (Fig. 3.14, panel C). The highest concentration of *Tz*cystatin B (10 µM) inhibited the activity of 1 µM *Tvi*CATL by approximately 70%. (Fig. 3.14, panel D).

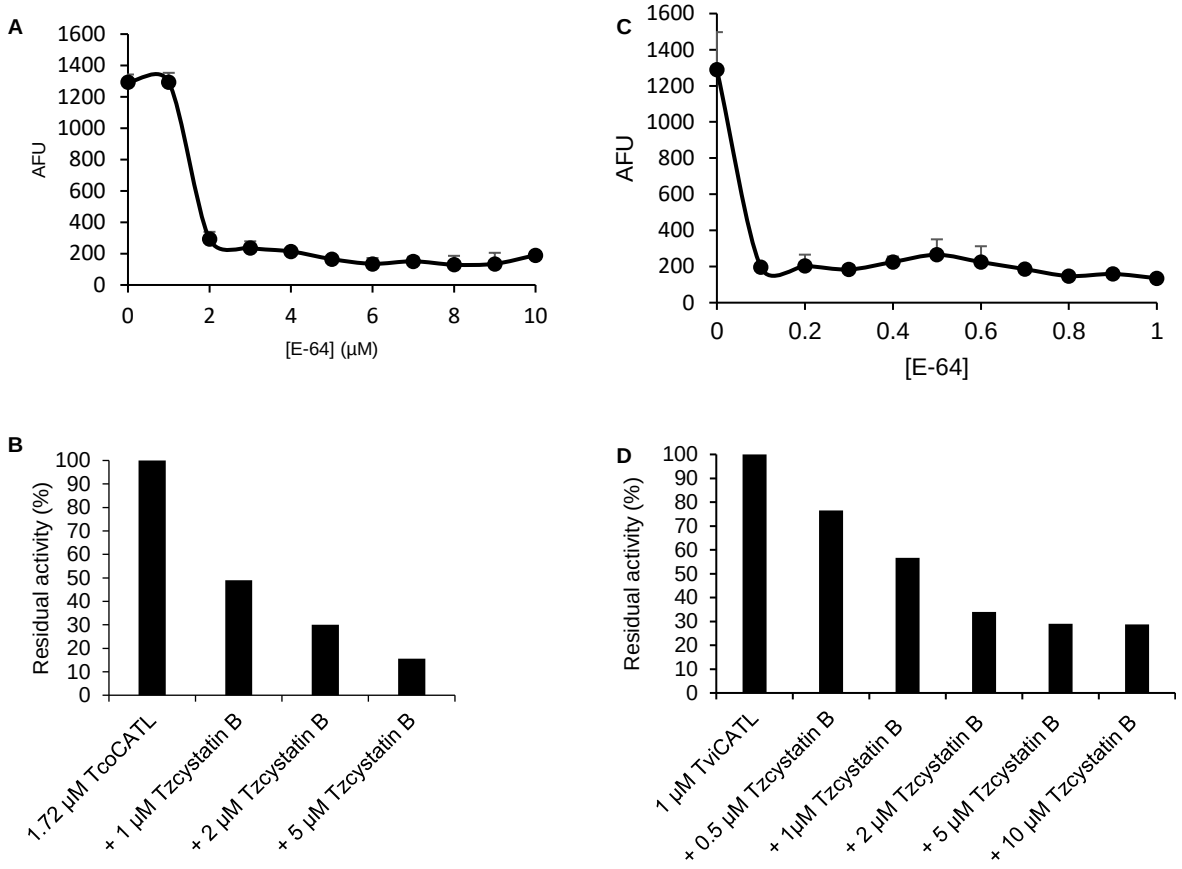

Figure 3.14: Analysis of the interaction of *Tco*CATL and *Tvi*CATL with *Tz*cystatin B. (A) Active site titration of *Tco*CATL by E-64 with the hydrolysis quantified using Z-Phe-Arg-AMC substrate. **(B)** *Tco*CATL (0.34 µM active protease) was incubated with 1, 2 or 5 µM of *Tz*cystatin B. **(C)** Active site titration of *Tvi*CATL by E-64. **(D)** *Tvi*CATL (0.1 µM active protease) was incubated with 0.5, 1, 2, 5 or 10 µM *Tz*cystatin B. The arbitrary fluorescence unit values represent the average of triplicate experiments.

The inhibitory activity of *Tz*cystatin B was also tested against a commercially sourced preparation of papain, a cysteine protease from *Carica papaya* L. latex. The active concentration of papain was titrated with E-64 and papain was found to be 40% active (Fig. 3.15, panel A). *Tz*cystatin B (5 µM) inhibited the enzymatic activity of papain by 40% (Fig.

3.15, panel B). Reverse zymography also showed that *Tz*cystatin B inhibited the digestion of gelatin by papain on a zymogram (Fig. 3.15, panel C).

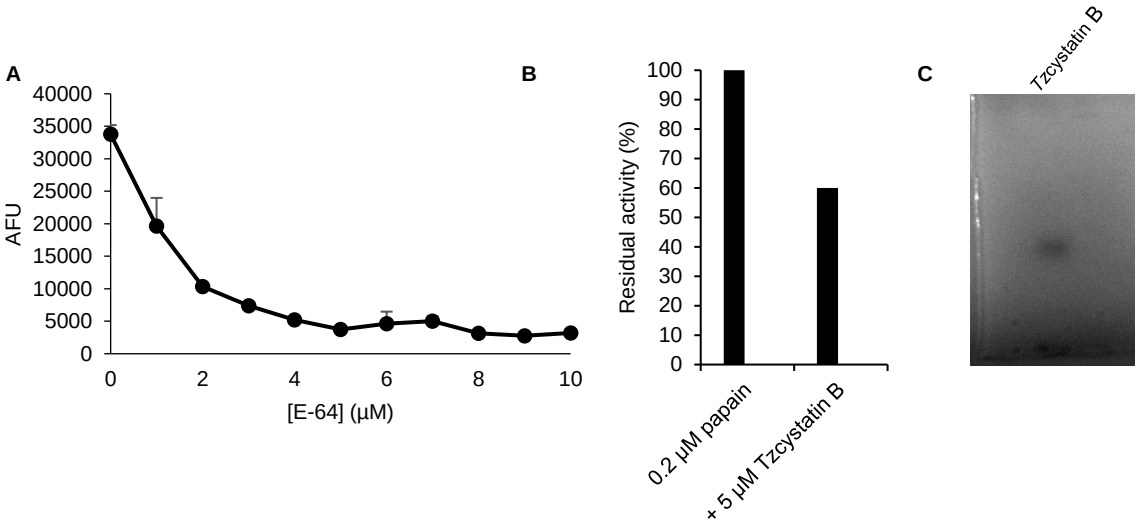

Figure 3.15: Analysis of the interaction of papain and *Tz*cystatin B. (A) Active site titration of papain by E-64. **(B)** Papain (0.08 μM active enzyme) was incubated with 5 μM of *Tz*cystatin B. **(C)**: 5 μM *Tz*cystatin B was electrophoresed on 10% Tris-tricine reducing SDS-PAGE gel and incubated in papain. The arbitrary fluorescence unit values represent the average of triplicate experiments.

The inhibitory activity of *Tz*cystatin B was also tested on the *Trichinella zimbabwensis* cathepsin B as well as the *Theileria parva* cysteine protease (Fig. 3.16). The enzymatic activity of 1 μM *T. zimbabwensis* cathepsin B was reduced by ~80% by 10 μM *Tz*cystatin B while the same concentration of *Tz*cystatin B reduced the activity of the *T. parva* cysteine protease by ~90% (Fig. 3.16, panels A and B).

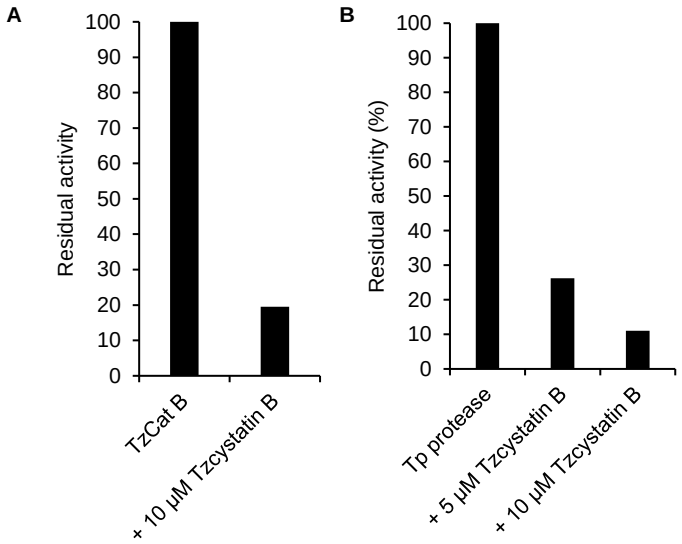

Figure 3.16: Analysis of the interaction of *Tz*cystatin B with cathepsin B from *T. zimbabwensis* and cysteine protease from *Theileria parva*. (A) 1 μM cathepsin B was incubated with 10 μM *Tz*cystatin B. **(B)** 1 μM *T. parva* cysteine protease was incubated with 5 μM and 10 μM of *Tz*cystatin B.

3.3.9 Production of chicken anti-*Tz*cystatin B IgY antibodies

The chicken anti-*Tz*cystatin IgY antibodies were isolated from eggs laid by chickens previously immunised with purified r*Tz*cystatin B protein. An ELISA was used to analyse the progress of antibody production by each chicken (Figure 3.17, panel A). Chicken 1 antibody production peaked during weeks 4,7 and 11 while antibody production from chicken 2 was inconsistent as no antibodies were obtained on day 3 and 13. Chicken 2 antibody production peaked during week 7 (Fig 3.17, panel A). The weeks where chicken anti-*Tz*cystatin IgY production was highest were pooled. Antibodies produced during weeks 4-6, 7-9, 11-13 by chicken 1 and antibodies produced during weeks 4-6, 7-9 and 11-12 by chicken 2 were pooled. A checkerboard ELISA was then performed using pooled antibodies from week 4-6 from both chicken 1 and chicken 2 to determine the lowest concentration of antibody that would give a signal (Fig. 3.17, panel B). A minimal concentration of 1 µg/ml shown to be the lowest concentration of chicken anti-*Tz*cystatin IgY to produce a signal (Fig. 3.17, panel B).

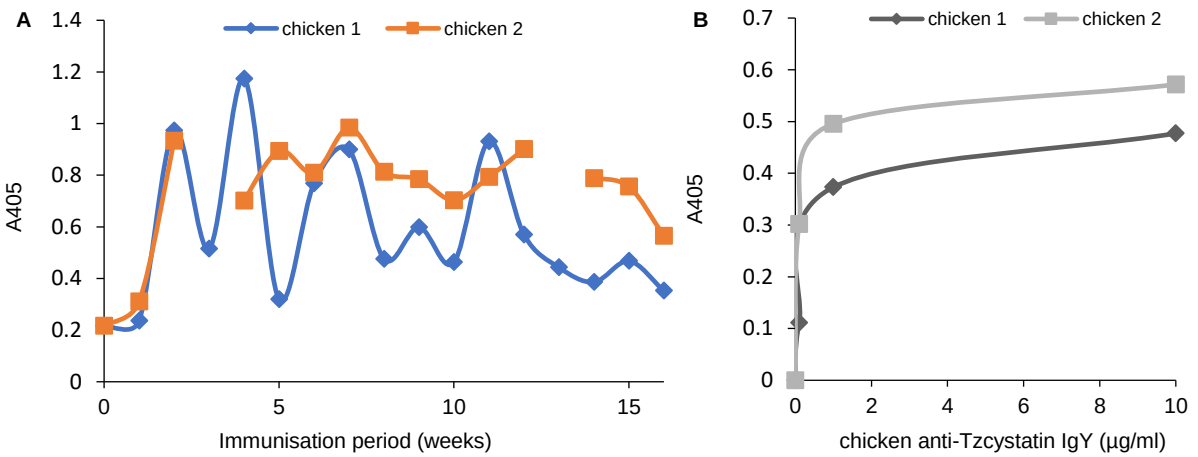

Figure 3.17: Analysis of the production of chicken anti-*Tz*cystatin B antibodies by ELISA. (A) ELISA plates were coated with 1 µg/ml of *Tz*cystatin B which was detected using chicken anti-cystatin IgY as a primary antibody and rabbit anti-chicken **(B)** ELISA plates were coated with 1 µg/ml of *Tz*cystatin B which was detected using the week 4-6 pool (10, 1, 0.1 µg/ml). The absorbance readings at 405 nm are averages of duplicate experiments.

3.3.10 Detection of native *Tz*cystatin B protein in crushed *T. zimbabwensis* muscle larvae

The pooled week 4-6 chicken anti-*Tz*cystatin IgY were used for the detection of native *Tz*cystatin B in a sample of isolated parasites that was crushed (Fig. 3.18, panel A). The *T. zimbabwensis* cystatin B native protein was not detected in the parasite by the chicken anti-*Tz*cystatin B IgY antibodies (panels B and C). However, the recombinant protein was detected.

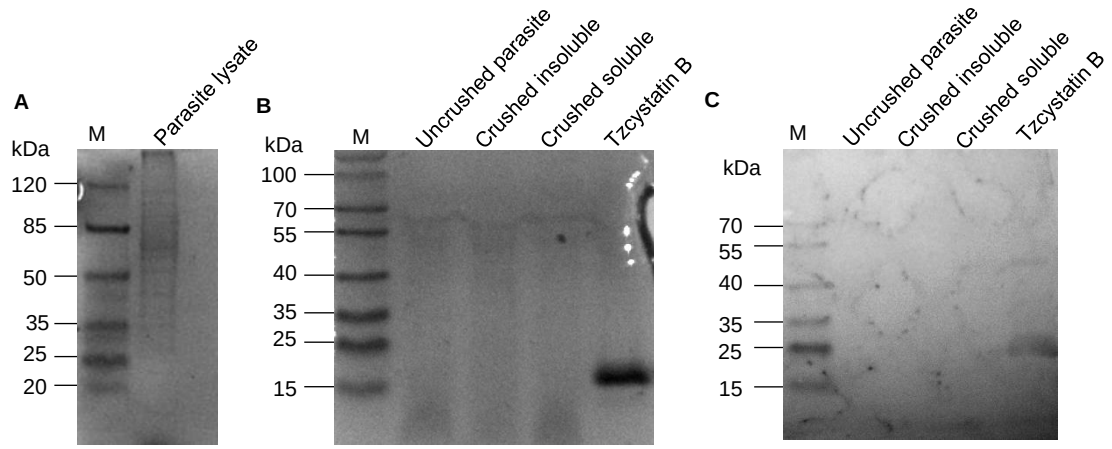

Figure 3.18: Detection of native *Tz*cystatin B in crushed and uncrushed *T. zimbabwensis* muscle larvae. (A) Isolated parasites were electrophoresed on a 10% Tris-tricine reducing SDS-PAGE gel. **(B)** The parasites were crushed and electrophoresed on a 10% Tris-tricine reducing SDS-PAGE gel along with a sample of recombinant *Tz*cystatin B. **(C)** The western blot was probed with chicken anti-cystatin as a primary antibody and rabbit anti-chicken IgY as a secondary antibody.

3.4 Discussion

In the present study, the *cystatin B* gene from *T. zimbabwensis* was amplified using cDNA synthesised from isolated mRNA, the amplicon was cloned and the protein recombinantly expressed in *E. coli* cells. The *Tz*cystatin B protein was purified, tested for inhibitory activity against cysteine proteases and used to raise antibodies in chickens. The antibodies were used for the confirmation of recombinant expression as well as the detection of the protein in *T. zimbabwensis* parasite extracts.

The 290 bp *Tzcystatin B* gene was amplified by PCR using cDNA as template which was synthesised from total RNA obtained from the *T. zimbabwensis* muscle larvae. Similarly, Tang *et al.* (2015) amplified the *T. spiralis TsCLP* gene by PCR using cDNA reverse transcribed from mRNA obtained from total RNA of intestinal infective larvae. On the contrary, the *H. polygrus*, *Hpcystatin,* and *N. brasiliensis Nippostatin* cystatin genes were amplified using cDNA reverse transcribed from RNA obtained from adult worms. The *Tzcystatin B* amplicon was then cloned into pGEM-T and pMD-19T cloning vectors. Following amplification, *Nippostatin* was also cloned into a pGEM-T cloning vector for sequencing purposes while *Hccystatin* was cloned into the pMD19-T cloning vector prior to subcloning into an expression vector. However, following gene amplification, the *TsCLP* amplicon was subcloned directly into the pET-28a expression vector. The *Ts*CLP had a molecular size of 45.9 kDa because of the presence of two 16.5 kDa domains in the N-terminus and a single domain in the C-terminus (Tang *et al.*, 2015).

The *Tzcystatin B* gene insert was subcloned into pET-28a and pET-32a expression vectors for recombinant expression. *Nippostatin* and *Hpcystatin* were both recombinantly expressed in pET-32a as well. This expression vector carries the His-tag, S-tag and thioredoxin-tag, the latter helps improve the solubility and thermal stability of the expressed protein, while the pET-28a vector contributes a His-tag which assists in protein purification by affinity chromatography (Costa *et al.*, 2014). Analysis of the recombinant expression of *Tz*cystatin B and purification by Ni-NTA affinity chromatography showed *Tz*cystatin B to have an apparent molecular weight of 16 kDa and 31 kDa in the pET-28 and pET-32a expression vectors respectively compared to *Hp*cystatin had a molecular weight of 16 kDa and Nippostatin 14 kDa as shown by SDS-PAGE.

In the present study, expression by auto-induction was found to produce higher yields of the protein in comparison to induction by IPTG for both pET28 and pET32a expression systems. Autoinducing medium enables high expression of the protein of interest because of attaining of high cell densities as a result of the presence sufficient nutrients; to illustrate, lactose is present which is consumed after the glucose in the medium has been consumed (El-Baky *et al.*, 2015).

Fusion tags such as the 12 kDa thioredoxin-tag, which is larger than the 11 kDa *Tz*cystatin B, that is being expressed, may interfere with the structure and function of the expressed protein (Paraskevopoulou and Falcone, 2018). To illustrate, the fusion tag may obstruct the substrate or ligand binding sites of the fusion protein (Fonda *et al.*, 2002) Treatment of the 31 kDa *Tz*cystatin B expressed in pET-32a with thrombin and enterokinase was expected to produce two cleavage products, the 11 kDa *Tz*cystatin B and the 20 kDa fusion tags which include the N-terminal and C-terminal His-tag, S-tag and thioredoxin-tag (Fig 1.5). However, multiple cleavage products were obtained except the expected 11 kDa *Tz*cystatin B cleavage product, possibly as result of cleavage at secondary sites as has been reported for the overexpressed GST-apoS100A13 calcium binding protein. (Rajalingam *et al.*, 2008). Cleavage of fusion tags from r*Hp*cystatin, expressed in the pET-32a vector to which a Tobacco Etch virus (TEV) recognition site was introduced, was achieved with the TEV protease (Sun *et al.*, 2013).

The purified 16 kDa *Tz*cystatin B protein expressed from the pET-28a construct was used for inhibition of protease activity assays. In other studies, the inhibitory activity of nippostatin, *Hc*cystatin and *A. viteae* cystatin were tested without prior cleavage of fusion tags. Recombinant Tzcystatin B (5 µM) was shown to inhibit 0.2 µM papain, 1.72 µM *Trypanosoma congolense Tco*CATL, 1 µM *T. vivax Tvi*CATL as well as 1 µM *T. zimbabwensis* cathepsin B using the Z-Phe-Arg-AMC peptide substrate. *Hc*cystatin was shown to inhibit 0.05 µM human cathepsin L, 0.05 µM human cathepsin B and 0.15 µM papain using the Z-Phe-Arg-AMC·HCl

peptide substrate as well as 0.05 µM human caspase 1 using Ac-Tyr-Val-Ala-Asp-7-amino-3-trifluoromethylcoumarin.

The immunisation of chickens with the *Tz*cystatin B antigen over the 16-week period showed, using an indirect ELISA that antibody production was highest between weeks 6-9. Native *Tz*cystatin B was not detected in the parasite lysates. In another study, Robinson and colleagues (2006) were able to detect *Ts*CLP in the stichosome of the *T*. *spiralis* parasite and not in new born larvae.

In conclusion, the *cystatin B* gene from *T. zimbabwensis* was identified using bioinformatics, cloned and the *Tz*cystatin B protein recombinantly expressed using the *E. coli* expression system. The purified r*Tz*cystatin B was used to raise antibodies in chickens and for activity assays. The chicken anti-*Tz*cystatin B antibodies enabled the detection of r*Tz*cystatin B in western blots and on ELISAs. The purified *Tz*cystatin B inhibited an endogenous cathepsin B-like protease as well as cathepsin L-like proteases from *T. congolense, T. vivax and T. parva.*

Chapter 4: General discussion

Trichinellosis is a meat-borne parasitic zoonotic disease that is acquired by the ingestion of raw or undercooked meat that is contaminated with infective *Trichinella* larvae (Wang *et al.*, 2017c). During the enteric phase of the infection, the infective larvae moult, mature into adults and produce offspring which enter the lymphatic system and begin the muscle phase of the infection (Gottstein *et al.*, 2009). There are nine species and three genotypes within the *Trichinella* genus which either form collagen capsules thus termed encapsulating or non-encapsulating; the non-encapsulating species include, *T. zimbabwensis*, *T. pseudospiralis* and *T. pupae* (Wang *et al.*, 2017a). This neglected tropical disease which continues to emerge and re-emerge in various countries has both health and economic impacts (Onkoba *et al.*, 2015; Wang *et al.*, 2017c). The clinical diagnosis of Trichinellosis has been a challenge due to the non-specific symptoms that the disease presents (Wang *et al.*, 2017c). There are direct methods of diagnosis which include muscle biopsies or post-mortem inspection of carcasses and indirect methods of diagnosis such as serological tests to detect Trichinellosis (Gómez-Morales *et al.*, 2014). Serological detection methods include the detection of parasite antigens in serum or tissue fluids and the detection of anti-*Trichinella* antibodies using techniques such as western blot, indirect ELISA and indirect fluorescent antibody test (Mukaratirwa *et al.*, 2013; Sun *et al.*, 2018). Treatment for *Trichinella* includes albendazole and mebendazole which are anthelmintics as well glucocorticosteroids (Gottstein *et al.*, 2009).

Sero-diagnostic methods for the detection of *Trichinella* utilise the *Trichinella* muscle larvae excretory/secretory (ES) antigens, cuticular antigens, and somatic antigens to detect anti-*Trichinella* IgG responses in the host (Yang *et al.*, 2016). The responses against the muscle larval ES antigens are only detected at least four weeks post infection hence classified as group II antigens (Yang *et al.*, 2016). The ES proteins that are released by the parasites are capable of interfering with both the initial recognition stage of the parasite by the host and the effector mechanisms of the host on the parasite (Hewitson *et al.*, 2009).

Excretory-secretory products include proteins such as proteases and protease inhibitors (Hewitson *et al.*, 2009). According to the MEROPS database (http://merops.sanger.ac.uk), classes of proteases, classified by their mechanism of action, include the aspartic, glutamic, metallo, threonine, serine and cysteine proteases as well as asparagine lyases. Mammalian serine proteases have key roles in complement activation, coagulation, inflammation and fibrinolysis, while cysteine proteases have roles in protein processing and antigen presentation (Zang and Maizels, 2001; Verma *et al.*, 2016).

There are three types of serine protease inhibitors which include the serpins, non-canonical canonical types of serine protease inhibitors; the latter comprises of ~20 families such as the Kazal, Kunitz, Pacifastatin and trypsin inhibitor-like (TIL) serine protease inhibitors (Krowarsch *et al.*, 2003; Yang *et al.*, 2017). The four types of cysteine protease inhibitors include the cystatin type 1 family, commonly referred to as the stefins, the cystatin type 2, the kininogens and the non-inhibitory cystatin homologues (Turk *et al.*, 2005). The parasite serine protease inhibitors help protect parasites from proteolysis (Song *et al.*, 2018b). In addition, these inhibitors have roles in the induction of the production cytokines which result in anti-inflammatory responses within the host (Dzik, 2006).

The ES products from the muscle larvae of the encapsulating *Trichinella spiralis*, a well-studied member of the *Trichinella* genus, have become the main target antigens shown to induce immune responses (Wang *et al.*, 2017a). These antigens have been classified into eight groups,TSL-1 to TSL-8, which are used in serological tests (Yang *et al.*, 2016). However, studies have shown that due to the absence of a collagen capsule, the non-encapsulating *T. pseudospiralis* elicited less of an inflammatory reaction in infected muscle tissue (Bruschi *et al.*, 2009). This indicates a potential difference in the ES products of encapsulating and non-encapsulating species (Wang *et al.*, 2017a). This difference may be better understood through the study of ES products from non-encapsulated species such as *T. zimbabwensis.*

The present study set out to identify endogenous serine and cysteine protease inhibitor genes from the *T. zimbabwensis* genome, using bioinformatics. The cystatins are a superfamily of cysteine protease inhibitors that bind tightly to, and block the active site of their target proteases upon interaction; however, this interaction is reversible (Turk *et al.*, 2002; Knox, 2007). The Kazal-type serine protease inhibitors are a family of canonical inhibitors that competitively bind to target serine proteases using their reactive centre loop (Rimphanitchayakit and Tassanakajon, 2010). The identified serine protease inhibitor Kazal-type 4 (*TzSPINK4*) and *Tzcystatin B* genes from *T. zimbabwensis* were cloned, recombinantly expressed as potential targets for antiparasitic interventions. The expressed proteins were purified, their interaction with proteases tested and they were used for antibody production. The antibodies were used for the detection of the recombinant proteins on western blots and ELISAs.

The *T. zimbabwensis* muscle larvae were isolated from the muscle tissue of Sprague Dawley rats using the pepsin-HCl digestion method. Total RNA was isolated from the parasites and cDNA reverse transcribed from the total RNA. The ~450 bp *TzSPINK4* and ~290 bp *Tzcystatin B* genes were each amplified by PCR using the synthesised cDNA as a template with gene specific primers. Each of the genes were cloned, and the exact sequence of the clones verified

by sequencing. The sequences of the clones were found to be congruent to the sequences obtained from NCBI Genbank. The conditions for recombinant expression were optimised for auto-induction and IPTG induction of expression within the *Escherichia coli* bacterial expression system.

The recombinant *Tz*cystatin B was expressed as a 16 kDa His-tagged protein and as a 32 kDa fusion protein that included a His-tag, S-tag and thioredoxin tag and purified by nickel affinity chromatography. Similar results were obtained for the recombinant expression of a cystatin from the gastrointestinal nematode *Nippostrongylus brasiliensis*. The recombinant cystatin from *N. brasiliensis*, nippostatin, was also expressed as a 16 kDa His-tagged protein which was purified by affinity chromatography (Dainichi *et al.*, 2001). In addition, the cystatin from the filarial nematode, *Acanthocheilonema viteae*, was expressed as a 17 kDa His-tagged protein (Hartmann *et al.*, 1997). The cystatin from a parasitic nematode, *Haemonchus contortus,* was expressed as a 35 kDa fusion protein that included a His-tag, S-tag and thioredoxin tag, which is similar to the size of the 32 kDa *Tz*cystatin (Dainichi *et al.*, 2001; Wang *et al.*, 2017b). Tobacco Etch Virus (TEV) protease cleavage was used for removal of the fusion tagfrom the affinity purified recombinant cystatin from *Heligmosoides polygrus*, a parasitic nematode.The cystatin had a size of 16 kDa following cleavage of the His-tag, S-tag and thioredoxin fusion protein (Sun *et al.*, 2013). The recombinant *Heligmosoides polygrus* cystatin has a higher molecular in comparison to *Tz*cystatin which would have a molecular weight of 11 kDa following fusion protein cleavage. The *T. spiralis* cystatin-like protein, *Ts*CLP was expressed as a 45.9 kDa His-tagged protein which is much larger in molecular size in comparison to the recombinant *Tz*cystatin proteins. The high molecular weight of *Ts*CLP may be attributed to the presence of three domains, two with a molecular weight of ~16.5 kDa; however, none of the domains contained the conserved QxVxG motif (Tang *et al.*, 2015).

The *Tz*SPINK4 protein as a 20 kDa His-tagged protein and as a 38 kDa fusion protein that included a His-tag, S-tag and thioredoxin tag. The expressed *Tz*SPINK4 proteins were purified by nickel affinity chromatography. The recombinant expression of Kazal-type serine protease inhibitors from other species within the *Trichinella* genus have not yet been reported. However, the expression of serine protease inhibitors from the serpin family has been reported. The interaction between serpins and target serine proteases is covalent and irreversible, resulting in the disruption of protease active site while the interaction between Kazal-type inhibitors and target serine proteases is non-covalent, tight-binding and does not result in the disruption of the active site (Krowarsch *et al.*, 2003). Two recombinant *Nasonia vitripenis* Kazal-type serine protease inhibitors, *Nv*KSPI-1 and *Nv*KSPI-2, were expressed as 33 and 36 kDa GST-fusion proteins. These inhibitors are present in the venom apparatus of the parasitic wasp and was shown to inhibit the activation of prophenoloxidase in the insect host haemolymph (Qian *et al.*,

2015). Knockdown studies showed that experimental animals without prophenoloxidase , a component of the immune system, were easier to infect (Lu *et al.*, 2014).

The His-tagged 16 kDa *Tz*cystatin B and 20 kDa *Tz*SPINK4 were used to immunise chickens to produce antibodies. The chicken anti-*Tz*cystatin B IgY and chicken anti-*Tz*SPINK4 IgY antibodies were shown to recognise the recombinant *Tz*cystatin B and *Tz*SPINK4 proteins respectively on a western blot and in an indirect ELISA. Antibodies against recombinant proteins from *Trichinella* have also been raised in mice and rabbits (Tang *et al.*, 2015; Song *et al.*, 2018b). Antibodies against the 45.9 kDa recombinant cystatin-like protein from *T. spiralis*, *Ts*CLP, were produced in rabbits and used to immunolocalise *Ts*CLP in the stichosome of the T. *spiralis* muscle larvae and adult worms (Tang *et al.*, 2015). Therefore, future studies may include immunolocalisation studies for the detection of the *Tz*cystatin B and *Tz*SPINK4 proteins in *Trichinella zimbabwensis* larvae as well as assessment of the presence of these inhibitors in other developmental stages of the parasite.

A purified recombinantly expressed 43 kDa *T. pseudospiralis* serpin (r*Tp*serpin) was detected by serum obtained from mice 60 days post infection. The rTpserpin was also detected in crude muscle larvae, adults and new born larvae using western blots, giving evidence that rTpserpin is expressed in all developmental stages of the parasite (Xu *et al.*, 2017b). Antibodies against a recombinantly expressed *T. spiralis* serine protease inhibitor (r*Ts*SPI) were able to inhibit the invasion of intestinal epithelial cells by the *Trichinella* parasites (Song *et al.*, 2018b). Therefore, antibodies against the ES proteins from *Trichinella* not only enable immunolocalisation studies, but were also shown to have protective roles. The assessment of whether *Tz*SPINK4 and *Tz*cystatin B can confer any immunoprotection may be carried out in future studies by immunising mice with *Tz*cystatin B and *Tz*SPINK4 and then challenging the immunised mice with *T. zimbabwensis* parasites. If the proteins are found to be protective, this may inform the development of vaccines.

It was demonstrated in the present study that *Tz*cystatin B inhibits papain from *Carica papaya*. This is an archetypal clan CA protease, hence the family of proteases is known as the papain family of proteases which also includes the mammalian lysosomal cathepsins (Turk *et al.*, 2005). The reactive site of cystatins, that contains the QxVxAxG motif, reversibly binds the catalytic site of papain and papain-like proteases (Wang *et al.*, 2017b). Turk *et al.* (2012) reported that cysteine cathepsin activity is largely regulated by endogenous cystatins, thyropins as well as serpins in a few cases. In order to determine if *Tz*cystatin B inhibits parasite cathepsin L- and B-like proteases, thecatalytic domain of cathepsin L from *Trypanosoma congolense (Tco*CATL), was recombinantly expressed and purified, while the previously expressed catalytic domain of cathepsin L from *T. vivax* (*Tvi*CATL) was purified for

the inhibition studies. Furthermore, a cathepsin B-like protease from *T. zimbabwensis*, *Tz*CATB and a cathepsin L-like protein from *Theileria parva* were available form parallel studies in our laboratory.

The *Tz*cystatin B inhibited the endogenous *T. zimbabwensis* cathepsin B (*Tz*CATB),the catalytic domains of the cathepsin L-like proteases from *Trypanosoma congolense* and *T. vivax,* protozoan parasites that cause nagana in cattle as well as a cathepsin L-like protein from *Theileria parva*, causal agent for east coast fever (Chamond *et al.*, 2010; Gachohi *et al.*, 2012). Previous studies have shown that T*co*CATL, also known as congopain, is strongly inhibited by the mammalian cystatins and kininogens (Chagas *et al.*, 1997; Lalmanach *et al.*, 2002), while mammalian stefin B inhibits *Tvi*CATL (Eyssen *et al.*, 2018).

Cystatins expressed from gastrointestinal nematodes have been reported to inhibit cathepsin and cathepsin-like proteases. The recombinantly expressed 35 kDa cystatin from *H. corticus* was shown to inhibit papain, human caspase 1, cathepsin B and cathepsin L (Wang *et al.*, 2017b). Similarly, the 16 kDa cystatin from *H. polygrus* was found to inhibit a variety of cathepsins including cathepsins B, C, L and S, while the *N. brasiliensis* nippostatin also inhibited cathepsins B and L (Dainichi *et al.*, 2001; Sun *et al.*, 2013)

The *Tz*SPINK4 did not inhibit trypsin, chymotrypsin or thrombin. Similarly, human SPINK6 also did not inhibit trypsin, chymotrypsin or human thrombin but was a selective kallikrein inhibitor (Meyer-Hoffert *et al.*, 2010).The 43 kDa recombinant *T. pseudospiralis* serpin, r*Tp*serpin, inhibited both pancreatic and human neutrophil elastase, mouse mast cell protease-1 and cathepsin G while the recombinant *T. spiralis* serine protease inhibitor, r*Ts*SPI, only inhibited pancreatic trypsin (Xu *et al.*, 2017b; Song *et al.*, 2018b).

Studies on the third domain of turkey ovomucoid (OMTKY3), a Kazal-type inhibitor in complex with bovine chymotrypsin Aα, human leukocyte elastase and S*treptomyces griseus* proteinase B showed that there were 12 positions of contact between the inhibitor and target serine protease which included the P_6, P_5, P_4, P_3, P_2, P_1, P_1', P_2', P_3' P_{14}' P_{15}' P_{18}' sites (Lu *et al.*, 2001; Rimphanitchayakit and Tassanakajon, 2010). However, It is the reactive P_1 site of Kazal-type inhibitors, usually the second amino acid located C-terminal to the second cysteine in the amino acid sequence that determines their specificity (Kreutzmann *et al.*, 2004; Rimphanitchayakit and Tassanakajon, 2010). This P_1 site interacts with the S_1 site of the target protease (Lu *et al.*, 1997). Studies have shown that this reactive P_1 site is variable and could include any one of the following ten amino acids; alanine, aspartic acid, glutamic acid, histidine, lysine, methionine, asparagine, arginine, serine and threonine (Lu *et al.*, 2001; Tian *et al.*, 2004). The *Tz*SPINK4 protein has a methionine residue in the P_1 site. Kazal-type inhibitors with methionine, arginine and alanine in the P_1 site have been found to inhibit either

pancreatic elastase, human neutrophil elastase or both (Rimphanitchayakit and Tassanakajon, 2010; Negulescu *et al.*, 2015). Therefore, future studies will include the assessment of the interaction of *Tz*SPINK4 with human neutrophil elastase and pancreatic elastase, cathepsin G as well as the kallikreins.

Antigens from *Trichinella spiralis* muscle larvae are commonly used in ELISA and western blot to diagnose Trichinellosis. However, there is a difference between the ES products of the encapsulating *T. spiralis* and non-encapsulating *T. pseudospiralis*, and possibly *T. zimbabwensis,* since the different species elicit different host pathological changes (Gómez-Morales *et al.*, 2018). The *Tz*cystatin B and *Tz*SPINK4 proteins identified, cloned and recombinantly expressed in the present study may constitute diagnostic antigens of muscle larvae of non-encapsulating species. Furthermore, assessment of the interaction of *Tz*cystatin B and *Tz*SPINK4 with cysteine and serine proteases respectively may provide insight into the functions of these inhibitors within the parasite and the host and may find application in the design of effective Trichinellosis therapeutics.

APPENDIX A

A. DNA coding sequences

The DNA coding sequences for the *SPINK4* and *cystatin B* genes from *T. zimbabwensis* were obtained by joining the coding sequences (CDS regions) within the shotgun sequence provided by NCBI Genbank.

ATGATTTCACTCGCTTGCTTGTTGTACTTGTTGATGAGCACTGCTGTTGTCACTTATGGTTTTCCG
ATGATTTTTCCAAGAGATCCATTTTGTACAATGTTCAGCCGTAATGGATTCTGTTATGATATTTATC
AACCGGTCTGTGGAACCGATGGAATAACATACGACAATGAATGCTGGCTCTGCTATCGTCTAACT
ATTGAACCATTGATAGTTCAAATTGCATACGACGGAGAATGTGTGGCAGATTATGATCCAATGAT
GCTGCAATTTCCTAGGGTAATTGGAAATGGTATTGCAGTGCCACCCCCATCGCCACCGTTTTTAC
TCAGTGGTGTTATTGGACTAAATTCAAAAGCTAAAATTGCTCATGCAAAGCCTGAAAACCACACGT
TATCTGTTGAAGATTTGCTGTCAAGCGAAATAGAAACT**CGTGCTGCTGATATCCCGTAA**

Figure A1: The coding sequences for the *Tz*SPINK4 gene. The gene-specific forward and reverse primer annealing sites are in bold while the start and stop codons are underlined.

ATGAGTAACATATGCGGAGGTGTCAAAGAGGAAAGAGAACCTACAGAAGCAGAAATGGCAATAG
CATTGGGTTTGAGATCTGACGTGGAGAATCAATTGAATAGAAAGTTCAAGCATTTTCGTCCAGTC
TCTATTCGTACGCAAATTGTCGCAGGCATAAATTACTTTTTTAAAGTTATGGTAGATGAAGATGAC
TTTATTCATCTTCGGGTTTTTAAAAATTTACAAAATGAAACTCAGTTGCACGGCGTACAGCATGGT
AAAAAACATTCTGATAAGC**TCGAATATTTTTAG**

Figure A2: The coding sequences for the *Tz*cystatin B gene. The gene-specific forward and reverse primer annealing sites are in bold while the start and stop codons are underlined.

B. Alignments

The DNA sequences obtained from the CAF sequencing facility from Stellenbosch University were translated into amino acid sequences using the BioEdit program were aligned with the sequences obtained from NCBI Genbank.

```
TzSPINK4 protein      -----MISLACLLYLLMSTAVVTYGFPMIFPRDPFCTMFSRNGFCYDIYQPVCGTDGITY    55
TzSPINK4 rev          LKRXFMISLAC-LYLLMSTAVVTYGFPMIFPRDPFCTMFSRNGFCYDIYQPVCGTDGITY    59
                           ****** **********************************************

TzSPINK4_protein      DNECWLCYRLTIEPLIVQIAYDGECVADYDPMMLQFPRVIGNGIAVPPPSPPFLLSGVIG    115
TzSPINK4_rev          DNECWLCYRLTIEPLIVQIAYDGECVADYDPMMLQFPXVIGNGIAVPPPSPPFLLSGVIG    119
                      ********************************** ********************

TzSPINK4 protein      LNSKAKIAHAKPENHTLSVEDLLSSEIETRAADIP150
TzSPINK4_rev          LNSKAKIAHAKPENHTXIC----------------138
                      ***************
```

Figure B1: Protein sequence alignment of recombinant clone used for cloning and expression of r*Tz*SPINK4 to the sequence obtained from NCBI Genbank.

```
TzcysB protein      --MSNICGGVKEEREPTEAEMAIALGLRSDVENQLNRKFKHFRPVSIRTQIVAGINYFFK      58
TzcysB fwd          EFMSNICGGVKEEREPTEAEMAIALGLRSDVENQLNRKFKHFRPVSIRTQIVAGINYFFK      60
                      ************************************************************

TzcysB_protein      VMVDEDDFIHLRVFKNLQNETQLHGVQHGKKHSDKLEYF        97
TzcysB fwd          VMVDEDDFIHLRVFKNLQNETQLHGVQHGKKHSDKLEYF        99
                    ************************************

TzcysB protein      --MSNICGGVKEEREPTEAEMAIALGLRSDVENQLNRKFKHFRPVSIRTQIVAGINYFFK      58
TzcysB_rev          EFMSNICGGVKEEREPTEAEMAIALGLRSDVENQLNRKFKHFRPVSIRTQIVAGINYFFK      60
                      ************************************************************

TzcysB protein      VMVDEDDFIHLRVFKNLQNETQLHGVQHGKKHSDKLEYF        97
TzcysB rev          VMVDEDDFIHLRVFKNLQNETRLHGVQHGKKHSDKLEYF        99
                    ********************:*******************
```

Figure B2: Protein sequence alignment of recombinant clone used for cloning and expression of r*Tz*cystatin B to the sequence obtained from NCBI Genbank.

REFERENCES

Abongwa, M., Martin, R. J. & Robertson, A. P. (2017) A brief review on the mode of action of antinematodal drugs. *Acta Veterinaria,* **67,** 137-152.

Andrade-Becerra, J. I., Pompa-Mera, E. N., Ribas-Aparicio, R. M. & Yépez-Mulia, L. (2017) Vaccination against *Trichinella spiralis*: Potential, Limitations and Future Directions. *Natural Remedies in the Fight Against Parasites***,** 219.

Antalis, T. M., Bugge, T. H. & Wu, Q. 2011. Chapter 1 - Membrane-Anchored Serine Proteases in Health and Disease. *In:* DI CERA, E. (ed.) *Progress in Molecular Biology and Translational Science.* Academic Press.

Athanasiadou, S., Jones, L. A., Burgess, S. T., Kyriazakis, I., Pemberton, A. D., Houdijk, J. G. & Huntley, J. F. (2011) Genome-wide transcriptomic analysis of intestinal tissue to assess the impact of nutrition and a secondary nematode challenge in lactating rats. *PloS One,* **6,** e20771.

Atkinson, H. J., Babbitt, P. C. & Sajid, M. (2009) The global cysteine peptidase landscape in parasites. *Trends in Parasitology,* **25,** 573-81.

Bai, X., Hu, X., Liu, X., Tang, B. & Liu, M. (2017) Current research of trichinellosis in China. *Frontiers in Microbiology,* **8,** 1472.

Barrett, A. J. & Rawlings, N. D. (1996) Families and clans of cysteine peptidases. *Perspectives in Drug Discovery and Design,* **6,** 1-11.

Blaxter, M. L., De Ley, P., Garey, J. R., Liu, L. X., Scheldeman, P., Vierstraete, A., Vanfleteren, J. R., Mackey, L. Y., Dorris, M., Frisse, L. M., Vida, J. T. & Thomas, W. K. (1998) A molecular evolutionary framework for the phylum Nematoda. *Nature,* **392,** 71-75.

Blisnick, A. A., Foulon, T. & Bonnet, S. I. (2017) Serine protease inhibitors in ticks: an overview of their role in tick biology and tick-borne pathogen transmission. *Frontiers in Cellular and Infection Microbiology,* **7,** 199.

Boulangé, A., Katende, J. & Authié, E. (2002) *Trypanosoma congolense*: expression of a heat shock protein 70 and initial evaluation as a diagnostic antigen for bovine trypanosomosis. *Experimental Parasitology,* **100,** 6-11.

Bradford, M. M. (1976) A rapid and sensitive method for the quantitation of microgram quantities of protein utilizing the principle of protein-dye binding. *Analytical Biochemistry,* **72,** 248-254.

Bromme, D. (2001) Papain-like cysteine proteases. *Current Protocols in Protein Science,* **Chapter 21,** Unit 21.2.

Bruschi, F., Chiumiento, L. & Del Prete, G. 2010. Immunodulation and Helminths: Towards New Strategies for Treatment of Immune-Mediated Diseases? *Detection of Bacteria, Viruses, Parasites and Fungi.* Springer.

Bruschi, F., Marucci, G., Pozio, E. & Masetti, M. (2009) Evaluation of inflammatory responses against muscle larvae of different *Trichinella* species by an image analysis system. *Veterinary Parasitology,* **159,** 258-262.

Bruschi, F. & Murrell, K. D. (2002) New aspects of human trichinellosis: the impact of new *Trichinella* species. *Postgraduate Medical Journal,* **78,** 15-22.

Caffrey, C. R., Goupil, L., Rebello, K. M., Dalton, J. P. & Smith, D. (2018) Cysteine proteases as digestive enzymes in parasitic helminths. *PLoS Neglected Tropical Diseases,* **12,** e0005840.

Castro, G. (1996) Chapter 86 Helminths: Structure, Classification, Growth, and Development. *Medical Microbiology*.

Chagas, J. R., Authié, E., Serveau, C., Lalmanach, G., Juliano, L. & Gauthier, F. (1997) A comparison of the enzymatic properties of the major cysteine proteinases from *Trypanosoma congolense* and *Trypanosoma cruzi*. *Molecular and Biochemical Parasitology,* **88,** 85-94.

Chakraborti, S. & Dhalla, N. S. (2017). *Proteases in Physiology and Pathology*, Springer.

Chamond, N., Cosson, A., Blom-Potar, M. C., Jouvion, G., D'archivio, S., Medina, M., Droin-Bergère, S., Huerre, M., Goyard, S. & Minoprio, P. (2010) *Trypanosoma vivax* infections: pushing ahead with mouse models for the study of Nagana. I. Parasitological, hematological and pathological parameters. *PLoS Neglected Tropical Diseases,* **4,** e792.

Chung, J.-Y., Bae, Y.-A., Na, B.-K. & Kong, Y. (2005) Cysteine protease inhibitors as potential antiparasitic agents. *Expert Opinion on Therapeutic Patents,* **15,** 995-1007.

Costa, S., Almeida, A., Castro, A. & Domingues, L. (2014) Fusion tags for protein solubility, purification and immunogenicity in *Escherichia coli*: the novel Fh8 system. *Frontiers in Microbiology,* **5,** 63.

Dainichi, T., Maekawa, Y., Ishii, K., Zhang, T., Nashed, B. F., Sakai, T., Takashima, M. & Himeno, K. (2001) Nippocystatin, a Cysteine Protease Inhibitor from *Nippostrongylus brasiliensis*, Inhibits

Antigen Processing and Modulates Antigen-Specific Immune Response. *Infection and Immunity,* **69,** 7380-7386.
Dale, J. W., Von Schantz, M. & Plant, N. (2011). *From genes to genomes: concepts and applications of DNA technology*, John Wiley & Sons.
De Ley, P. (2006) A quick tour of nematode diversity and the backbone of nematode phylogeny. *WormBook*, 1-8.
Di Cera, E. (2009) Serine proteases. *Internation Union of Biochemistry and Molecular Biology Life,* **61,** 510-515.
Dubin, G. (2005) Proteinaceous cysteine protease inhibitors. *Cellular and molecular life sciences,* **62,** 653-669.
Duffy, M. S., Cevasco, D. K., Zarlenga, D. S., Sukhumavasi, W. & Appleton, J. A. (2006) Cathepsin B homologue at the interface between a parasitic nematode and its intermediate host. *Infection and Immunity,* **74,** 1297-304.
Dzik, J. M. (2006) Molecules released by helminth parasites involved in host colonization. *Acta Biochimica Polonica,* **53,** 33-64.
El-Baky, N. A., Linjawi, M. H. & Redwan, E. M. (2015) Auto-induction expression of human consensus interferon-alpha in *Escherichia coli*. *BioMed Central Biotechnology,* **15,** 14.
ElsäSser, B., Zauner, F. B., Messner, J., Soh, W. T., Dall, E. & Brandstetter, H. (2017) Distinct roles of catalytic cysteine and histidine in the protease and ligase mechanisms of human legumain as revealed by DFT-based QM/MM simulations. *ACS Catalysis,* **7,** 5585-5593.
Eyssen, L. E.-A., Vather, P., Jackson, L., Ximba, P., Biteau, N., Baltz, T., Boulangé, A., Büscher, P. & Coetzer, T. H. (2018) Recombinant and native *Tvi*CATL from *Trypanosoma vivax*: enzymatic characterisation and evaluation as a diagnostic target for animal African trypanosomosis. *Molecular and Biochemical Parasitology,* **223,** 50-54.
Farady, C. J. & Craik, C. S. (2010) Mechanisms of macromolecular protease inhibitors. *ChemBioChem,* **11,** 2341-2346.
Farina, F., Pasqualetti, M., Ilgova, J., Cardillo, N., Ercole, M., Aronowicz, T., Krivokapich, S., Kasny, M. & Ribicich, M. (2017) Evaluation of the infectivity and the persistence of *Trichinella patagoniensis* in muscle tissue of decomposing guinea pig (*Cavia porcellus*). *Parasitology Research,* **116,** 371-375.
Feidas, H., Kouam, M. K., Kantzoura, V. & Theodoropoulos, G. (2014) Global geographic distribution of *Trichinella* species and genotypes. *Infection, Genetics and Evolution,* **26,** 255-266.
Fink, E., Rehm, H., Gippner, C., Bode, W., Eulitz, M., Machleidt, W. & Fritz, H. (1986) The primary structure of bdellin B-3 from the leech *Hirudo medicinalis*. Bdellin B-3 is a compact proteinase inhibitor of a "non-classical" Kazal type. It is present in the leech in a high molecular mass form. *Biological chemistry Hoppe-Seyler,* **367,** 1235-42.
Fonda, I., Kenig, M., Gaberc-Porekar, V., Pristovaek, P. & Menart, V. (2002) Attachment of histidine tags to recombinant tumor necrosis factor-alpha drastically changes its properties. *Scientific World Journal,* **2,** 1312-25.
Friedrich, T., Kröger, B., Bialojan, S., Lemaire, H. G., Höffken, H., Reuschenbach, P., Otte, M. & Dodt, J. (1993a) A Kazal-type inhibitor with thrombin specificity from *Rhodnius prolixus*. *Journal of Biological Chemistry,* **268,** 16216-16222.
Friedrich, T., Kroger, B., Bialojan, S., Lemaire, H. G., Hoffken, H. W., Reuschenbach, P., Otte, M. & Dodt, J. (1993b) A Kazal-type inhibitor with thrombin specificity from *Rhodnius prolixus*. *The Journal of Biological Chemistry,* **268,** 16216-22.
Gachohi, J., Skilton, R., Hansen, F., Ngumi, P. & Kitala, P. (2012) Epidemiology of East Coast fever (*Theileria parva* infection) in Kenya: past, present and the future. *Parasites & Vectors,* **5,** 194.
Goldring, J. D. & Coetzer, T. H. (2003) Isolation of chicken immunoglobulins (IgY) from egg yolk. *Biochemistry and Molecular Biology Education,* **31,** 185-187.
Goldring, J. D., Thobakgale, C., Hiltunen, T. & Coetzer, T. H. (2005) Raising antibodies in chickens against primaquine, pyrimethamine, dapsone, tetracycline, and doxycycline. *Immunological Investigations,* **34,** 101-114.
Gómez-Morales, M. A., Ludovisi, A., Amati, M., Bandino, E., Capelli, G., Corrias, F., Gelmini, L., Nardi, A., Sacchi, C. & Cherchi, S. (2014) Indirect versus direct detection methods of *Trichinella* spp. infection in wild boar (*Sus scrofa*). *Parasites & Vectors,* **7,** 171.
Gómez-Morales, M. A., Ludovisi, A., Amati, M., Cherchi, S., Tonanzi, D. & Pozio, E. (2018) Differentiation of *Trichinella* species (*Trichinella spiralis*/*Trichinella britov*i versus *Trichinella pseudospiralis*) using western blot. *Parasites & Vectors,* **11,** 631.
Gottstein, B., Pozio, E. & Nöckler, K. (2009) Epidemiology, diagnosis, treatment, and control of trichinellosis. *Clinical Microbiology Reviews,* **22,** 127-145.

Goyal, P. K., Wheatcroft, J. & Wakelin, D. (2002) Tyvelose and protective responses to the intestinal stages of *Trichinella spiralis*. *Parasitology International,* **51,** 91-8.
Goździk, K., Odoevskaya, I., Movsesyan, S. & Cabaj, W. (2017) Molecular identification of *Trichinella* isolates from wildlife animals of the Russian Arctic territories. *Helminthologia,* **54,** 11-16.
Grote, A., Caffrey, C. R., Rebello, K. M., Smith, D., Dalton, J. P. & Lustigman, S. (2018) Cysteine proteases during larval migration and development of helminths in their final host. *PLoS Neglected Tropical Diseases,* **12,** e0005919.
Gu, Y., Li, J., Zhu, X., Yang, J., Li, Q., Liu, Z., Yu, S. & Li, Y. (2008) *Trichinella spiralis*: characterization of phage-displayed specific epitopes and their protective immunity in BALB/c mice. *Experimental Parasitology,* **118,** 66-74.
Guo, A. (2015) Comparative analysis of cystatin superfamily in platyhelminths. *PloS One,* **10,** e0124683.
Habib, H. & Fazili, K. M. (2007) Plant protease inhibitors: a defense strategy in plants. *Biotechnology and Molecular Biology Reviews,* **2,** 68-85.
Haider, S. R., Reid, H. J. & Sharp, B. L. 2012. Tricine-sds-page. *Protein electrophoresis.* Springer.
Han, C., Yu, J., Zhang, Z., Zhai, P., Zhang, Y., Meng, S., Yu, Y., Li, X. & Song, M. (2019) Immunomodulatory effects of Trichinella spiralis excretory-secretory antigens on macrophages. *Experimental Parasitology,* **196,** 68-72.
Hanspal, J. S., Bushell, G. R. & Ghosh, P. (1983) Detection of protease inhibitors using substrate-containing sodium dodecyl sulfate-polyacrylamide gel electrophoresis. *Analytical Biochemistry,* **132,** 288-293.
Hartmann, S., Kyewski, B., Sonnenburg, B. & Lucius, R. (1997) A filarial cysteine protease inhibitor down-regulates T cell proliferation and enhances interleukin-10 production. *European Journal of Immunology,* **27,** 2253-2260.
Hartmann, S. & Lucius, R. (2003) Modulation of host immune responses by nematode cystatins. *International Journal for Parasitology,* **33,** 1291-1302.
Hasnain, S. Z., Mcguckin, M. A., Grencis, R. K. & Thornton, D. J. (2012) Serine protease (s) secreted by the nematode *Trichuris muris* degrade the mucus barrier. *PLoS Neglected Tropical Diseases,* **6,** e1856.
Heussen, C. & Dowdle, E. B. (1980) Electrophoretic analysis of plasminogen activators in polyacrylamide gels containing sodium dodecyl sulfate and copolymerized substrates. *Analytical Biochemistry,* **102,** 196-202.
Hewitson, J. P., Grainger, J. R. & Maizels, R. M. (2009) Helminth immunoregulation: the role of parasite secreted proteins in modulating host immunity. *Molecular and Biochemical Parasitology,* **167,** 1-11.
Hunkapiller, M. W., Forgac, M. D. & Richards, J. H. (1976) Mechanism of action of serine proteases: tetrahedral intermediate and concerted proton transfer. *Biochemistry,* **15,** 5581-5588.
Hutchinson, E., Avery, A. & Vandewoude, S. (2005) Environmental enrichment for laboratory rodents. *Institute for Laboratory Animal Research Journal,* **46,** 148-161.
Ilic, N., Gruden-Movsesijan, A. & Sofronic-Milosavljevic, L. (2012) *Trichinella spiralis*: shaping the immune response. *Immunologic Research,* **52,** 111-9.
Janeway Jr, C. A., Travers, P., Walport, M. & Shlomchik, M. J. 2001. The complement system and innate immunity. *Immunobiology: The Immune System in Health and Disease. 5th edition.* Garland Science.
Jia, B. & Jeon, C. O. (2016) High-throughput recombinant protein expression in *Escherichia coli*: current status and future perspectives. *Open Biology,* **6,** 160196.
Kalinska, M., Meyer-Hoffert, U., Kantyka, T. & Potempa, J. (2016) Kallikreins–the melting pot of activity and function. *Biochimie,* **122,** 270-282.
Kanai, Y., Inoue, T., Mano, T., Nonaka, N., Katakura, K. & Oku, Y. (2007) Epizootiological survey of *Trichinella* spp. infection in carnivores, rodents and insectivores in Hokkaido, Japan. *The Japanese Journal of Veterinary Research,* **54,** 175-82.
Klotz, C., Ziegler, T., Daniłowicz-Luebert, E. & Hartmann, S. 2011. Cystatins of parasitic organisms. *Cysteine Proteases of Pathogenic Organisms.* Springer.
Knox, D. (2007) Proteinase inhibitors and helminth parasite infection. *Parasite immunology,* **29,** 57-71.
Ko, R. C., Fan, L., Lee, D. L. & Compton, H. (2009) Changes in host muscles induced by excretory/secretory products of larval *Trichinella spiralis* and *Trichinella pseudospiralis*. *Parasitology,* **108,** 195-205.
Kocięcka, W. (2000) Trichinellosis: human disease, diagnosis and treatment. *Veterinary Parasitology,* **93,** 365-383.

Korhonen, P. K., Pozio, E., La Rosa, G., Chang, B. C., Koehler, A. V., Hoberg, E. P., Boag, P. R., Tan, P., Jex, A. R. & Hofmann, A. (2016) Phylogenomic and biogeographic reconstruction of the *Trichinella* complex. *Nature Communications,* **7,** 10513.

Kreutzmann, P., Schulz, A., Standker, L., Forssmann, W. G. & Magert, H. J. (2004) Recombinant production, purification and biochemical characterization of domain 6 of LEKTI: a temporary Kazal-type-related serine proteinase inhibitor. *Journal of Chromatography. B, Analytical technologies in the Biomedical and Life sciences,* **803,** 75-81.

Krowarsch, D., Cierpicki, T., Jelen, F. & Otlewski, J. (2003) Canonical protein inhibitors of serine proteases. *Cellular and Molecular Life Sciences,* **60,** 2427-2444.

La Grange, L. J., Marucci, G. & Pozio, E. (2009) *Trichinella zimbabwensis* in wild Nile crocodiles (*Crocodylus niloticus*) of South Africa. *Vet Parasitol,* **161,** 88-91.

Lalmanach, G., Boulangé, A., Serveau, C., Lecaille, F., Scharfstein, J., Gauthier, F. & Authié, E. (2002) Congopain from *Trypanosoma congolense*: drug target and vaccine candidate. *Biological Chemistry,* **383,** 739-749.

Lee, J.-Y., Song, S.-M., Moon, E.-K., Lee, Y.-R., Jha, B. K., Danne, D.-B. S., Cha, H.-J., Yu, H. S., Kong, H.-H. & Chung, D.-I. (2013) Cysteine protease inhibitor (AcStefin) is required for complete cyst formation of *Acanthamoeba*. *Eukaryotic Cell,* **12,** 567-574.

Lihua, X., Una, R. & Yaoyu, F. (2015). *Biology of Foodborne Parasites,* Bosa Roca, United States, Taylor & Francis Inc.

Long, S. R., Wang, Z. Q., Jiang, P., Liu, R. D., Qi, X., Liu, P., Ren, H. J., Shi, H. N. & Cui, J. (2015) Characterization and functional analysis of *Trichinella spiralis* Nudix hydrolase. *Experimental Parasitology,* **159,** 264-73.

Lu, A., Zhang, Q., Zhang, J., Yang, B., Wu, K., Xie, W., Luan, Y.-X. & Ling, E. (2014) Insect prophenoloxidase: the view beyond immunity. *Frontiers in Physiology,* **5,** 252.

Lu, S. M., Lu, W., Qasim, M. A., Anderson, S., Apostol, I., Ardelt, W., Bigler, T., Chiang, Y. W., Cook, J., James, M. N., Kato, I., Kelly, C., Kohr, W., Komiyama, T., Lin, T. Y., Ogawa, M., Otlewski, J., Park, S. J., Qasim, S., Ranjbar, M., Tashiro, M., Warne, N., Whatley, H., Wieczorek, A., Wieczorek, M., Wilusz, T., Wynn, R., Zhang, W. & Laskowski, M., Jr. (2001) Predicting the reactivity of proteins from their sequence alone: Kazal family of protein inhibitors of serine proteinases. *Proceedings of the National Academy of Sciences of the United States of America,* **98,** 1410-5.

Lu, W., Apostol, I., Qasim, M. A., Warne, N., Wynn, R., Zhang, W. L., Anderson, S., Chiang, Y. W., Ogin, E., Rothberg, I., Ryan, K. & Laskowski, M. (1997) Binding of amino acid side-chains to S1 cavities of serine proteinases. *Journal of Molecular Biology,* **266,** 441-461.

Macdonald, A. S., Araujo, M. I. & Pearce, E. J. (2002) Immunology of Parasitic Helminth Infections. *Infection and Immunity,* **70,** 427-433.

Magrone, T., Jirillo, E. & Miragliotta, G. (2014) The impact of helminths on the human microbiota: therapeutic correction of disturbed gut microbial immunity. *Jirillo E, Magrone T, Miragliotta G. Immune Response to Parasitic Infections. Immunity to Helminths and Novel Therapeutical Approaches. Eds. Elsevier,* **2,** 235-254.

Meyer-Hoffert, U., Wu, Z., Kantyka, T., Fischer, J., Latendorf, T., Hansmann, B., Bartels, J., He, Y., Gläser, R. & Schröder, J.-M. (2010) Isolation of SPINK6 in human skin selective inhibitor of kallikrein-related peptidases. *Journal of Biological Chemistry,* **285,** 32174-32181.

Meyer-Hoffert, U., Wu, Z. & Schröder, J.-M. (2009) Identification of lympho-epithelial Kazal-type inhibitor 2 in human skin as a kallikrein-related peptidase 5-specific protease inhibitor. *PloS One,* **4,** e4372.

Mitreva, M. & Jasmer, D. P. (2006) Biology and genome of *Trichinella spiralis*.

Mitsudo, K., Jayakumar, A., Henderson, Y., Frederick, M. J., Kang, Y. A., Wang, M., El-Naggar, A. K. & Clayman, G. L. (2003) Inhibition of serine proteinases plasmin, trypsin, subtilisin A, cathepsin G, and elastase by LEKTI: a kinetic analysis. *Biochemistry,* **42,** 3874-3881.

Mukaratirwa, S., La Grange, L. & Pfukenyi, D. M. (2013) *Trichinella* infections in animals and humans in sub-Saharan Africa: a review. *Acta Tropica,* **125,** 82-89.

Nagano, I., Wu, Z., Nakada, T., Matsuo, A. & Takahashi, Y. (2001) Molecular cloning and characterization of a serine proteinase inhibitor from *Trichinella spiralis*. *Parasitology,* **123,** 77-83.

Neghina, R., Moldovan, R., Marincu, I., Calma, C. L. & Neghina, A. M. (2012) The roots of evil: the amazing history of trichinellosis and *Trichinella* parasites. *Parasitology Research,* **110,** 503-508.

Negulescu, H., Guo, Y., Garner, T. P., Goodwin, O. Y., Henderson, G., Laine, R. A. & Macnaughtan, M. A. (2015) A Kazal-type serine protease inhibitor from the defense gland secretion of the subterranean termite *Coptotermes formosanus* Shiraki. *PloS One,* **10,** e0125376.

Nishimiya, D., Kawaguchi, Y., Kodama, S., Nasu, H., Yano, H., Yamaguchi, A., Tamura, M. & Hashimoto, R. (2019) A protein scaffold, engineered SPINK2, for generation of inhibitors with high affinity and specificity against target proteases. *Scientific Reports,* **9,** 1-11.

Nutman, T. B. (2015) Looking beyond the induction of Th2 responses to explain immunomodulation by helminths. *Parasite immunology,* **37,** 304-313.

Onkoba, N. W., Chimbari, M. J. & Mukaratirwa, S. (2015) Malaria endemicity and co-infection with tissue-dwelling parasites in Sub-Saharan Africa: a review. *Infectious Diseases of Poverty,* **4,** 35.

Ortega, Y. R. & Sterling, C. R. (2018). *Foodborne parasites*, Springer.

Paraskevopoulou, V. & Falcone, F. (2018) Polyionic tags as enhancers of protein solubility in recombinant protein expression. *Microorganisms,* **6,** 47.

Parkinson, J., Mitreva, M., Whitton, C., Thomson, M., Daub, J., Martin, J., Schmid, R., Hall, N., Barrell, B. & Waterston, R. H. (2004) A transcriptomic analysis of the phylum Nematoda. *Nature Genetics,* **36,** 1259.

Pei, J. & Grishin, N. V. (2009) The Rho GTPase inactivation domain in Vibrio cholerae MARTX toxin has a circularly permuted papain-like thiol protease fold. *Proteins: Structure, Function, and Bioinformatics,* **77,** 413-419.

Pike, R. & Dennison, C. (1989) Protein fractionation by three phase partitioning (TPP) in aqueous/t-butanol mixtures. *Biotechnology and Bioengineering,* **33,** 221-228.

Pol, E. & Björk, I. (2001) Role of the single cysteine residue, Cys 3, of human and bovine cystatin B (stefin B) in the inhibition of cysteine proteinases. *Protein Science,* **10,** 1729-1738.

Pozio, E. (2016) Adaptation of *Trichinella spp*. for survival in cold climates. *Food and Waterborne Parasitology,* **4,** 4-12.

Pozio, E., Foggin, C., Marucci, G., La Rosa, G., Sacchi, L., Corona, S., Rossi, P. & Mukaratirwa, S. (2002a) *Trichinella zimbabwensis* n. sp.(Nematoda), a new non-encapsulated species from crocodiles (*Crocodylus niloticus)* in Zimbabwe also infecting mammals. *International Journal for Parasitology,* **32,** 1787-1799.

Pozio, E., Foggin, C. M., Marucci, G., La Rosa, G., Sacchi, L., Corona, S., Rossi, P. & Mukaratirwa, S. (2002b) Trichinella zimbabwensis n.sp. (Nematoda), a new non-encapsulated species from crocodiles (Crocodylus niloticus) in Zimbabwe also infecting mammals. *Int J Parasitol,* **32,** 1787-99.

Pozio, E., Zarlenga, D. & La Rosa, G. (2001) The detection of encapsulated and non-encapsulated species of *Trichinella* suggests the existence of two evolutive lines in the genus. *Parasite,* **8,** S27-S29.

Qian, C., Fang, Q., Wang, L. & Ye, G.-Y. (2015) Molecular cloning and functional studies of two Kazal-type serine protease inhibitors specifically expressed by *Nasonia vitripennis* venom apparatus. *Toxins,* **7,** 2888-2905.

Qu, Z.-G., Ma, X.-T., Li, W.-H., Zhang, N.-Z., Yue, L., Cui, J.-M., Cai, J.-P., Jia, W.-Z. & Fu, B.-Q. (2015) Molecular characterization of a cathepsin F-like protease in *Trichinella spiralis*. *Parasites & Vectors,* **8,** 652.

Rajalingam, D., Kathir, K. M., Ananthamurthy, K., Adams, P. D. & Kumar, T. K. S. (2008) A method for the prevention of thrombin-induced degradation of recombinant proteins. *Analytical Biochemistry,* **375,** 361-363.

Ranasinghe, S. & Mcmanus, D. P. (2013) Structure and function of invertebrate Kunitz serine protease inhibitors. *Developmental & Comparative Immunology,* **39,** 219-227.

Rawlings, N. D., Barrett, A. J. & Bateman, A. (2012) MEROPS: the database of proteolytic enzymes, their substrates and inhibitors. *Nucleic Acids Research,* **40,** D343-50.

Rawlings, N. D., Barrett, A. J. & Finn, R. (2015) Twenty years of the MEROPS database of proteolytic enzymes, their substrates and inhibitors. *Nucleic Acids Research,* **44,** D343-D350.

Rimphanitchayakit, V. & Tassanakajon, A. (2010) Structure and function of invertebrate Kazal-type serine proteinase inhibitors. *Developmental & Comparative Immunology,* **34,** 377-386.

Roberts, R. J., Belfort, M., Bestor, T., Bhagwat, A. S., Bickle, T. A., Bitinaite, J., Blumenthal, R. M., Degtyarev, S., Dryden, D. T., Dybvig, K., Firman, K., Gromova, E. S., Gumport, R. I., Halford, S. E., Hattman, S., Heitman, J., Hornby, D. P., Janulaitis, A., Jeltsch, A., Josephsen, J., Kiss, A., Klaenhammer, T. R., Kobayashi, I., Kong, H., Kruger, D. H., Lacks, S., Marinus, M. G., Miyahara, M., Morgan, R. D., Murray, N. E., Nagaraja, V., Piekarowicz, A., Pingoud, A., Raleigh, E., Rao, D. N., Reich, N., Repin, V. E., Selker, E. U., Shaw, P. C., Stein, D. C., Stoddard, B. L., Szybalski, W., Trautner, T. A., Van Etten, J. L., Vitor, J. M., Wilson, G. G. & Xu, S. Y. (2003) A nomenclature for restriction enzymes, DNA methyltransferases, homing endonucleases and their genes. *Nucleic Acids Res,* **31,** 1805-12.

Robinson, M. W., Massie, D. H. & Connolly, B. (2007) Secretion and processing of a novel multi-domain cystatin-like protein by intracellular stages of *Trichinella spiralis*. *Molecular and Biochemical Parasitology,* **151,** 9-17.
Rostami, A., Gamble, H. R., Dupouy-Camet, J., Khazan, H. & Bruschi, F. (2017) Meat sources of infection for outbreaks of human trichinellosis. *Food Microbiology,* **64,** 65-71.
Sajid, M. & Mckerrow, J. H. (2002) Cysteine proteases of parasitic organisms. *Molecular and biochemical parasitology,* **120,** 1-21.
Scalf, C. S., Chariker, J. H., Rouchka, E. C. & Ashley, N. T. (2019) Transcriptomic analysis of immune response to bacterial lipopolysaccharide in zebra finch (*Taeniopygia guttata*). *Biomed Central Genomics,* **20,** 647.
Schägger, H. (2006) Tricine–sds-page. *Nature Protocols,* **1,** 16.
Sigle, L. T. & Ramalho-Ortigão, M. (2013) Kazal-type serine proteinase inhibitors in the midgut of *Phlebotomus papatasi*. *Memórias do Instituto Oswaldo Cruz,* **108,** 671-678.
Smythe, A. B., Holovachov, O. & Kocot, K. M. (2019) Improved phylogenomic sampling of free-living nematodes enhances resolution of higher-level nematode phylogeny. *Biomed Central Evolutionary Biology,* **19,** 121.
Sofronic-Milosavljevic, L., Ilic, N., Pinelli, E. & Gruden-Movsesijan, A. (2015) Secretory Products of *Trichinella spiralis* Muscle Larvae and Immunomodulation: Implication for Autoimmune Diseases, Allergies, and Malignancies. *Journal of Immunology Research,* **2015,** 523875.
Song, Y. Y., Wang, A. L., Na Ren, H., Qi, X., Sun, G. G., Liu, D. R., Jiang, P., Zhang, X., Cui, J. & Wang, Q. Z. (2018a) Cloning, expression and characterisation of a cysteine protease from *Trichinella spiralis*. *Folia Parasitologica,* **65**.
Song, Y. Y., Zhang, Y., Ren, H. N., Sun, G. G., Qi, X., Yang, F., Jiang, P., Zhang, X., Cui, J. & Wang, Z. Q. (2018b) Characterization of a serine protease inhibitor from *Trichinella spiralis* and its participation in larval invasion of host's intestinal epithelial cells. *Parasites & vectors,* **11,** 499.
Sotiropoulou, G., Pampalakis, G. & Diamandis, E. P. (2009) Functional roles of human kallikrein-related peptidases. *Journal of Biological Chemistry,* **284,** 32989-32994.
Steinhoff, M., Buddenkotte, J. R., Shpacovitch, V., Rattenholl, A., Moormann, C., Vergnolle, N., Luger, T. A. & Hollenberg, M. D. (2004) Proteinase-activated receptors: transducers of proteinase-mediated signaling in inflammation and immune response. *Endocrine Reviews,* **26,** 1-43.
Sun, G. G., Song, Y. Y., Jiang, P., Ren, H. N., Yan, S. W., Han, Y., Liu, R. D., Zhang, X., Wang, Z. Q. & Cui, J. (2018) Characterization of a *Trichinella spiralis* putative serine protease. Study of its potential as sero-diagnostic tool. *PLoS Neglected Tropical Diseases,* **12,** e0006485.
Sun, Y., Liu, G., Li, Z., Chen, Y., Liu, Y., Liu, B. & Su, Z. (2013) Modulation of dendritic cell function and immune response by cysteine protease inhibitor from murine nematode parasite *Heligmosomoides polygyrus*. *Immunology,* **138,** 370-381.
Tang, B., Liu, M., Wang, L., Yu, S., Shi, H., Boireau, P., Cozma, V., Wu, X. & Liu, X. (2015) Characterisation of a high-frequency gene encoding a strongly antigenic cystatin-like protein from Trichinella spiralis at its early invasion stage. *Parasites & vectors,* **8,** 78.
Terpe, K. (2003) Overview of tag protein fusions: from molecular and biochemical fundamentals to commercial systems. *Applied Microbiology and Biotechnology,* **60,** 523-533.
Tian, M., Huitema, E., Da Cunha, L., Torto-Alalibo, T. & Kamoun, S. (2004) A Kazal-like extracellular serine protease inhibitor from Phytophthora infestans targets the tomato pathogenesis-related protease P69B. *Journal of Biological Chemistry,* **279,** 26370-26377.
Todorova, V. K. (2000) Proteolytic enzymes secreted by larval stage of the parasitic nematode *Trichinella spiralis*. *Folia Parasitologica,* **47,** 141-145.
Tormo, N., Del Remedio Guna, M., Teresa Fraile, M., Dolores Ocete, M., Garcia, A., Navalpotro, D., Chanzá, M., Luis Ramos, J. & Gimeno, C. (2011) Immunity to Parasites. *Current Immunology Reviews,* **7,** 25-43.
Turk, B., Turk, D. & Salvesen, G. S. (2002) Regulating cysteine protease activity: essential role of protease inhibitors as guardians and regulators. *Current Pharmaceutical Design,* **8,** 1623-1637.
Turk, B., Turk, D. & Salvesen, G. S. (2005) Regulating cysteine protease activity: essential role of protease inhibitors as guardians and regulators. *Medicinal Chemistry Reviews-Online,* **2,** 283-297.
Turk, B., Turk, D. & Turk, V. (2000) Lysosomal cysteine proteases: more than scavengers. *Biochimica et Biophysica Acta (BBA)-Protein Structure and Molecular Enzymology,* **1477,** 98-111.
Turk, V. & Bode, W. (1991) The cystatins: Protein inhibitors of cysteine proteinases. *FEBS Letters,* **285,** 213-219.

Turk, V., Stoka, V., Vasiljeva, O., Renko, M., Sun, T., Turk, B. & Turk, D. (2012) Cysteine cathepsins: from structure, function and regulation to new frontiers. *Biochimica et Biophysica Acta (BBA)-Proteins and Proteomics,* **1824,** 68-88.

Van Wyk, S. G., Du Plessis, M., Cullis, C. A., Kunert, K. J. & Vorster, B. J. (2014) Cysteine protease and cystatin expression and activity during soybean nodule development and senescence. *BioMedCentral Plant Pathology,* **14,** 294.

Verma, S., Dixit, R. & Pandey, K. C. (2016) Cysteine proteases: modes of activation and future prospects as pharmacological targets. *Frontiers in Pharmacology,* **7,** 107.

Walden, H. S. 2013. Chapter 25 - *Trichinella*. *In:* MORRIS, J. G. & POTTER, M. E. (eds.) *Foodborne Infections and Intoxications (Fourth Edition).* San Diego: Academic Press.

Wang, B., Wang, Z. Q., Jin, J., Ren, H. J., Liu, L. N. & Cui, J. (2013a) Cloning, expression and characterization of a Trichinella spiralis serine protease gene encoding a 35.5kDa protein. *Experimental Parasitology,* **134,** 148-154.

Wang, L., Wang, Z. Q., Hu, D. D. & Cui, J. (2013b) Proteomic analysis of *Trichinella spiralis* muscle larval excretory-secretory proteins recognized by early infection sera. *BioMed research international,* **2013**.

Wang, Y., Bai, X., Zhu, H., Wang, X., Shi, H., Tang, B., Boireau, P., Cai, X., Luo, X. & Liu, M. (2017a) Immunoproteomic analysis of the excretory-secretory products of *Trichinella pseudospiralis* adult worms and newborn larvae. *Parasites & Vectors,* **10,** 579.

Wang, Y., Wu, L., Liu, X., Wang, S., Ehsan, M., Yan, R., Song, X., Xu, L. & Li, X. (2017b) Characterization of a secreted cystatin of the parasitic nematode *Haemonchus contortus* and its immune-modulatory effect on goat monocytes. *Parasites & Vectors,* **10,** 425.

Wang, Z.-Q. & Cui, J. (2008) [Diagnosis and treatment of trichinellosis]. *Zhongguo ji sheng chong xue yu ji sheng chong bing za zhi = Chinese journal of parasitology & parasitic diseases,* **26,** 53-57.

Wang, Z.-Q., Shi, Y.-L., Liu, R.-D., Jiang, P., Guan, Y.-Y., Chen, Y.-D. & Cui, J. (2017c) New insights on serodiagnosis of trichinellosis during window period: early diagnostic antigens from *Trichinella spiralis* intestinal worms. *Infectious Diseases of Poverty,* **6,** 41.

Wu, Z., Matsuo, A., Nakada, T., Nagano, I. & Takahashi, Y. (2001) Different response of satellite cells in the kinetics of myogenic regulatory factors and ultrastructural pathology after *Trichinella spiralis* and *T. pseudospiralis* infection. *Parasitology,* **123,** 85-94.

Xu, D., Wu, Z., Nagano, I. & Takahashi, Y. (1997) A muscle larva of *Trichinella pseudospiralis* is intracellular, but does not form a typical cyst wall. *Parasitology International,* **46,** 1-5.

Xu, J., Bai, X., Wang, L. B., Shi, H. N., Van Der Giessen, J. W., Boireau, P., Liu, M. Y. & Liu, X. L. (2017a) Immune responses in mice vaccinated with a DNA vaccine expressing serine protease-like protein from the new-born larval stage of *Trichinella spiralis*. *Parasitology,* **144,** 712-719.

Xu, J., Yu, P., Wu, L., Liu, M. & Lu, Y. (2019) Regulatory effect of two *Trichinella spiralis* serine protease inhibitors on the host's immune system. *Scientific Reports,* **9,** 17045.

Xu, N., Liu, X., Tang, B., Wang, L., Shi, H. N., Boireau, P., Liu, M. & Bai, X. (2017b) Recombinant *Trichinella pseudospiralis* serine protease inhibitors alter macrophage polarization in vitro. *Frontiers in Microbiology,* **8,** 1834.

Yang, J., Pan, W., Sun, X., Zhao, X., Yuan, G., Sun, Q., Huang, J. & Zhu, X. (2015a) Immunoproteomic profile of *Trichinella spiralis* adult worm proteins recognized by early infection sera. *Parasites & Vectors,* **8,** 20.

Yang, L., Mei, Y., Fang, Q., Wang, J., Yan, Z., Song, Q., Lin, Z. & Ye, G. (2017) Identification and characterization of serine protease inhibitors in a parasitic wasp, *Pteromalus puparum*. *Scientific Reports,* **7,** 15755.

Yang, Y., Cai, Y. N., Tong, M. W., Sun, N., Xuan, Y. H., Kang, Y. J., Vallée, I., Boireau, P., Peng Cheng, S. & Liu, M. Y. (2016) Serological tools for detection of *Trichinella* infection in animals and humans. *One Health,* **2,** 25-30.

Yang, Y., Jun Wen, Y., Cai, Y. N., Vallée, I., Boireau, P., Liu, M. Y. & Cheng, S. P. (2015b) Serine proteases of parasitic helminths. *The Korean journal of parasitology,* **53,** 1.

Yepez-Mulia, L., Hernandez-Bello, R., Arizmendi-Puga, N., Fonseca-Linan, R. & Ortega-Pierres, G. (2007) Contributions to the study of Trichinella spiralis TSL-1 antigens in host immunity. *Parasite Immunol,* **29,** 661-70.

Yiu, W. H., Wong, D. W., Chan, L. Y., Leung, J. C., Chan, K. W., Lan, H. Y., Lai, K. N. & Tang, S. C. (2014) Tissue kallikrein mediates pro-inflammatory pathways and activation of protease-activated receptor-4 in proximal tubular epithelial cells. *PloS One,* **9,** e88894.

Zang, X. & Maizels, R. M. (2001) Serine proteinase inhibitors from nematodes and the arms race between host and pathogen. *Trends in Biochemical Sciences,* **26,** 191-197.

Zarlenga, D. S., Chute, M. B., Martin, A. & Kapel, C. M. (2001) A single, multiplex PCR for differentiating all species of *Trichinella*. *Parasite,* **8,** S24-6.
Zerovnik, E. (2006). *Human stefins and cystatins*, Nova Publishers.
Zhan, J. H., Yao, J. P., Liu, W., Hu, X. C., Wu, Z. D. & Zhou, X. W. (2013) Analysis of a novel cathepsin B circulating antigen and its response to drug treatment in *Trichinella*-infected mice. *Parasitol Res,* **112,** 3213-22.
Zhang, G., Guo, J. & Wang, X. 2009. Immunochromatographic lateral flow strip tests. *Biosensors and Biodetection.* Springer.
Zhang, N., Li, W. & Fu, B. (2018) Vaccines against *Trichinella spiralis*: progress, challenges and future prospects. *Transboundary and Emerging Diseases,* **65,** 1447-1458.
Zhang, Z., Mao, Y., Li, D., Zhang, Y., Li, W., Jia, H., Zheng, J., Li, L. & Lu, Y. (2016) High-level expression and characterization of two serine protease inhibitors from *Trichinella spiralis*. *Veterinary Parasitology,* **219,** 34-39.
Zhu, C., Han, H., Li, J., Xu, L., Liu, F., Wu, K. & Liu, X. (2019) Hepatitis B Virus X Protein-Induced Serine Protease Inhibitor Kazal Type 1 Is Associated with the Progression of HBV-Related Diseases. *BioMed research international,* **2019**.
Zolfaghari Emameh, R., Purmonen, S., Sukura, A. & Parkkila, S. (2018) Surveillance and diagnosis of zoonotic foodborne parasites. *Food science & nutrition,* **6,** 3-17.